DESIGN AND ANALYSIS OF MULTI-FREQUENCY BROADBAND MICROSTRIP ANTENNAS

by

Pradeep Kumar

A thesis submitted for fulfillment of the requirements

for

the degree of

Doctor of Philosophy

in

Electronics and Communication Engineering

DEPARTMENT OF ELECTRONICS AND COMMUNICATION ENGINEERING
JAYPEE UNIVERSITY OF INFORMATION TECHNOLOGY,
WAKNAGHAT, SOLAN-173215, INDIA

Roll No. 061760 **2009**

JAYPEE UNIVERSITY OF INFORMATION TECHNOLOGY
(Established by H.P. State Legislative vide Act No. 14 of 2002)
Waknaghat, P.O. Dumehar Bani, Kandaghat, Distt. Solan - 173215 (H.P.) INDIA
Website : www.juit.ac.in
Phone No. (91) 01792-257999 (30 Lines)
Fax: (91) 01792 245362

Date: 29.05.09

CERTIFICATE

This is to certify that ***Mr. Pradeep Kumar*** has completed the research work for the full period prescribed by the university for Ph.D. and that the thesis entitled "***Design and Analysis of Multi-frequency Broadband Microstrip Antennas***" authored by him embodies the results of his own investigations conducted during the period he worked as Ph.D. research scholar in the Department of Electronics and Communication Engineering, Jaypee University of Information Technology, Waknaghat, Solan, India.

(Dr. G. Singh)
Supervisor

(Dr. Sunil Bhooshan)
Co-supervisor

ABSTRACT

Microstrip antennas have been in the spotlight ever since their introduction in the early nineteen sixties. A strong demand has arisen in many areas for small, lightweight and low profile antennas, for example, wireless communications, satellite communication terminals, phased arrays, electronic warfare, missile telemetry, altimeters, biological telemetry, navigation, radar, surveillance, radiometers and low probability of intercept systems. In its basic form, microstrip antennas are similar to parallel plate capacitors. Both have parallel plates of metal layer and sandwiched dielectric substrate between them. But in microstrip antennas, one of these metal plates is infinitely extended to form the ground plane whereas the smaller metal plate is described as radiating patch. Since the size of the patch is often proportional to the wavelength of the propagating signal, this class of antenna is classified as resonant antennas. So far, several shapes of microstrip patches, such as rectangular, circular, triangular, semicircular, sectoral and annular etc, are successfully used as radiating antenna elements employed in various communication and control devices.

The microstrip patch antenna feeding techniques can be classified into two categories — contact feeding and non-contact feeding. In the contact feeding method, the RF power is fed directly to the radiating patch using a connector element such as microstrip line and coaxial probe. In the non-contacting feeding methods, electromagnetic field coupling is established to transfer power between microstrip line and radiating patch such as aperture coupling and proximity coupling. The feeding technique influences the input impedance, which is often exploited for matching purposes. As the antenna efficiency depends on the transfer of power to the radiating element, feeding technique plays a vital role in the design process. The main objectives of antenna analysis are to predict the radiation characteristics such as radiation patterns, gain as well as near-field characteristics, input impedance, impedance bandwidth, mutual coupling and antenna efficiency. Various techniques have been proposed and used to determine microstrip antenna characteristics. The analytical techniques include the transmission line model, generalized transmission line model, cavity model and multiport network model.

Circular disc microstrip patch antennas offer performance similar to that of the rectangular microstrip antennas and are slightly smaller than the latter. In some applications, such as arrays, circular geometries offer certain advantages over the other configurations and it can easily be modified to produce a range of impedance values, radiation patterns and frequency of operation. For an efficient interface between the free-space wave and the guided wave in the feed transmission line, the input impedance of an antenna must be matched to the characteristic impedance of the transmission line. Thus, the antenna characteristics can be classified into two main categories: radiation characteristics, which are used to describe the way the antenna radiates or receives energy to or from space and input characteristics, which are used to specify the performance of the antenna looking into its terminals. Radiation characteristics include the radiation pattern, gain, directivity, effective aperture, polarization etc. and the input characteristics are specified in terms of the input impedance, bandwidth, reflection coefficient, voltage standing wave ratio etc.

The major disadvantages of the microstrip antennas are narrow impedance bandwidth and low efficiency. The impedance bandwidth of a microstrip antenna can be increased by using various techniques such as by using thicker substrate, by reducing the dielectric constant, by using gap-coupled multiple resonators and by loading the patch. However, the use of thicker substrate causes spurious radiation and there are practical limitations in decreasing the value of dielectric constant. The concept of the two gap-coupled circular microstrip patch antenna is a significant technique to enhance the impedance bandwidth among the aforementioned methods. The investigation presented in this thesis principally addresses the probe fed two gap-coupled circular microstrip patch antenna. Using the concept of gap-coupling, the gap-coupled circular microstrip patch antenna is designed for dual frequency operation. In the gap-coupled microstrip antenna, two patches are placed close to each other. One patch is excited by coaxial probe feeding technique and the other is excited by the gap-coupling. The numerical model for computation of the resonant frequency of the two gap-coupled circular microstrip antennas has been developed using the concept of cavity model. The resonant frequency of the two gap-coupled circular patches is computed and the mode number is also evaluated. The gap-

coupled circular microstrip patch antenna generates two close resonances. The computed results are compared with reported literature. An extensive comparison with the method-of-moments based commercially available simulator IE3D is also performed. By the concept of current density distribution, the mode prediction is also carried out.

The trend for technology in recent times is towards the miniaturization and demand for more compact and robust designs has been growing. In wireless devices, the antenna still remains a matter of concern as regards to its size. Microstrip antennas and arrays are extensively used in several applications; however, they are limited by their size, inspite of their other advantages. However, using high dielectric constant substrates increases the surface wave effect, which yields poor performance in terms of radiation efficiency. One effective way to reduce the size of the microstrip patch antenna size is by loading the microstrip patch with a shorting post. The concept of two gap-coupled circular microstrip antenna loaded with a shorting post in the feed patch provides a triple frequency operation. The size of the gap-coupled circular microstrip antennas can be minimized by using the zero mode. The resonant frequency of the zero mode is less than the two modes generated by the gap-coupled circular microstrip antennas. So, the size of gap-coupled microstrip antennas can be reduced for same frequency applications. The numerical model for computing the resonant frequency of shorting post loaded two gap-coupled circular microstrip antennas has been presented. The cavity model is used and the resonant frequency of the shorting post loaded gap-coupled circular patches is computed. The computed results are compared with simulated results.

One can think that the antenna as equivalent complex impedance, which draws exactly the same amount of complex power from the transmission line, which is known as the antenna input impedance. The real part accounts for the radiated power and the power dissipated in the antenna. The reactive part accounts for the reactive power stored in the near-field of the antenna. The theoretical model for analysis of the input impedance of two gap-coupled circular microstrip patch antennas has been developed. The circuit theory approach is used and the input impedance is calculated. The concept of coupled microstrip lines is applied to the coupled circular microstrip antennas. The theoretical results are compared with reported literature of coupled microstrip lines. The frequency

characteristics of the input impedance of the two gap-coupled circular microstrip patch antenna with gap-distance between the feed patch and parasitic patch as well as the feed position in the feed patch has been studied. The theoretical results are compared with the simulated results. The numerical model for calculating the input impedance of two gap-coupled circular microstrip path antennas loaded with shorting post also has been developed. The variation of input impedance of two gap-coupled circular microstrip antennas loaded with shorting post, with the gap distance between adjacent edges of the patch as well as with the diameter of the shorting post has been studied.

For the analysis of gap-coupled microstrip antennas/antenna arrays, consideration of mutual coupling is an important parameters. Different antenna parameters like antenna element separation, frequency, substrate thickness, dielectric constant, near field scatters and direction of arrival of the incoming wave are key parameters affecting the mutual coupling resulting in the change of antenna characteristics like gain, beamwidth and input impedance. The numerical model for computation of the mutual impedance between the gap-coupled circular microstrip patch antennas has been developed. The mutual admittance between two circular microstrip patches is analyzed using the concept of cavity model and reaction theorem. Variation of mutual impedance with the gap distance between adjacent edges of fed patch and parasitic patch is shown. As the gap between the adjacent edges increases, the coupling is weaker and vice-versa. The analyzed results are compared with the other reported literature. The numerical computation of mutual coupling between gap-coupled circular microstrip antennas loaded with shorting post has been presented. The cavity model and reaction theorem is used and the mutual admittance is computed. The mutual impedance decreases on increasing the gap distance between adjacent edges of feed and parasitic patch and vice versa. The effect of variation of diameter of the shorting post on mutual impedance is also shown. The mutual impedance decreases on increasing the diameter of the shorting post and vice versa.

An innovative design of a cross patch antenna on a substrate with ground plane partially removed has been presented. The antenna is fed by a microstrip line. The impedance matching is good over the band of interest and pattern is stable over the frequency range. Two antennas with different dimensions are presented. The proposed

antennas can be used for wideband communication applications.

In the present thesis, two gap-coupled circular microstrip patch antennas are designed for dual frequency operation. The numerical model for calculating the resonant frequency has been presented. The concept of coupled microstrip lines is applied to the coupled circular microstrip antennas and the numerical model for calculating the input impedance has been presented. The two gap-coupled circular microstrip patch antenna is loaded with a shorting post and designed for triple frequency applications. Also the size of the designed antenna can be reduced. The numerical model for calculating the resonant frequency of gap-coupled circular microstrip patch antennas loaded with a shorting post is presented. The concept of coupled microstrip lines is applied to the coupled circular microstrip antennas loaded with shorting post and the numerical model for calculating the input impedance has been presented. The reaction theorem and cavity model is used and the theoretical model for calculating the mutual impedance of the two gap-coupled circular microstrip patch antennas loaded and without loading has been presented. A novel cross patch antenna is designed for wideband applications.

TABLE OF CONTENTS

LIST OF FIGURES

LIST OF TABLES

CHAPTER 1

INTRODUCTION

1.1 Introduction

The concept of microstrip radiators was first proposed by Deschamps in 1953 [1] and a patent in 1955. The considerable attention to microstrip antennas was given in 1970s due to the availability of good substrates with low loss tangent and attractive thermal and mechanical properties. The first practical microstrip antennas were developed by Howell [2] and Munson [3]. In microstrip antennas a metallic patch is fabricated on a grounded substrate [4]. Microstrip antennas are suitable for aerospace, missile, aircraft, mobile communication applications etc. [5-7].

In their basic form, microstrip antennas are similar to parallel plate capacitors. Both have parallel plates of metal layer and a sandwiched dielectric substrate between them. But in microstrip antennas, one of these metal plates is infinitely extended to form the ground plane; where as the smaller metal plate is described as radiating patch [5]. Since the size of the patch is often proportional to the wavelength of the propagating signal, this class of antenna is classified as resonant antennas. So far, several shapes of microstrip patches, such as rectangular, circular, triangular, semicircular, sectoral and annular etc, are successfully used as radiating antenna elements employed in various communication and control devices [5].

The most basic type of a microstrip patch antenna consisting of a circular radiating element is shown in Fig. 1.1. When the patch is excited by a feed line, charge is distributed on the underside of the patch and the ground plane. At a particular instant of time the attractive forces between the underside of the patch and the ground plane tend to hold a large amount of charge, and also the repulsive forces push the charges to the edge of the patch, creating a large density of charge at the edges. These are the sources of fringing field. Radiation from microstrip antennas can occur from the fringing fields between the periphery of the patch and the ground plane [5].

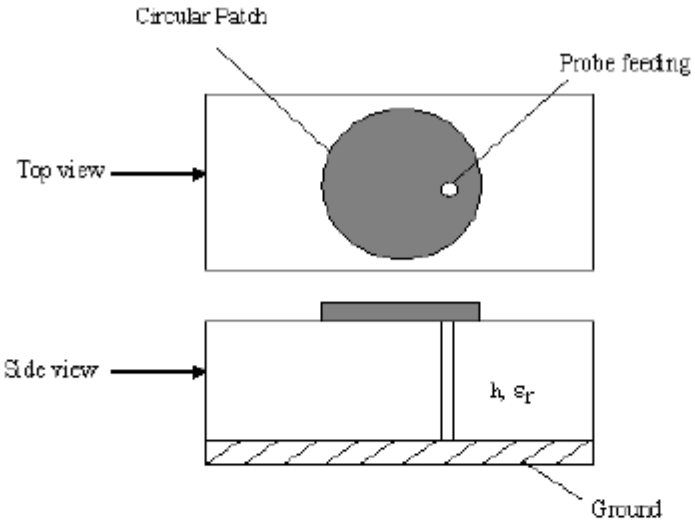

Fig. 1.1 Schematic of circular microstrip patch antenna.

Microstrip antennas have several advantages compared to conventional antennas. Some of the principal advantages of microstrip antennas compared to conventional antennas are light weight, low volume and thin profile configuration, low fabrication cost, conformability to mounting hosts, isotropic radiation characteristics, negligible human body effect, no cavity backing is required, feed lines and matching network can be fabricated [4]. However, microstrip antennas also have some limitations compared to conventional antennas. The major disadvantages are narrow impedance bandwidth, low gain, large ohmic loss in the feed structure of arrays, most microstrip antennas radiate into half-space, complex feed structures required for high performance, spurious radiation from feeds and junctions, and the size of microstrip antennas becomes larger at lower frequencies. Microstrip antennas fabricated on a substrate with a high dielectric constant are strongly preferred for easy integration with MMIC RF front-end circuitry, however, use of high dielectric constant leads to poor efficiency and narrow bandwidth [4].

The bandwidth of the antenna can be increased by using various techniques such as by using a thicker substrate or by loading a patch. The use of thicker substrates causes spurious radiation [4]. Loading can be done by use of various forms like stub loading, slots, shorting posts, parasitic couplings, substrate loading, superstrate cover, resistors,

capacitors, diodes, and by gap coupling patches with slightly different resonant frequencies.

Microstrip antennas can be excited by two methods contacting and non-contacting. In the contacting method, microstrip antennas are directly fed using a connector element such as a microstrip line and/or coaxial probe. They can also be excited indirectly using electromagnetic coupling (proximity) or by the aperture coupling method, in which there is no direct metallic contact between the feed line and the patch. Since the feeding technique influences the input impedance, it is often exploited for matching purposes. Also, as the antenna efficiency depends on the transfer of power to the radiating element, feeding technique plays a vital role in the design process.

Microstrip line feed patch antennas are easy to fabricate because both the feed line and the radiating elements are printed on the same substrate. The impedance matching associated with this class of antennas is also simpler compared to other methods. Although these antennas have low spurious radiation, often the radiation from the feed line increases the cross-polarization level. Also, the thick substrate associated with these antennas (for bandwidth improvement) introduces surface waves that deteriorate the antenna performance. In the millimeter-wave range, the size of the feed line is comparable to the patch size, leading to increased undesired radiation. Typically, the patches are feed from their edge and the edge impedance should be matched with the impedance of the feed line for maximum power transfer. Since the input impedance of the patch gradually decreases from maximum at the edge (150 to 300 Ω) to minimum at the center, insets are often used to connect the feed line to a relatively low impedance spot of the patch.

The coaxial or probe feed arrangement is one in which the center conductor of the coaxial connector is soldered to the patch. The main advantage of this feed is that it can be placed at any desired location inside the patch to match its input impedance; other advantages are that it can be easily fabricated and has low spurious radiation [5]. The main disadvantage of a coaxial feed antenna is the requirement of drilling a hole in the substrate to reach the bottom part of the patch. Other disadvantages include narrow

bandwidth, difficult to theoretically model, and its asymmetrical non planar configuration.

Aperture coupling is a method of indirectly exciting the patch, where the electromagnetic fields are coupled from the microstrip feed line to the radiating patch through an electrically small aperture or slot, cut in the ground plane. The advantage of this feeding technique is that the radiator is shielded from the feed structure by the ground plane. Another important advantage is the freedom of selecting two different substrates; one for the feed line and another for the radiating patch. Since both substrates can be optimized simultaneously, the need for a compromise between radiation and propagation requirements can be avoided. This flexibility in choosing the appropriate substrates also minimizes unwanted surface waves, spurious coupling between antenna elements and thereby increasing the efficiency as well as the bandwidth of the antenna. However, the fabricating process of this class of antenna is difficult and can easily deteriorate the performance due to small errors in the alignment of the different layers. In this study an aperture coupled stacked patch antenna is also designed for beam scanning purposes.

Proximity coupling is another coupling method which does not involve the direct contact of the feed line. But unlike aperture coupling, this method uses electromagnetic coupling between the feed line and the radiating patches, printed on separate substrates [5]. The advantage of this coupling is that it yields the largest bandwidth compared to other coupling methods; it is somewhat easy to model and has low spurious radiation. The disadvantage is that it is more difficult to fabricate.

The flow chart presented in Fig. 1.2 describes the general approach of designing and implementing the microstrip antennas. Firstly, either the designer applies available design techniques for the desired specifications or the designer develops an innovative idea of the design. The approximate size of the microstrip antennas is calculated in the section of preliminary design. With the help of microstrip antenna simulators such as IE3D, CST Microwave Studio, HFSS, ANSOFT etc., the design of an antenna is optimized. The optimized design of the microstrip antenna is fabricated and the measured results are compared with the desired results. If the measured results are in agreement with the

simulated results, the antenna is finally designed. The numerical analysis of the designed antenna is done for further designing.

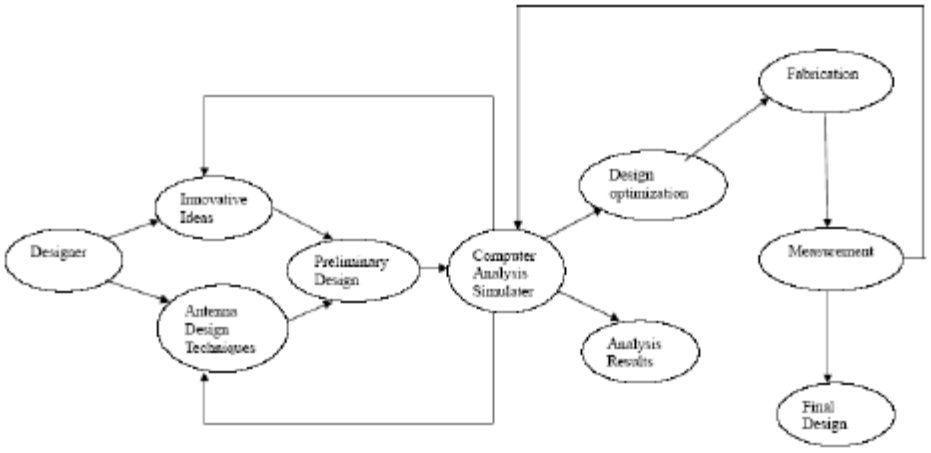

Fig. 1.2 Flow chart of designing microstrip antennas.

An antenna acts as an interface between a guided wave and free space wave. One of the most important characteristics of an antenna is its directional property that is its ability to concentrate radiated power in a certain direction or receive power from a preferred direction. The directional property of an antenna is characterized in terms of a pattern which applies to the antenna as a transmitter or as a receiver. For an efficient interface between the free space wave and the guided wave in the feed transmission line, the input impedance of an antenna must be matched to the characteristic impedance of the transmission line. Thus, the antenna characteristics can be classified into two main categories that is radiation characteristics and input characteristics. Radiation characteristics are used to describe the way the antenna radiates or receives energy to or from space and input characteristics are used to specify the performance of the antenna looking into its terminals. Radiation characteristics include the radiation pattern, gain, directivity, effective aperture and polarization. The input characteristics are specified in terms of the input impedance, bandwidth, reflection coefficient and voltage standing wave ratio.

1.2 Analytical Methods of Microstrip Antennas

The objectives of antenna analyses are to predict the radiation characteristics such as radiation patterns, gain as well as input characteristics such as input impedance, impedance bandwidth, mutual coupling and antenna efficiency. Many techniques have been proposed and used to determine microstrip antenna characteristics [8-9]. The analytical techniques include the transmission line model, generalized transmission line model, cavity model and multiport network model. Numerical methods of analysis include integral equation analysis in the spectral domain, integral equation analysis in the space domain and the finite difference time domain approach.

The transmission line model is the easiest of all but it yields the least accurate results and it lacks the versatility. Rectangular and square patches have a physical shape derived from microstrip transmission lines. Therefore, these antennas can be modeled as sections of transmission lines. Similarly, circular patches, annular tings and sectors of circular patches and annular rings can be modeled in terms of sections of radial transmission lines [8-10]. Therefore, the transmission line model is one of the most intuitively appealing models for a microstrip antenna. The original transmission model was prepared by Munson [3]. Two important shortcomings of the model like the neglection of mutual coupling between the equivalent slots are eliminated by Derneryd [11, 12].

The cavity model is more accurate and more complex than the transmission line model. Microstrip patch antennas are narrowband resonant antennas. They can be termed as lossy cavities. Therefore, the cavity model becomes a natural choice to analyze the patch antennas. A cavity model was advanced by Lo et al [13-15]. In this model, the interior region of the patch is modeled as a cavity bounded by electric walls on the top and bottom, and a magnetic wall all along the periphery. Since thin substrates are used, the field inside the cavity is uniform along the thickness of the substrate.

The multiport network model for analyzing the microstrip antenna is an extension of the cavity model [16]. In this method the electromagnetic fields underneath the patch and outside the patch are modeled separately. The patch is analyzed as a two-dimensional planar network, with a multiple number of probes located around the periphery. The multiport impedance matrix of the patch is obtained from its two-dimensional Green's

function. The fringing fields are incorporated by adding an equivalent edge admittance network. The segmentation method is then used to find the overall impedance matrix.

Full wave models are very versatile and can provide very accurate results. The Method-of-Moments (MoM), the Finite Difference Time Domain (FDTD) method, the Finite Element Method (FEM) all belong to this category, they are suitable for volumetric configurations. The FEM is most popular amongst these methods and in this method the region of interest is divided into any number of finite surfaces or volume elements depending upon the planar or volumetric structures to be analyzed. These discretized units, generally referred to as finite elements, are well defined geometrical shapes, such as triangular elements for planar configurations and tetrahedral and prismatic elements for three dimensional configurations. However, they are most complex models and usually give less physical insight. These methods of analysis are based on the electric current distribution on the patch conductor and the ground plane and give results for any arbitrarily shaped antenna with good accuracy, but they are time-consuming and resource intensive. On the other hand, the models other than numerical models offer both simplicity and physical insight. In the cavity model the analysis problem reduces to that of finding the edge voltage distribution for a given excitation and for a specified mode. For a thin patch, this model offers accurate results suitable for most engineering applications. Hence this model can form the basis of study of the radiation mechanism of circular disk antennas.

Circular disc antennas offer performance similar to that of the rectangular microstrip antennas. The circular disc tends to be slightly smaller than the rectangular disc. In some applications, such as arrays, circular geometries offer certain advantages over the other configurations. The circular disk can be easily modified to produce a range of impedance values, radiation patterns and frequency of operation.

1.3 Analysis of Circular Microstrip Antenna

The circular microstrip disk antenna has been studied extensively [17-31]. Various methods of analysis have been applied to the circular disk antenna, including the cavity model [13, 21], mode matching with edge admittance [22-24], the generalized

transmission line model [8, 9, 25], an integral equation approach [26-28] and FDTD [29]. The cavity model, mode matching with edge admittance and generalized transmission line model are applicable to thin substrate only because the variation of the field along the substrate thickness is assumed to be negligible. For the cavity model, the bases for this assumption are the following observations for thin substrates ($h << \lambda_0$) (r, ϕ and z are the components of cylindrical coordinate system, z is the direction of propagation, and the center of the patch is at origin):

a) The fields in the interior region do not vary with z, i.e. $\frac{\partial}{\partial z} = 0$, because the substrate is very thin.
b) The electric field is z directed only, and the magnetic field has only transverse components in the region bounded by the patch metallization and the ground plane. This observation provides for the electric walls at the top and bottom.
c) The electric current in the patch has no component normal to the edge of the patch metallization, which implies that the tangential components of the magnetic field along the edge is negligible, and a magnetic wall can be placed along the periphery.

Therefore, the electric field within the substrate has only a z component and the magnetic field essentially has only radial and azimuthal components. The component of the current normal to the edge of the microstrip disc approaches zero at the edge. This implies that the tangential component of the magnetic field at the edge of the disc is vanishingly small. With these assumptions, the microstrip disc can be modeled as a cylindrical cavity, bounded at its top and bottom by electric walls and on its edge by a magnetic wall. Thus the fields within the dielectric region of the microstrip cavity, corresponding to TM_{mnp} modes, can be determined by solving the wave equation (Helmholtz equation) for a cavity.

$(\nabla^2 + k^2)E = 0$, where $k = 2\pi / \lambda_o$

After application of boundary conditions, the fields are derived. For each mode configuration, a radius can be found that results in a resonance corresponding to the zeroes of the derivative of the Bessel function.

1.4 Bandwidth Enhancement Techniques of Microstrip Antennas

As discussed previously, narrow bandwidth is a major disadvantage of microstrip antennas in practical applications. Many bandwidth-enhancement or broadband techniques for microstrip antennas have been reported. One bandwidth enhancement technique uses coplanar directly coupled and gap-coupled parasitic patches [30]. Decreasing the quality factor of a microstrip antenna is also an effective way of increasing the antenna's impedance bandwidth. This kind of bandwidth-enhancement technique includes the use of a thick air or foam substrate [31–41] and the loading of a chip resistor on a microstrip antenna with a thin dielectric substrate [42, 43]. Another effective bandwidth-enhancement technique is to excite two or more resonant modes of similar radiating characteristics at adjacent frequencies to form a wide operating bandwidth. Such bandwidth-enhancement techniques include the loading of suitable slots in a radiating patch [44–51] or the integration of cascaded microstrip line sections (microstrip reactive loading) into a radiating patch [52–56].

The bandwidth of microstrip antennas is inversely proportional to their quality factor. By changing the substrate parameters such as dielectric constant and thickness, the quality factor can be varied. By decreasing the dielectric constant the bandwidth of the microstrip antennas can be increased [57]. The quality factor of a resonator is defined as the ratio of energy stored to the power radiated. On decreasing the dielectric constant energy stored decreases and the power radiated increases, so the quality factor decreases, hence the bandwidth increases. Similarly, on increasing the thickness of the substrate the stored energy decreases, hence quality factor decreases and bandwidth of the antenna increases [57]. But there are many disadvantages of increasing the thickness of the substrate and of using lower dielectric constants, such as increasing surface wave power resulting poor radiation efficiency. Thicker substrates with microstrip edge feed will give rise to increased spurious radiation from the microstrip step in width and other discontinuities etc.

The effect of stacking of patches was first studied in 1978 [58]. In this technique an another patch is placed above the main patch separated by the dielectric substrate matarials. The stacked patch configuration has been analyzed using the integral equation

approach [59], the lossy transmission line model [60] and the cavity model [61]. Impedance bandwidths of 10% to 29% have been achieved with probe feed stacked patches [62-64] and 18% to 67 % for aperture coupled stacked patches [59, 65-67].

Another configuration, by which the bandwidth of microstrip antennas can be improved, is the gap-coupled structure. In this structure, a parasitic patch is placed close to the feed patch and gets excited through the coupling between the patches. If the resonant frequencies f_1 and f_2 of these two patches are close to each other, then broad bandwidth is obtained as shown in Fig. 1.3. The overall input VSWR will be the superposition of the responses of the two resonators resulting in a wide bandwidth [68]. By adjusting the feed location and various dimension parameters of the gap-coupled microstrip antennas, the bandwidth can be enhanced. If the dimensions of the feed patch and parasitic patch are same, due to coupling the coupled structure creates two different resonant frequencies.

The basic configuration of two dipoles gap-coupled to a radiating patch was reported in 1979 [69]. When two patches were gap-coupled to the main patch along the radiating edges, a maximum bandwidth up to 5.1 times that of a single rectangular patch antenna was obtained [70]. This type of parasitic coupling along the nonradiating edges yielded 4 times the bandwidth [71]. A similar configuration consisting of short circuited quarter wave patches coupled to a half wave patch along the radiating edges yielded 5.35 times the bandwidth [72]. In another example, two quarter long short circuited patches with coupling along the radiating edge were studied. The bandwidth was found to be about 2.4 times [72].

In [73], two gap coupled rectangular patch antennas are used. In this paper a rectangular patch is excited and coupled with a parasitic element. The theoretical analysis is performed and the bandwidth of the antenna is improved up to eight times than the single rectangular patch antenna. In [74], two semicircular gap-coupled microstrip antennas and two triangular gap coupled microstrip antennas are discussed. In this literature [74], the analysis is carried out using the multiport network model. Semicircular and triangular gap coupled microstrip antennas yield bandwidth which is more than twice the bandwidth of the corresponding circular and equilateral patches, respectively.

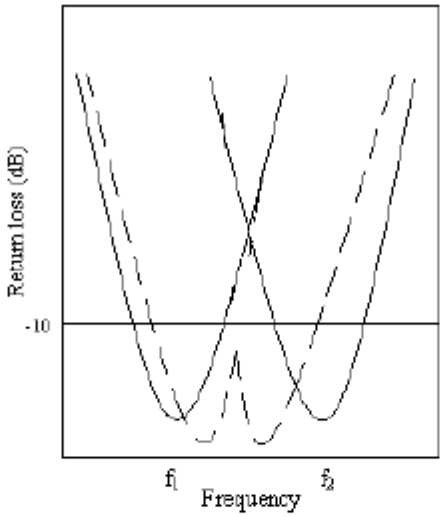

Fig 1.3 Return loss plot, dotted line for coupled resonators, and continuous line for individual resonators.

In [70], three rectangular gap-coupled microstrip antennas are used. A two-dimensional approach using the impedance Green's function and segmentation method has been used for analysis. The obtained bandwidth of the antenna is five times that of a single rectangular patch antenna. In [75] the structure used in [70] is modified. In this literature [75] various stacked combinations of multiple rectangular patches on thick air dielectric substrate are presented. In all configurations only one rectangular patch at the bottom layer is fed with a co-axial line and other patches are parasitically coupled. A parametric study has been carried out using method-of-moment based IE3D software. The configuration with three rectangular patches stacked on a single feed patch yielded a bandwidth of 830 MHz (25.7%) with more than 10 dB gain within the bandwidth. Higher gain is achieved when three patches are stacked on the three gap-coupled rectangular patches.

In [76], a compact broadband antenna is designed and fabricated using a gap-coupled microstrip antenna with photonic band gap. The gap-coupled microstrip antenna consists of a number of parasitic elements which are gap-coupled to driven patch. The measured

center frequency of the gap-coupled patch antenna and conventional patch antenna is 2.568 GHz and 2.483 GHz respectively. The impedance bandwidth has been observed four times greater than conventional microstrip patch antenna at VSWR 2:1. A photonic band gap has been applied to suppress surface waves propagating on the substrate which improves the radiation pattern and bandwidth.

In [77], a different type of triangular gap-coupled microstrip antenna is presented. In this configuration two triangular patches are kept in such a way that a rectangular structure is formed. A parametric study is carried out using MoM based software. This configuration yields 2.38 times large bandwidth as compared to the equilateral triangular microstrip antenna.

In [68], the configuration presented in [75] is modified for ultra wideband application. The antenna has three rectangular patches at the bottom and two patches on the top layers exciting the bottom patch by a coaxial feed. Only the bottom patch is fed and the other patches are electromagnetically coupled. The bandwidth obtained for the antenna is 3.25 GHz. The radiation is in the broad side direction, and the variation in the pattern is very small over the entire bandwidth. At 4.3 GHz the gain is 7.5 dB. The bandwidth and return loss are proper for ultra wideband applications.

In [78], experimental investigations on three hybrid coupled circular microstrip antennas are reported. In this the coupling between the patches is increased by shorting the patches to obtain dual, triple and wideband responses. This makes this configuration more suitable for wideband applications as compared to the gap coupled rectangular patches.

1.5 Miniaturization Techniques of Microstrip Antennas

The trend for technology in recent times is towards miniaturization and the demand for more compact and robust designs has been growing. The revolution in semiconductor manufacturing and device design methodologies has helped to achieve very high data rates transmission and compact size. In wireless devices, the antenna still remains a matter of concern as regards to its size. In some applications, operation at two or more discrete bands and an arbitrary separation of bands is desired. Further all bands may be

required to have the same polarization, radiation pattern and input impedance characteristics. There are various techniques for reducing the size of the microstrip antennas.

By loading the patch, the size of microstrip patch antennas can be decreased. The range of applications of microstrip antennas and their performance can be improved considerably by suitable loading them. Loading can take various forms such as stub loading, slots, shorting posts, parasitic couplings, substrate loading, superstrate cover, resistors, capacitors and diodes.

Fixed or variable capacitors can be used to change the resonant frequency of a microstrip antenna. Capacitive loading lowers the resonance frequency. The use of a varactor diode to obtain the frequency agile microstrip antennas was first reported in 1982 by Bhartia and Bahl [79]. In this article, two varactor diodes are embedded in the patch. A frequency tuning range of about 30% was achieved depending upon the diode characteristics and the position of the diode in the patch. The junction capacitance of the diode, which is parallel to the equivalent circuit of the patch, is used to tune out tank circuit inductance and therefore the resonant frequency of the microstrip antenna can be changed. As the reverse bias voltage of the diode is increased, the junction capacitance decreases and the resonant frequency of the loaded microstrip antenna increases, until it equals that of the unloaded microstrip antenna. The efficiency of the varactor diode loaded microstrip antenna becomes a function of the reverse bias voltage, because of the power dissipated in the diodes [80]. The efficiency varies from 95% at high reverse bias to about 30% at low bias. The varactor diode loaded microstrip antenna can be designed to operate at two vastly different frequencies [81].

Circular polarization is a requirement for satellite communications and compactness is a desirable feature for mobile or airborne applications. Compact circularly polarized antennas can be realized by starting with the circularly polarized configurations and loading them with shorts and/or slots. A circular disk loaded with four slots has been developed by Bokhari et al. [82] for circular polarization. The measured resonant frequency for the antenna is about 0.8 times the resonant frequency of the unloaded disk. A simple mechanical tuning mechanism for the axial ratio is also discussed. A square

ring antenna is designed for orthogonal polarizations, like a square patch, in [83]. The size of this antenna is smaller because the average circumference of the antenna equals one wavelength. This square ring antenna [83] is loaded with a narrow slit in one of the arms in [84]. The center frequency of the antenna is 2180 MHz with the 3 dB axial ratio bandwidth of 21 MHz. In [85], the square microstrip antenna is loaded with two pairs of slits to reduce the size of the antenna. The resonant frequency is decreased from 2318 MHz to 1849 MHz (i.e. 20 % reduction) and the size of the antenna is reduced by 36%. A similar antenna with a superstrate loading is described in [86]. In [87], the rectangular patch is loaded with four symmetric shorts. This antenna resonates at two resonances near 2.5 GHz. In [88], a circular microstrip antenna is loaded with a cross slot of unequal slot lengths. The slots cross each other orthogonally at the center of the circular disk. The degenerate modes of the circular disk experience unequal loading due to unequal slot lengths. The resonant frequency of the antenna decreases monotonically with increasing the slot length. Therefore, the resonant frequency can be controlled by changing the slot length. The size of the antenna was reduced by about 36% compared to the circular microstrip antenna without slots. In [89], an equilateral triangular microstrip antenna is loaded with a cross slot. This loaded triangular antenna supports two degenerate modes.

In many applications, operation in more than one discrete band with an arbitrary separation of band is desired. In such cases, a microstrip antenna capable of operating in multiple bands is highly desirable. This may be done using shorting pin and slots combined [90], only slots [91], step slots [92] etc. A dual-frequency, dual-linearly polarized microstrip antenna is an increasingly important requirement. Such an antenna can be made using a rectangular patch with inclined slot in the ground plane for impedance matching [93]. An unslotted circular patch with two input ports, for dual-frequency or dual-polarization operation, has been reported by Murakami et al [94]. The slot dimensions are selected for maximum isolation between the two modes of operation. Pozar [95] has used stacked square patches to obtain dual-frequency operation. Circular polarization is achieved by aperture coupling of the lower patch by a crossed slot. Loading by cross slots has been used to obtain dual-frequency dual-polarization operation of a rectangular patch [96]. The antenna size reduction at the lowest frequency is about

40% and the cross-polar performance is better than that of pin loaded antennas. A similar antenna with probe feed has also been studied in [97]. In another report, a square slot has been cut at the center of the rectangular patch [98]. The ring antenna has lower resonant frequencies because the surface currents have to travel along the slot perimeter to reach the other end, which is a longer distance. The first two modes of the ring are excited by feeding along the diagonal of the ring. Another variation of the ring antenna is obtained when the central square slot is rotated by 45° [99]. This antenna can accommodate a larger slot size therefore larger reduction in size. The radiation pattern remains same with the rotation of slot. In [100], by etching the microstrip patch as the Sierpinski carpet, the size of the microstrip antenna is reduced up to a maximum of 33.9%.

High dielectric permittivity will also maintain the compactness of the structure whereas low dielectric permittivity will provide more efficient result. The bandwidth of microstrip patch antennas can also be increased by increasing the thickness of the substrate material [101, 102]. The major disadvantage of increasing thickness is the reduced efficiency since the large portion of the input power is dissipated in the resistor which takes away the available power that can be radiated by antenna. Further more, reducing the height of the structure may appear to be a suitable solution, but it may lead to a reduced impedance bandwidth and lower radiation efficiency. This is often a tradeoff in realizing compact antennas while maintaining performance characteristics. A high permittivity substrate is a poor choice for widening the antenna bandwidth, since the bandwidth of a microstrip antenna is best for low dielectric constant substrates and if substrate thickness is increased in an attempt to improve bandwidth, spurious feed radiation increases and surface wave power increases. As a patch antenna radiates, a portion of the total available power for direct radiation becomes trapped along the surface of the substrate. This trapped electromagnetic energy leads to the development of surface waves. In fact, the ratio of the power that radiates into the substrate compared to the power that radiates into air is approximately ($\varepsilon^{3/2}$: 1). The power launched into surface waves is power which will eventually be lost, hence the excitation of surface waves lowers the overall radiation efficiency of the antenna. The surface waves are spread out in a cylindrical fashion around the excitation point with field amplitudes decreasing with

distance. They are incident on the ground plane, get reflected from there and then meet the dielectric-air interface, which also reflects them. Following this zigzag path, they finally reach the boundaries of the microstrip structure where they are reflected back and diffracted by edges giving rise to end-fire radiation. For microstrip patch antennas, reduction in thickness of substrate, in general, will lower the efficiency and bandwidth [103].

By loading of a microstrip antenna with a shorting post, the size of the microstrip antenna can be reduced as well as multi-frequency operation, change of polarization etc can be achieved. Depending on the application, the shorting pin may be located at the edge or at the center of the patch. The analysis of the post loaded microstrip antenna has been carried out using the transmission line model [104, 105], cavity model [106, 107], multiport network model [108], integral equation approach [109] and FDTD technique [110, 111]. In [112], rectangular and circular microstrip antennas are loaded with shorting pin/post. The antenna is fed by probe feeding. Two resonant frequencies are observed for loaded rectangular microstrip antennas. The computed values are 461.5 MHz and 1.701 GHz and the measured values are 462 MHz and 1.677 GHz [108], when the antenna is loaded at the mid point of the edge. When the shorting post is moved to the corner of the patch, the computed resonant frequency changed to 369.5 MHz and 1.708 GHz. The measured frequencies are 381 MHz and 1.717 GHz [110]. The decrease in the resonant frequency for the lower resonance is about 20 %. The variation of the lower resonant frequency with the location of shorting post is also shown. The resonant frequency decreases as the shorting post moves from center to the corner, i.e. the maximum size reduction is achieved in this position of short. In [113], the rectangular microstrip antenna is loaded with a shorting post at the center line of the patch. This type of loading produces two lowest resonant frequencies with the same polarization. The size reduction of the antenna at the lowest frequency is roughly 2.6. In a recent work [114], an analytical theory for the eigenfrequencies and eigenmodes of shorting post loaded microstrip antennas is presented. It is shown that the zero mode of the unloaded microstrip antenna plays a central role for reducing the lowest operating frequency of the loaded microstrip antenna. For a circular patch loaded with single post, it was shown that

a larger shorting post radii lead to stronger suppression of the inductive part of the shorting-post impedance and, therefore, resonates at higher resonant frequencies. The lowest values for the resonant frequency are obtained when positioning the shorting post at the edge of the patch. In general, the resonant frequencies obtainable from a loaded circular patch are larger than those of a rectangular patch of equal cross section. It is also seen that the sensitivity of the resonance frequency against variations of the shorting-post position of the circular patch is stronger than in the rectangular patch.

A dual frequency compact antenna capable of receiving both linearly and circularly polarized radiation has been reported in [115]. It generates linear polarization at the lower frequency and circular polarization at the upper frequency. It consists of a square patch with two symmetrical shorting pins. A reduction factor of 5 in area has been achieved at the lower frequency end. In [116], the shorting post is used in rectangular microstrip antennas to generate the triple frequency operations.

1.6 Organization of Thesis

The organization of the present thesis is as follows: In chapter 2, an expression for the resonant frequency of two gap-coupled circular microstrip patch antennas is derived by using the concept of cavity model and circuit theory. The overall structure is divided into two regions and fields in each region are evaluated from the solution of the appropriate Helmholtz equation for TM modes. Evaluation of the constants using the boundary conditions leads to a transcendental equation and the resonant frequencies for different modes are determined from the solution of the transcendental equation. In the proposed model, the equivalent circuit for the gap distance has been utilized. However, to compensate for the edge effects, an empirically generated correction factor has also been incorporated. It is shown that such a combination leads to a very accurate model of the gap-coupled circular microstrip antenna and it leads to dual frequency operation with closely spaced resonances. The computed results are compared with the simulated as well as previously reported literatures. The simulation is performed by using the MoM based commercially available simulator IE3D.

In chapter 3, an expression for the resonant frequency of two gap-coupled circular microstrip patch antennas loaded with shorting post is derived by using the similar approach as in chapter 2. It is shown that such combination leads to a very accurate model of the two gap-coupled circular microstrip antenna loaded with shorting post. The variation of resonant frequency with the gap distance between adjacent edges as well as with the diameter of the shorting post is also analyzed.

In chapter 4, the theoretical analysis of the input impedance of two gap-coupled circular microstrip patch antennas has been carried out using circuit theory approach. The concept of coupled microstrip lines is applied to the gap-coupled circular microstrip antennas and the input impedance is calculated. The frequency characteristics of the input impedance of the gap-coupled circular microstrip patch antenna with the gap distance between the feed patch and parasitic patch as well as the feed position in the feed patch has been studied. The theoretical results are compared with the simulated results as well as other reported literature.

In chapter 5, the theoretical analysis of the input impedance of two gap-coupled circular microstrip patch antennas loaded with shorting post has been carried out using circuit theory approach as in chapter 4. The frequency characteristics of the input impedance of the gap-coupled circular microstrip patch antenna with gap-distance between the feed patch and parasitic patch as well as the diameter of shorting post has been studied.

In chapter 6, the numerical computation of the mutual coupling between two gap-coupled circular microstrip patch antennas has been presented. The mutual admittance is computed by using the cavity model and reaction theorem for two circular patches and the computed results are compared with the reported literature. The mutual admittance of the two gap-coupled circular microstrip antenna loaded with shorting post is analyzed. The analyzed results are compared with the simulated results.

In chapter 7, an innovative design of the cross patch antenna on the substrate with ground plane partially removed is presented. The antenna is fed by a microstrip line and yields an omnidirectional pattern. Two antennas with different dimensions are presented. Optimization of design leads to a bandwidth of 28% with sufficient directivity. The

proposed antennas can be used for wideband communication applications. Finally, chapter 8 concludes the thesis and explores its future scope.

CHAPTER 2

NUMERICAL COMPUTATION OF RESONANT FREQUENCY OF GAP-COUPLED CIRCULAR MICROSTRIP ANTENNAS

2.1 Introduction

As discussed in the previous chapter, one of the major disadvantages of microstrip patch antennas is their narrow impedance bandwidth [117] and the gap-coupling is one of the potential methods by which the bandwidth of microstrip antennas can be increased [118, 119]. In many applications, multi-operating frequencies are desired which can be achieved by using the gap-coupling. In gap-coupled microstrip antennas, two patches are placed nearby with some small gap. One patch is fed by any appropriate feeding technique and the other patch, that is the parasitic patch, is excited by gap-coupling. The two gap-coupled microstrip structure generates two close resonances. The frequencies of the two resonances can be adjusted by changing various parameters like the gap distance between adjacent edges of patches, the radius of feed patch and the radius of the parasitic patch and the resulting impedance bandwidth can be enhanced. As shown in Fig. 1.3, the overall bandwidth of the gap-coupled microstrip structures can be enhanced as compared to individual patches. The gap-coupled microstrip structures can be used for dual frequency operation and by adjusting different parameters the desired two resonant frequencies can be obtained.

In this chapter, a numerical model for computing the resonant frequency of the two gap-coupled circular microstrip antenna is presented. A similar structure has been reported in [78], but the reported literature has been presented only on experimental results. In [78] gap-coupled circular patches with different radii in a small gap distance are fabricated. For increasing the coupling the circular patches are shorted.

2.2 Antenna configuration

The geometrical configuration of a two gap-coupled circular microstrip antenna is shown in Fig. 2.1. The patch of radius $r_1 = 15\,\text{mm}$ is the feed patch and other patch of radius $r_2 = 15\,\text{mm}$ is the parasitic patch. The parasitic patch is excited by the gap-coupling whereas the feed patch is excited by the probe feeding technique. The parasitic patch introduces another resonance near the main resonance and by proper adjustment of the structure parameters, the bandwidth can be enhanced. The height and relative permittivity of the substrate is $h = 1.59\,\text{mm}$ and $\varepsilon_r = 2.2$, respectively. The gap distance between the adjacent edges of the feed patch and parasitic patch is s. The thickness of the patches is neglected.

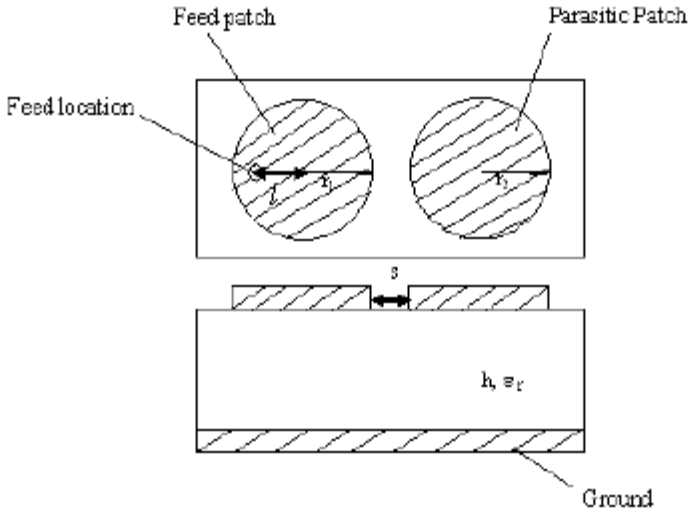

Fig. 2.1 Geometrical configuration of the two gap-coupled circular microstrip patch antennas.

2.3 Analysis

The analytical configuration of the proposed gap coupled circular patch microstrip antenna is shown in Fig. 2.2. The central patch of radius 'r_1' is the feed and a parasitic patch of same radius is placed around the central patch as shown in Fig. 2.2.

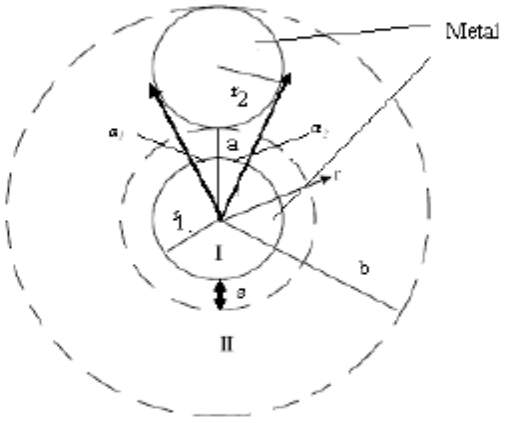

Fig. 2.2 Analytical configuration of the two gap-coupled circular microstrip patch antennas (without feeding system).

We consider two concentric regions region I and region II as shown in Fig. 2.2. The radius of region I is 'r_1'. The inner radius of region II is 'a' and the outer radius is 'b'. The separation between region I and region II is denoted by 's'. We now consider the field expressions for a given TM_{np} mode in these two regions [120].

In region I ($0 \le r \le r_1$), the wave equation for the electric field between patch and ground plane can be written as:

$$\left(\nabla^2 + k^2\right)\vec{E} = 0 \tag{2.1}$$

where $k = \dfrac{2\pi\sqrt{\varepsilon_r}}{\lambda_0}$

The above wave equation can be written in the cylindrical co-ordinate system as

$$\frac{1}{r}\frac{\partial}{\partial r}\left(r\frac{\partial E}{\partial r}\right) + \frac{1}{r^2}\frac{\partial^2 E}{\partial \phi^2} + k^2 E = 0 \tag{2.2}$$

The electric field in the cavity must satisfy the above wave equation and the magnetic wall boundary condition. The solution of the above equation in cylindrical coordinates is

$$E_z^1 = -j\omega\mu C_1 J_n(kr)\cos n\phi \tag{2.3}$$

where E_z^1 is the axial electric field for region I, ω and k are the angular frequency and propagation constant for the TM_{np} mode, respectively. $J_n(x)$ is the Bessel function of first kind of order n and C_1 is the amplitude constants for region I.

The azimuthal magnetic field for region I can be calculated as [120]:

$$H_\phi^1 = -\frac{j}{\omega\mu}\frac{\partial E_z}{\partial r} \tag{2.4}$$

$$H_\phi^1 = -kC_1 J_n'(kr)\cos n\phi \tag{2.5}$$

where $J_n'(x)$ is the first derivative of $J_n(x)$ with respect to x.

The radial magnetic field component H_r^1 can be calculated as:

$$H_r^1 = \frac{j}{\omega\mu\rho}\frac{\partial E_z}{\partial \phi} \tag{2.6}$$

$$H_r^1 = -\left(\frac{n}{r}\right)C_1 J_n(kr)\sin n\phi \tag{2.7}$$

In region II ($a \le r \le b$), the solution of the equation (2.2) in cylindrical coordinates is

$$E_z^2 = -j\omega\mu[C_2 J_n(kr) + C_3 N_n(kr)]\cos n\phi \tag{2.8}$$

Using equation (2.4) the expression for H_ϕ^2 can be written as

$$H_\phi^2 = -k[C_2 J_n'(kr) + C_3 N_n'(kr)]\cos n\phi \tag{2.9}$$

Using equation (2.6) the expression for H_r^2 can be written as

$$H_r^2 = -\left(\frac{n}{r}\right)[C_2 J_n'(kr) + C_3 N_n'(kr)]\sin n\phi \tag{2.10}$$

where $N_n(x)$ is the Bessel function of second kind of order n, and $N_n'(x)$ is the first derivative of $N_n(x)$ with respect to x. C_2 and C_3 are the amplitude constants for the region II.

Considering the parasitic patch in isolation the boundary condition of vanishing H_ϕ^2 can be applied as:

$$H_\phi^2 = 0 \qquad \text{for} \qquad a \le r \le b \quad \text{and} \quad \alpha_1 \le \phi \le \alpha_2 \tag{2.11}$$

Thus

$$\frac{C_3}{C_2} = -\frac{\int_a^b J_n'(kr)rdr}{\int_a^b N_n'(kr)rdr} = \frac{I_2}{I_1} \tag{2.12}$$

Therefore, the field expression in region II can be rewritten as:

$$E_z^2 = -j\omega\mu C_n^2 F_n^2(kr)\cos n\phi \tag{2.13}$$

$$H_\phi^2 = -kC_n^2 F_n^{2\prime}(kr)\cos n\phi \tag{2.14}$$

where C_n^2 is a constant dependant on the given mode 'n' and

$$F_n^2(kr) = J_n(kr)I_1 - I_2 N_n(kr) \tag{2.15}$$

Similarly, the field expression for the region I is:

$$E_z^1 = -j\omega\mu C_n^1 F_n^1(kr)\cos n\phi \tag{2.16}$$

$$H_\phi^1 = -kC_n^1 F_n^{1\prime}(kr)\cos n\phi \tag{2.17}$$

where C_n^1 is a constant and

$$F_n^1(kr) = J_n(kr) \tag{2.18}$$

If we consider the central patch to be isolated, then its resonant frequency is obtained using the following equation

$$J_n'(ka_e) = 0 \tag{2.19}$$

where a_e is the effective radius of the feed circular patch. We now consider the gap between the two regions at the point of coupling between the two patches as a π-type network [121]. It is shown in Fig. 2.3.

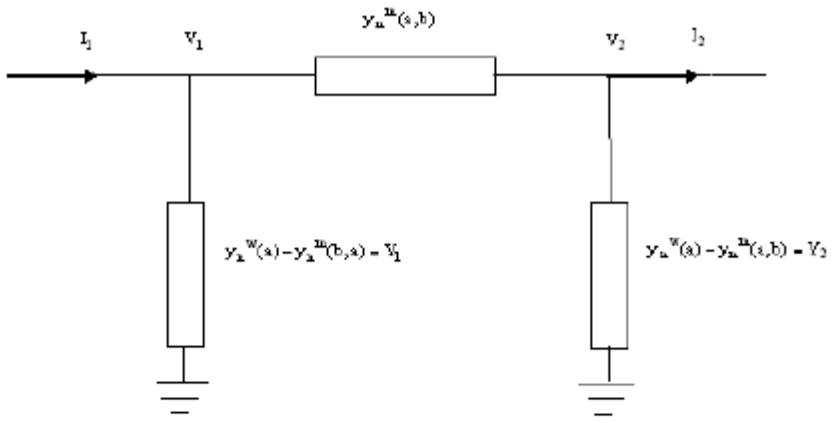

Fig. 2.3 Equivalent circuit diagram of the gap-coupled microstrip antenna.

In Fig. 2.3, $y_n^W(a/b)$ are the wall admittances of individual patches and $y_n^m(a,b)$ is the mutual admittance between the two patches.

Here, $y_n^m = \frac{1}{j\omega M}$

where M denotes magnetic coupling and is given by

$$M = \int_0^{hh}\int_0^{\mu_0 q}\frac{}{4\pi\times s} dl_1 dl_2$$

where h is the substrate height and q is a correction factor. The expression for magnetic coupling is derived for infinitely thin cylindrical lines. However, to take account for substantial area of each cylinder the empirical correction factor q is utilized. This varies from 3 for tight coupling to 0.1 for loose coupling. From the condition of discontinuity of current in these two regions we can write:

$$r_1 H_\phi^1(r_1) - aH_\phi^2(a) = E_z^1(r_1)Y_1 - E_z^2(a)Y_2 \qquad (2.20)$$

using this expression, we obtain

$$\frac{C_n^2}{C_n^1}=\frac{r_1F_n^1{}'(kr_1)+\frac{j\omega\mu}{k}F_n^1(kr_1)Y_1}{aF_n^2{}'(ka)-\frac{j\omega\mu}{k}F_n^2(ka)Y_2} \tag{2.21}$$

The small gap normal component of the electric field is continuous at c, where $c=\frac{b+a}{2}$

Therefore $E_Z^1(r)=E_Z^2(r)$ at $r=c$

From this

$$\frac{C_n^2}{C_n^1}=\frac{F_n^1(kc)}{F_n^2(kc)} \tag{2.22}$$

Equating expression (2.21) and (2.22) we get

$$\frac{F_n^1(kc)}{F_n^2(kc)}-\frac{r_1F_n^1{}'(kr_1)+\frac{j\omega\mu}{k}F_n^1(kr_1)Y_1}{aF_n^2{}'(ka)-\frac{j\omega\mu}{k}F_n^2(ka)Y_2}=0 \tag{2.23}$$

The above transcendental equation for gap-coupled circular microstrip patch antennas gives the resonant frequency of a given TM_{np} mode.

2.4 Results and Discussion

Ray and Kumar [78] have demonstrated a schematic of a central patch of diameter 31 mm gap-coupled to two circular patches of diameter 30 mm and 32 mm, respectively. The patches are etched on a substrate of $\varepsilon_r = 4.3$ and height $h = 1.59$ mm. Using experiments, the authors have demonstrated that impedance loops are being formed at the frequencies 2.42 GHz and 2.58 GHz. Table 2.1 compares the results with the present approach. The percentage of error shown by the present approach is within ± 3.48%. For further validation of the proposed model the results for two gap-coupled patches as shown in Fig. 2.1, are compared with the MoM based software IE3D from M/S Zeland Software in table 2.2.

Table 2.1: Comparison of the resonant frequency of the two gap-coupled circular microstrip patch antenna between experiment [78] and proposed approach, (gap distance s = 1.0 mm, ε_r = 4.3, h = 1.59 mm).

Experiment [78]		Present approach			
f_1	f_2	f_1	n	f_2	n
2.42 GHz	2.58 GHz	2.48 GHz	1	2.67 GHz	2

Table 2.2: Comparison of the resonant frequency of the two gap coupled circular microstrip patch antennas between simulated and proposed approach (radius = 15 mm (both), gap distance s = 0.5 mm, ε_r = 2.2, h = 1.59 mm).

Mode number	Simulated	Computed
n=1	3.68 GHz	3.66 GHz
n=2	3.76 GHz	3.80 GHz

Further, the resonant frequency for given 'n' is computed for different gap sizes. A comparison with the simulation is also made in table 2.3. The agreement is excellent.

To validate the presentation of mode numbers the simulated current density on the patches are presented in Fig. 2.4 and in Fig. 2.5. It is seen that the mode numbers are predicted accurately. In this case, the colour of current density towards 'Red' is higher and towards 'Blue' is lower. The current density of 'Yellow' is in between 'Red' and 'Blue'. The right hand side patch is the feed patch of circular cross-section. In Fig. 2.4 it is seen that on the feed patch a small yellow region and a blue region exists. This accounts for the TM_{11} mode. The two blue regions in Fig. 2.5 convey the existence of the TM_{21} mode. From the current distribution data it is also observed that the parasitic patch is excited when the resonant frequency of the combined structure is close to its self resonance which is 3.7 GHz for the TM_{11} mode.

Table 2.3 Variation of the resonant frequency of TM_{np} modes of the two gap-coupled circular microstrip antennas with the gap distance between adjacent edges of feed patch and parasitic patch.

Gap distance between the adjacent edges of feed and parasitic patch (s) (mm)	n=1 Resonant frequency (GHz)		n=2 Resonant frequency (GHz)	
	computed	simulated	computed	simulated
0.2	3.70	3.70	3.9	-
0.5	3.66	3.68	3.8	3.76
0.75	3.63	3.65	3.78	3.75
1.0	3.6	3.64	3.76	3.74
1.5	3.67	3.63	3.74	3.74
2.0	3.63	3.58	3.72	3.73

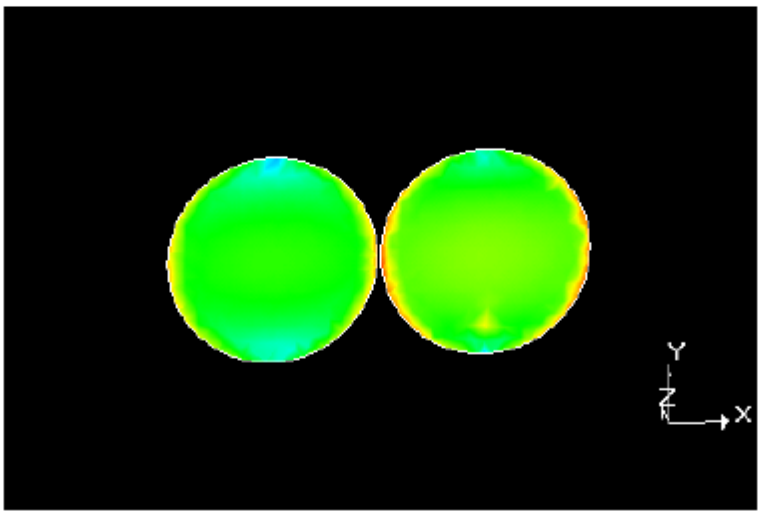

Fig. 2.4 Simulated current density distribution of the two gap-coupled circular microstrip patch antenna at 3.66 GHz.

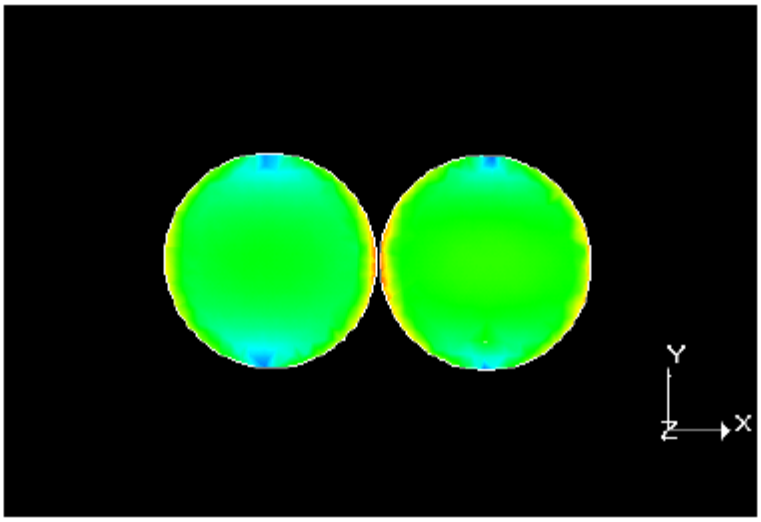

Fig. 2.4 Simulated current density distribution of the two gap-coupled circular microstrip patch antenna at 3.77 GHz.

2.5 Conclusion

A numerical model for gap-coupled circular microstrip patches has been developed. The comparison between the computation and simulated results as well reported literature shows good agreement for the resonant frequency. Since the cavity model analysis is used in conjunction with circuit theory, the mode number prediction is also done. The same is validated through obtaining the current distribution for full-wave solutions. The proposed model can be extended to multiple resonators as well as the analysis with different patch sizes.

CHAPTER 3

COMPUTATION OF RESONANT FREQUENCY OF SHORTING POST LOADED GAP-COUPLED CIRCULAR MICROSTRIP ANTENNAS

3.1 Introduction

Microstrip patch antennas are resonant antennas with many favorable characteristics, such as low cost, light weight and low profile [122-125]. The main limitation is the narrow impedance bandwidth, which is known to be approximately proportional to the volume of the antenna measured in wavelength. Thus the impedance bandwidth of a basic patch antenna can be optimized by selecting a low permittivity substrate, which maximizes the resonant length of the patch, and by maximizing the patch width and the substrate thickness. However, many applications, such as inside portable radio devices, the space allowed for the antenna is limited, which restricts the antenna size. Furthermore, the size may be limited by feeding technique, radiation pattern and efficiency related constraints [16]. Besides increasing the size, the bandwidth of microstrip antennas can be increased by artificially decreasing its efficiency. In many cases, it is, however, unacceptable. Although, as pointed out in [16], the manufacturing simplicity of this technique has a definite appeal. In some applications, it can outweigh the disadvantage of decreased gain. One of the methods of miniaturization of microstrip antennas is loading the microstrip patch with a shorting post [116, 126-129]. Microstrip antennas loaded with a shorting post can also be used for multiple frequency operation [130] and it generates one more mode as compared to microstrip antennas without shorting post. It is shown in literature that a circular microstrip antenna loaded with shorting post has two modes that is TM_{01} and TM_{11} [131, 132].

In this chapter, the two gap-coupled circular microstrip antennas loaded with a shorting post is analyzed. It generates three modes that is the TM_{01}, TM_{11} and TM_{21}

modes. The numerical computation of the resonant frequency of the shorting post loaded gap-coupled microstrip antenna is analyzed and the results are compared with that of simulations. The simulation work is carried out by using the commercially available simulator IE3D based on MoM.

3.2 Antenna Geometry

The geometrical configuration of two gap-coupled circular microstrip antennas loaded with a shorting post is shown in Fig. 3.1. The patch of radius r_1 = 15 mm is the feed patch and the other patch of radius r_2 = 15 mm is the parasitic patch. The parasitic patch is excited by the gap-coupling whereas the feed patch is excited by the coaxial probe feeding technique. The feed patch is shorted by a shorting post of diameter p as shown in Fig. 3.1. The height and permittivity of the antenna substrate is h = 1.59 mm and ε_r = 2.2, respectively. The gap distance between the adjacent edges of the patches is s. The thickness of the patches is neglected.

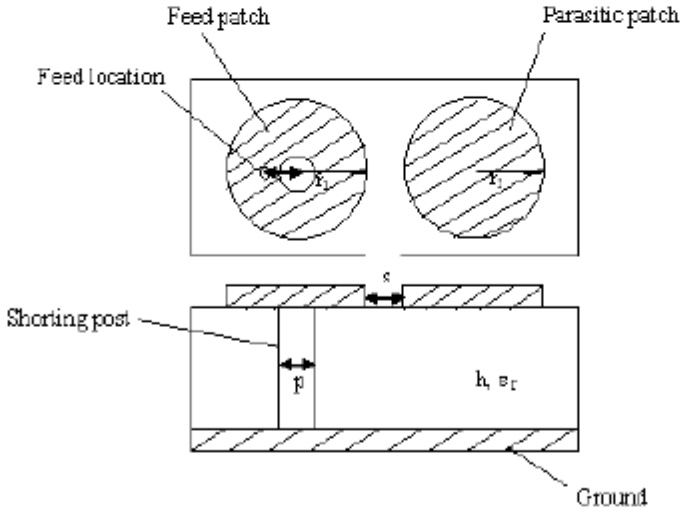

Fig. 3.1 Geometrical configuration of the two gap-coupled circular microstrip antenna loaded with a shorting post.

3.3 Field Expression and Mode Prediction

The analytical configuration of a shorting post loaded gap-coupled circular microstrip antenna is shown in Fig. 3.2. The structure is divided into two concentric regions; region I and region II as shown in Fig. 3.2. The inner radius of region II is 'a' and the outer radius of region II is 'b'. Now we consider the field expressions for a given TM_{np} mode in these two regions. In region I ($0 \le r \le r_1$), we apply the wave equation in cylindrical coordinates that is equation (2.2). The solution of equation (2.2) in region I is:

$$E_z^1 = -j\omega\mu[C_1 J_n(kr) + C_2 N_n(kr)]\cos n\phi \tag{3.1}$$

From equation (2.4),

$$H_\phi^1 = -k[C_1 J_n'(kr) + C_2 N_n'(kr)]\cos n\phi \tag{3.2}$$

From equation (2.6),

$$H_r^1 = -\left(\frac{n}{r}\right)[C_1 J_n(kr) + C_2 N_n(kr)]\sin n\phi \tag{3.3}$$

The terms incorporated in above expressions have their usual meanings. C_1 and C_2 are the amplitude constants for region I.

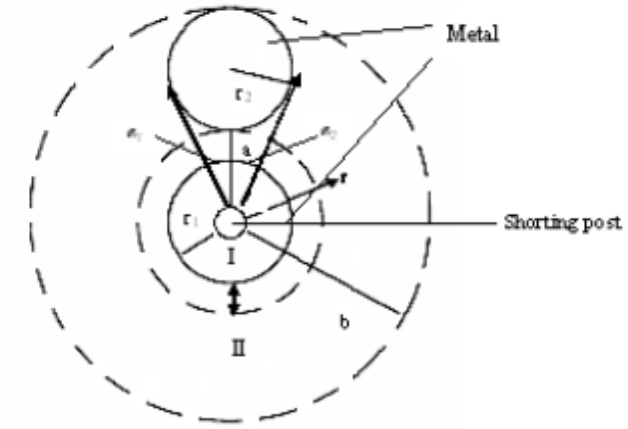

Fig. 3.2 Analytical configuration of the shorting post loaded gap-coupled circular microstrip antennas.

In region II ($a \le r \le b$) , the solution of equation (2.2) is

$$E_z^2 = -j\omega\mu[C_3 J_n(kr) + C_4 N_n(kr)]\cos n\phi \tag{3.4}$$

From equation (2.4),

$$H_\phi^{(2)} = -k[C_3 J_n'(kr) + C_4 N_n'(kr)]\cos n\phi \tag{3.5}$$

From equation (2.6),

$$H_r^2 = -\left(\frac{n}{r}\right)[C_3 J_n'(kr) + C_4 N_n'(kr)]\sin n\phi \tag{3.6}$$

where C_3 and C_4 are the amplitude constants for region II. Considering the parasitic patch in isolation the boundary condition of vanishing H_ϕ^2 can be applied as in equation (2.11).

$$\frac{C_4}{C_3} = -\frac{\int_b^c J_n'(kr)rdr}{\int_b^c N_n'(kr)rdr} = \frac{I_2}{I_1} \tag{3.7}$$

Therefore the field expression in region II can be rewritten as:

$$E_z^2 = -j\omega\mu C_n^2 F_n^2(kr)\cos n\phi \tag{3.8}$$

$$H_\phi^2 = -kC_n^2 F_n^{2\prime}(kr)\cos n\phi \tag{3.9}$$

where C_n^2 is a constant dependant on given mode 'n' and

$$F_n^2(kr) = J_n(kr)I_1 - I_2 N_n(kr) \tag{3.10}$$

Similarly,

$E_z^1 = 0$ for $r = p/2$

$$\frac{C_1}{C_2} = -\frac{N_n(kp/2)}{J_n(kp/2)} = \frac{I_3}{I_4} \tag{3.11}$$

Thus the field expression in region I is:

$$E_z^1 = -j\omega\mu C_n^1 F_n^1(kr)\cos n\phi \tag{3.12}$$

$$H_\phi^1 = -kC_n^1 F_n^{1\prime}(kr)\cos n\phi \tag{3.13}$$

where C_h^1 is a constant and

$$F_n^1(kr) = J_n(kr)I_3 - N_n(kr)I_4 \tag{3.14}$$

Now we consider the gap between the two regions at the point of coupling between the two patches as a π-type network as shown in Fig. 2.2. From the equation of discontinuity of current in these two regions, that is equation (2.20), the following expression can be obtained:

$$\frac{C_n^2}{C_n^1} = \frac{r_1 F_n^{1\prime}(kr_1) + \frac{j\omega\mu}{k} F_n^1(kr_1) Y_1}{aF_n^{2\prime}(ka) - \frac{j\omega\mu}{k} F_n^2(ka) Y_2} \tag{3.15}$$

For small gap distance, the normal component of electric field is continuous at r' where $r' = \frac{b+a}{2}$

Therefore $E_z^1(r) = E_z^2(r)$ at $r = r'$

From this

$$\frac{C_n^2}{C_n^1} = \frac{F_n^1(kr')}{F_n^2(kr')} \tag{3.16}$$

Equating expression (3.14) and (3.15) we get

$$\frac{F_n^1(kr')}{F_n^2(kr')} - \frac{r_1 F_n^{1\prime}(kr_1) + \frac{j\omega\mu}{k} F_n^1(kr_1) Y_1}{aF_n^{2\prime}(ka) - \frac{j\omega\mu}{k} F_n^2(ka) Y_2} = 0 \tag{3.17}$$

The above transcendental equation gives the resonant frequency of a given TM_{np} mode.

3.4 Results and discussion

For simulation, we consider a schematic of feed patch and parasitic patch of the same diameter as shown in Fig. 3.1. The patches are placed on substrate of relative permittivity $\varepsilon_r = 2.2$ and height $h = 1.59$ mm. Fig. 3.3 to Fig. 3.8 compare the analyzed results with that of simulations with IE3D. In Fig. 3.3, the variation of the resonant frequency of the TM_{01} mode with the radius of shorting post is shown. In Fig. 3.4, the variation of

resonant frequency of the TM_{11} mode with radius of shorting post is shown. In Fig. 3.5, the variation of resonant frequency of the TM_{21} mode with radius of shorting post is shown. The resonant frequency increases on increasing the radius of shorting post. In Fig. 3.6, the variation of the resonant frequency of the TM_{01} mode with the gap distance between adjacent edges of the feed patch and parasitic patch is shown. In Fig. 3.7, the variation of the resonant frequency of the TM_{11} mode with the gap distance between adjacent edges of the feed patch and parasitic patch is shown. In Fig. 3.8, the variation of resonant frequency of the TM_{21} mode with the gap distance between adjacent edges of the feed patch and parasitic patch is shown. The resonant frequency decreases on increasing the gap between adjacent edges. The analyzed results show good agreement with simulated results.

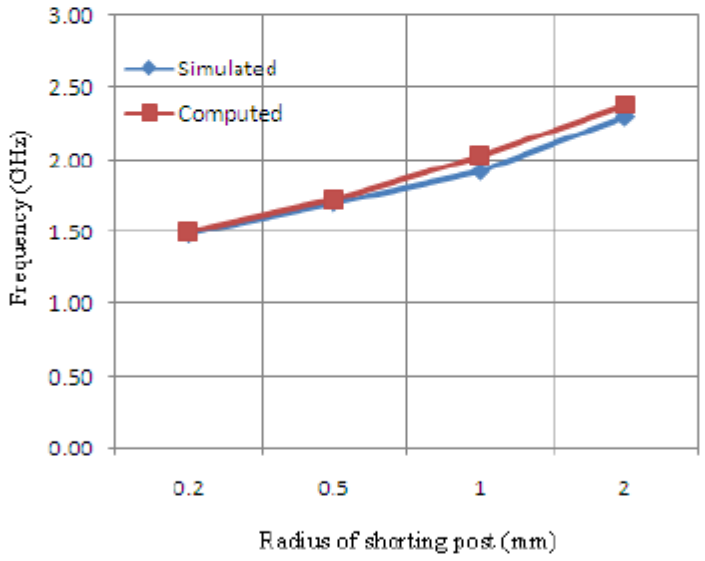

Fig. 3.3 Variation of the resonant frequency of the TM_{01} mode with increasing radius of shorting post with gap distance, s = 0.5 mm.

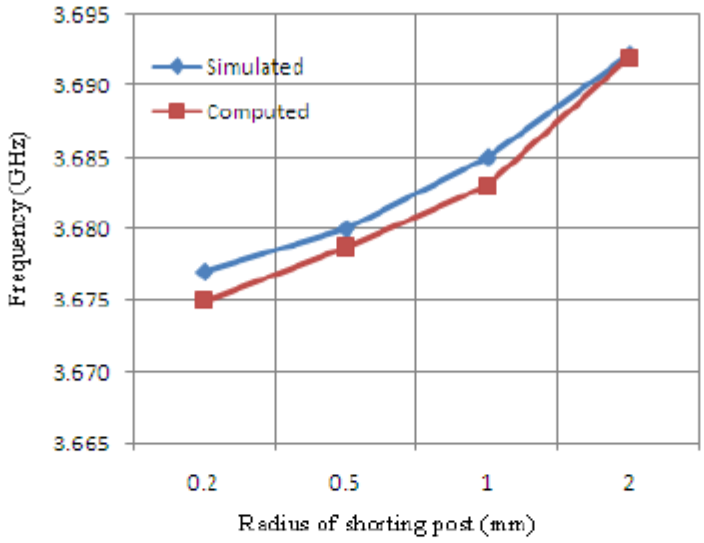

Fig. 3.4 Variation of the resonant frequency of the TM_{11} mode with increasing radius of shorting post with gap distance, s = 0.5 mm.

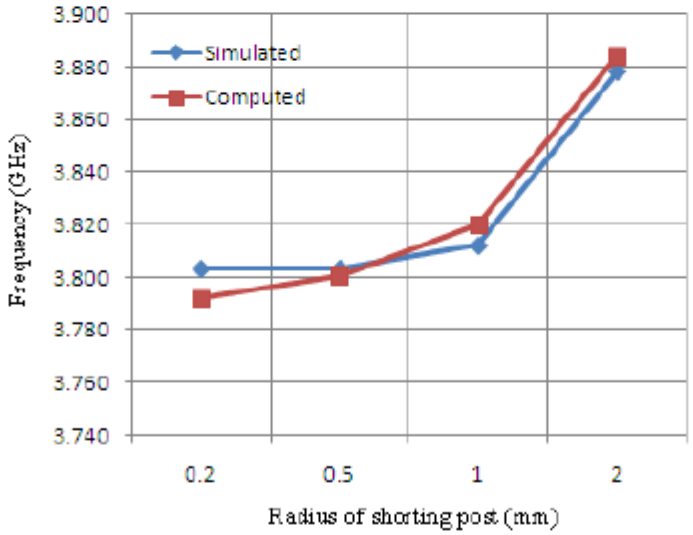

Fig. 3.5 Variation of the resonant frequency of the TM_{21} mode with increasing radius of shorting post with gap distance, s = 0.5 mm.

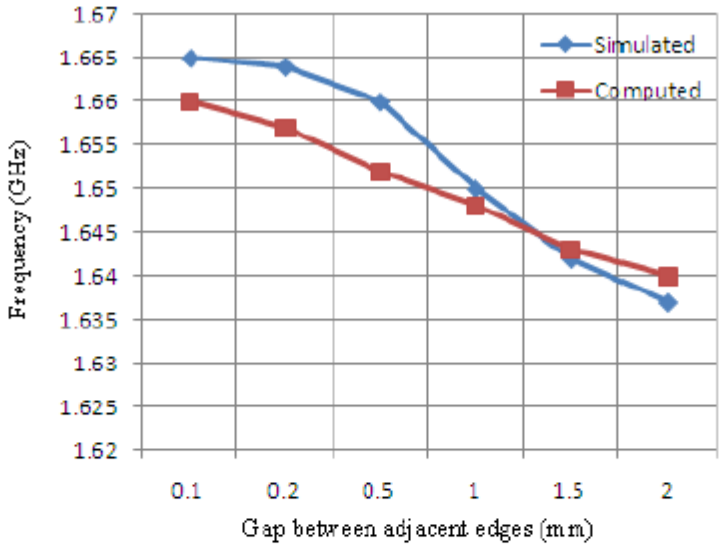

Fig. 3.6 Variation of the resonant frequency of TM_{01} mode with increasing gap distance between adjacent edges with radius of shorting post = 0.5 mm.

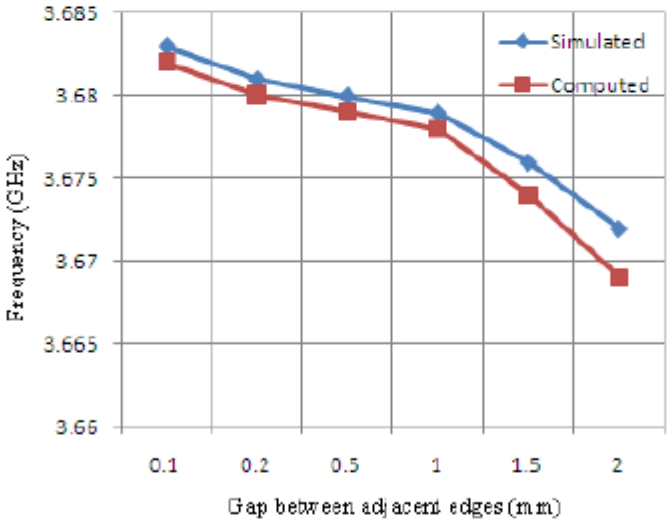

Fig. 3.7 Variation of the resonant frequency of TM_{11} mode with increasing gap distance between adjacent edges with radius of shorting post = 0.5 mm.

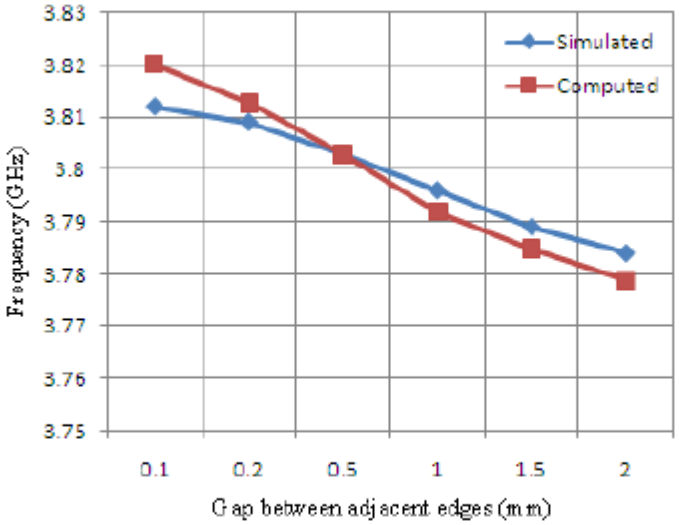

Fig. 3.8 Variation of the resonant frequency of TM_{21} mode with increasing gap distance between adjacent edges with radius of shorting post = 0.5 mm.

To validate the presentation of mode numbers the simulated current densities on the patches are presented in Fig. 3.9, 3.20 and 3.11. It is seen that the mode numbers are predicted accurately. In this case, the colour of current density towards 'Red' is higher potential and 'Blue' is the minimum potential. The left hand side patch is the feed patch and the right side patch is the parasitic patch. In Fig. 3.9, the yellow region is at the center of the feed patch and the blue region at the surroundings of the green region conveys the TM_{01} mode. In Fig. 3.10, it is seen that on the feed patch a yellow region and a blue region exists. This accounts for the TM_{11} mode. The two blue regions in Fig. 3.11 convey the existence of the TM_{21} mode.

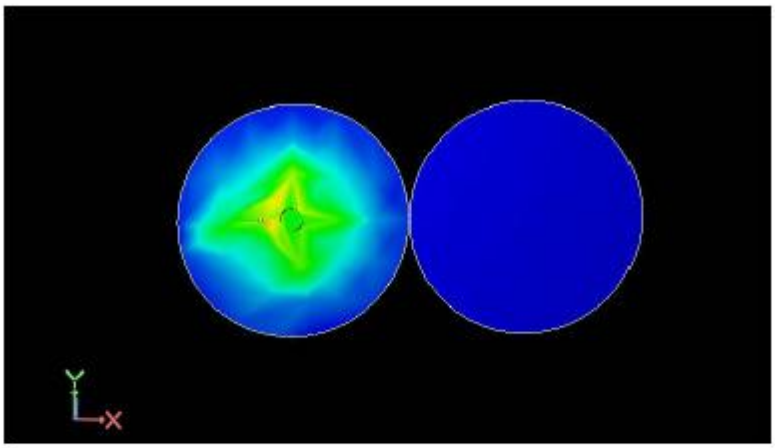

Fig. 3.9 Simulated current density at 2.149 GHz (gap distance between adjacent edges = 0.1 mm, radius of shorting post = 1.5 mm).

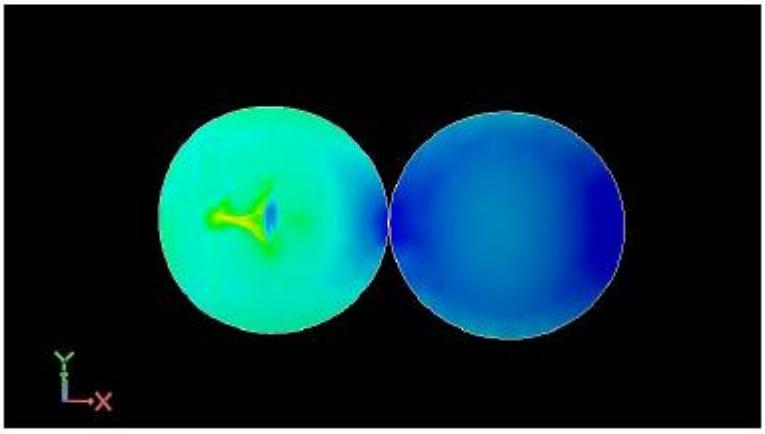

Fig. 3.10 Simulated current density at 3.6912 GHz (gap distance between adjacent edges = 0.1 mm, radius of shorting post = 1.5 mm).

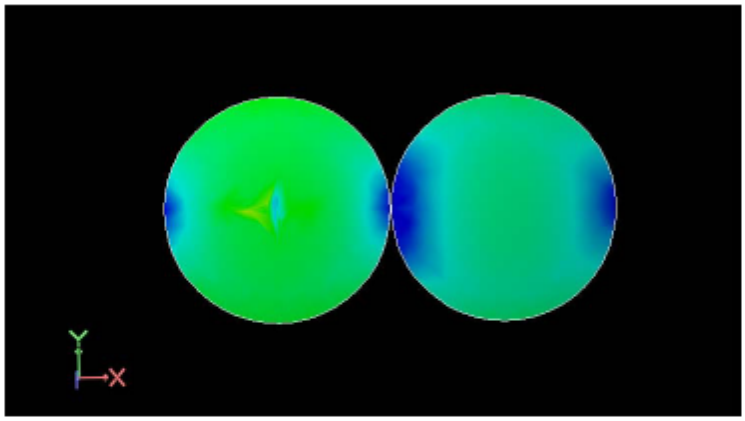

Fig. 3.11 Simulated current density at 3.8474 GHz (gap distance between adjacent edges = 0.1 mm, radius of shorting post = 1.5 mm).

3.5 Conclusion

In the present chapter, a numerical model for the resonant frequency of shorting post loaded two gap-coupled circular microstrip patch antennas has been investigated. The comparison between the computed and simulated results shows good agreement in the resonant frequency. Since the cavity model analysis is used in conjunction with circuit theory, the mode number prediction is also performed. The two gap-coupled circular microstrip antennas loaded with shorting post can be used for triple frequencies operation. The proposed model can be extended to multiple resonators as well as analysis with different patch sizes.

CHAPTER 4

THEORETICAL INVESTIGATION OF INPUT IMPEDANCE OF GAP-COUPLED CIRCULAR MICROSTRIP PATCH ANTENNAS

4.1 Introduction

The impedance bandwidth and input impedance are potential properties of microstrip patch antennas that are strongly affected by the substrate thickness. The straightforward approach to increase the bandwidth is by increasing the thickness of the substrate supporting the microstrip patch. However, limitations still exist on the ability to effectively feed the patch on a thick substrate and radiation efficiency can degrade with increasing substrate thickness [133]. Techniques to overcome this problem include using parasitic tuning elements, external matching, and separating the antenna and feed [133]. Recently, more progress has been made to broaden the bandwidth of microstrip patch antennas [133-135]. Pozar [133] listed the bandwidths for microstrip antennas with several shapes such as narrow rectangular, square, wide rectangular, and circular. The ways to enhance the bandwidth of microstrip antennas are: parasitic elements [71, 136, 137], aperture coupling [138], [139], and impedance matching network [140]. A broad-band matching design procedure with external matching has been presented in [141] to improve the bandwidth characteristics of several microstrip patch antennas. Ray et al [142] have designed dual and triple frequency band operation gap-coupled microstrip patch antennas and Ansari et al [143] have presented the analysis of a gap-coupled stacked annular ring microstrip antenna. The effects of the several geometrical design parameters on the input impedance of stacked short circuited patch antennas have been discussed first in [144] and more thoroughly in [145]. The design of open circuited patches with coplanar parasitic has been presented in [146]. The effects of various geometrical design parameters on the input impedance of a shorted patch with coplanar

parasitic have been studied in [147]. The impedance bandwidth of a small resonant antenna is known to depend on the antenna size [148, 149]. Therefore any extra bandwidth, obtained by optimizing the antenna performance can be trade off for smaller size. The constraint requirements to decrease the antenna size and to increase the number of antenna elements that can be filled into a given volume make bandwidth optimization especially important in the case of internal mobile phone antennas, which is currently one of the main application areas of the microstrip type small antennas.

In this chapter, the concept of coupled microstrip lines [149] is extended for the two gap-coupled circular microstrip patch antennas to analyze the input impedance by using the circuit theory approach and the results are compared with the simulated results. Comparison of these results shows good agreement with simulated results. In the analysis, the total capacitance of a microstrip patch antenna is taken as parallel plate capacitance and two fringing capacitances for both even and odd mode. Since there is another patch that is the parasitic element in the proposed two gap-coupled circular microstrip patch antennas, so there is another fringing capacitance at the adjacent edge of the patches.

4.2 Antenna Configuration

The geometrical configuration of two gap-coupled circular microstrip antennas is shown in Fig 2.1. The patch of radius $r_1 = 15\text{mm}$ is the feed patch and other patch of radius $r_2 = 15\text{mm}$ is the parasitic patch. The parasitic patch is excited by the gap-coupling whereas the feed patch is excited by the coaxially probe feeding technique. The location of probe is at distance $l = 4\text{ mm}$, from the center of the patch as shown in Fig. 2.1. Microstrip patch antennas, generally, used either microstrip line or coaxial probe feed technique. These two feeding techniques are very similar in operation, and offer essentially one degree of freedom in the design of the antenna element through the positioning of the feed point to adjust the input impedance level. Coaxially fed microstrip antennas have two key exciting sources, namely, the probe electric current and the coaxial electric field. In the calculation of the input impedance of probe-driven microstrip antennas on thin substrates, the effects of the probe results in an additional inductive

component to the input impedance. The probe inductance has been accounted by several authors through use of a simple formula [150-153]. The parasitic patch introduces another resonance near the main resonance and proper adjustment of the structure parameters, bandwidth can be enhanced. The height and relative permittivity of the substrate is $h = 1.59\text{mm}$ and $\varepsilon_r = 2.2$, respectively. The gap distance between the adjacent edges of the feed patch and parasitic patch is s. The thickness t of the patches is neglected.

4.3 Formulation

Coupled microstrip structures can be characterized for two modes which are known as odd and even modes [149, 154]. The properties of the coupled microstrip patches have been determined by the self and mutual inductance and capacitance between the patches. Under the quasi-transverse electromagnetic mode approximation the self-inductance can be expressed in term of self-capacitance by using simple relations. For most of the practical circuits using symmetric microstrip patches the mutual-inductance and mutual-capacitance are interrelated to each other so it is not necessary to determine each separately. Therefore, only capacitance parameters are evaluated for the two gap-coupled circular microstrip patch antennas. The capacitances can be expressed in terms of even and odd mode values for propagation [149]. The total capacitance of the coupled structure can be determined using Fig. 4.1 and Fig. 4.2 for the even mode and odd mode, respectively. From Fig. 4.1 the total capacitance for the even mode C_E is given by [149]:

$$C_E = C_P + C_F + C_{F'} \tag{4.1}$$

where C_P is the parallel plate capacitance between the metallic patch and the ground plane and is given by:

$$C_P = \frac{\varepsilon_0 \varepsilon_r A}{h} \tag{4.2}$$

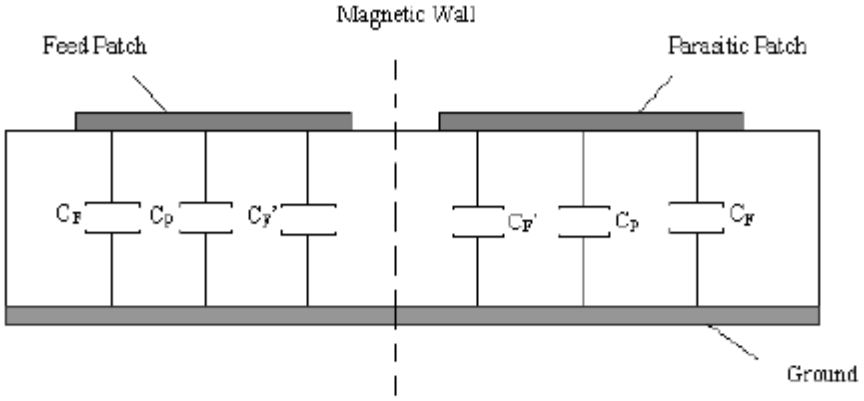

Fig. 4.1 Even-mode capacitances of the two gap-coupled circular microstrip patch antenna.

where A is the surface area of the patch, ε_r is the relative dielectric permittivity of the substrate and ε_0 is the permittivity of free-space. C_F is the fringing capacitance due to edge conductor and given by:

$$C_F = \frac{1}{2}\left[\frac{\sqrt{\varepsilon_{eff}}}{cZ_C} - C_P\right] \tag{4.3}$$

where $c = 3\times10^8$ m/s that is velocity of light in vacuum, Z_C is the characteristic impedance and ε_{eff} is the effective dielectric permittivity of the substrate. C_F' is the fringing capacitance due to parasitic patch and given by:

$$C_F' = \frac{C_F}{1+A\left(\frac{h}{s}\right)\tanh\left(\frac{10s}{h}\right)}\sqrt{\frac{\varepsilon_r}{\varepsilon_{eff}}} \tag{4.4}$$

where $A = \exp\left(-0.1\exp\left(2.33-\frac{2.53C}{2h}\right)\right)$ and C is the circumference of the patch. With the help of equations (4.1) to (4.4), the even mode-capacitance of two gap-coupled circular microstrip patch antennas is calculated. From Fig. 4.2, the total capacitance for the odd- mode (C_O) is given by [149]:

$$C_O = C_P + C_F + C_{gd} + C_{ga} \tag{4.5}$$

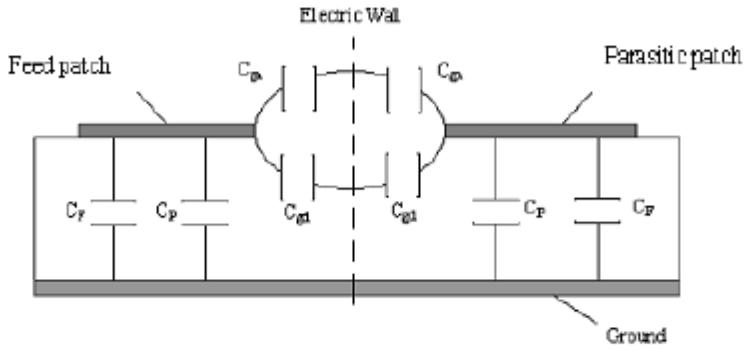

Fig. 4.2 Odd-mode capacitances of the two gap-coupled circular microstrip patch antenna.

where C_{gd} is the capacitance between the two structures through the dielectric region and given by:

$$C_{gd} = \frac{\varepsilon}{\pi}\ln\left(\coth\left(\frac{\pi s}{4h}\right)\right) + 0.65C_F\left(\frac{0.02\sqrt{\varepsilon_r}}{s/h} + 1 - \frac{1}{\varepsilon_r^2}\right) \tag{4.6}$$

and C_{ga} is the capacitance between the structures through air and given by:

$$C_{ga} = \frac{K(k')\varepsilon_0}{2K(k)} \tag{4.7}$$

where $K(k)$, $K(k')$ are elliptic functions, k and k' are:

$$k = \frac{s/h}{s/h + 2(C/h)} \text{ and } k' = \sqrt{1-k^2}$$

The approach of coupled microstrip lines presented in [149] is applied to the two gap-coupled microstrip patch antennas. With the help of equation (4.1)-(4.7), the capacitances of the two gap-coupled circular microstrip patch antenna for the odd and even modes are calculated and compared with the coupled microstrip lines as in [149]. For this comparison the cross-sectional area of the coupled circular microstrip patches and coupled microstrip lines are considered same. In the present results of table 4.1, the

height of the substrate is taken unity. The even and odd mode capacitances of the coupled circular microstrip patches and coupled microstrip lines are shown in table 4.1.

The equivalent circuit model of the two gap-coupled circular microstrip patch antenna for the even mode is shown in Fig. 3. From Fig. 3, the input impedance for the even mode is calculated. Z_1 and Z_2 are the impedances of feed path and parasitic patch, respectively and given as [155].

$$Z_1 = Z_2 = \frac{R}{1+Q_T^2\left(\frac{f}{f_r}-\frac{f_r}{f}\right)^2} + jRQ_T\frac{\left(\frac{f_r}{f}-\frac{f}{f_r}\right)}{1+Q_T^2\left(\frac{f}{f_r}-\frac{f_r}{f}\right)^2} \tag{4.8}$$

where R is the resonant resistance of the resonant parallel RLC circuit. f_r is the resonant frequency and Q_T is quality factor associated with system loss including radiation from the walls (Q_R), losses in dielectric (Q_D), and losses in conductor (Q_C). Q_T can be calculated by [4, 155]:

$$Q_T = \frac{1}{\frac{1}{Q_R}+\frac{1}{Q_C}+\frac{1}{Q_D}} \tag{4.9}$$

$$Q_R = \frac{4\pi(\alpha^2-1)\varepsilon_r^{3/2}}{h\alpha^3 F\left(\alpha/\sqrt{\varepsilon_r}\right)} \tag{4.10}$$

where

$$F(x) = \frac{4}{x^3}\left\{2xJ_0(2x) + (x^2-1)\int_0^{2x} J_0(t)dt\right\} \tag{4.11}$$

Table 4.1 Comparison of coupled microstrip lines by Garg [149] and our approach to coupled microstrip antennas. ($\varepsilon_r = 9.7$).

Coupled microstrip lines [149] (L=1)				Proposed approach for gap coupled circular microstrip antennas			
w/h	s/h	C_E(pF)	C_O(pF)	r1/h	s/h	C_E(pF)	C_O(pF)
0.2	0.05	60.3	215	0.253	0.05	57.99	222.3
0.2	0.20	66.1	149	0.253	0.20	62.3	155.2
0.2	0.50	75.7	117	0.253	0.50	70.41	122.5
0.2	1.00	83.5	98.5	0.253	1.00	78.28	102.8
0.2	2.00	89.9	87.2	0.253	2.00	85.8	90.58
0.5	0.05	90.1	258	0.399	0.05	87.9	260.7
0.5	0.20	95.4	188	0.399	0.20	92.3	190.9
0.5	0.50	105	155	0.399	0.50	100.8	157.5
0.5	1.00	114	136	0.399	1.00	109.3	137.4
0.5	2.00	122	124	0.399	2.00	117.6	124.7
1.0	0.05	136	313	0.564	0.05	133	311
1.0	0.20	141	241	0.564	0.20	137.4	239.7
1.0	0.50	150	207	0.564	0.50	146	206
1.0	1.00	159	187	0.564	1.00	154.7	185.5
1.0	2.00	168	174	0.564	2.00	163.4	172.6
2.0	0.05	223	408	0.798	0.05	220.3	402.1
2.0	0.20	228	334	0.798	0.20	224.6	330.1
2.0	0.50	237	300	0.798	0.50	233.2	295.9
2.0	1.00	246	279	0.798	1.00	241.9	275.3
2.0	2.00	255	266	0.798	2.00	250.5	262.2

$$F(x) = 2.666667378 - 1.066662519x^2 + 0.209534311x^4 - 0.019411347x^6 + 0.001044121x^8 - 0.000049747x^{10} \quad (4.12)$$

$$Q_D = \frac{1}{\tan\delta} \tag{4.13}$$

where $\tan\delta$ is the dielectric loss tangent and α is the n^{th} zero of first derivative of the Bessel function of first order.

$$Q_C = \frac{h}{\delta_s} \tag{4.14}$$

where δ_s is the skin depth and given by:

$$\delta_s = \frac{1}{\sqrt{\pi f \mu_0 \sigma}} \tag{4.15}$$

$$R = \frac{1}{G_T}\frac{J_1^2(kl)}{J_1^2(kr_1)} \tag{4.16}$$

where G_T includes the conductance due to ohmic, dielectric and radiation losses, and l is the distance of feed point from the center.

$$G_T = G_R + G_D + G_C \tag{4.17}$$

where

$$G_R = \frac{2.39}{4\mu_0 f_r h Q_R} \tag{4.18}$$

$$G_D = \frac{2.39\tan\delta}{4\mu_0 f_r h} \tag{4.19}$$

$$G_C = \frac{2.39\pi(\pi f_r \mu_0)^{-3/2}}{4h^2\sqrt{\sigma}} \tag{4.20}$$

$$J_1(t) = t(0.5 - 0.56249985\left(\frac{t}{3}\right)^2 + 0.21093573\left(\frac{t}{3}\right)^4 - 0.03954289\left(\frac{t}{3}\right)^6 + 0.00443319\left(\frac{t}{3}\right)^8 - 0.0031761\left(\frac{t}{3}\right)^{10} \tag{4.21}$$

X_L is the inductance due to probe feeding and given by [153]:

$$X_L = j\frac{3.77fh}{c}\log\left(\frac{c}{\pi f d_0}\right) \tag{4.22}$$

where d_0 is the diameter of the feed probe. The conductance, inductance and the capacitance in the Fig. 4.3 and Fig. 4.4 are given by [156]:

$$Y_1 = Y_2 = \frac{1}{R} \tag{4.23}$$

$$L_1 = L_2 = \frac{R}{2\pi f_r Q_T} \tag{4.24}$$

$$C_1 = C_2 = \frac{Q_T}{2\pi f_r R} \tag{4.25}$$

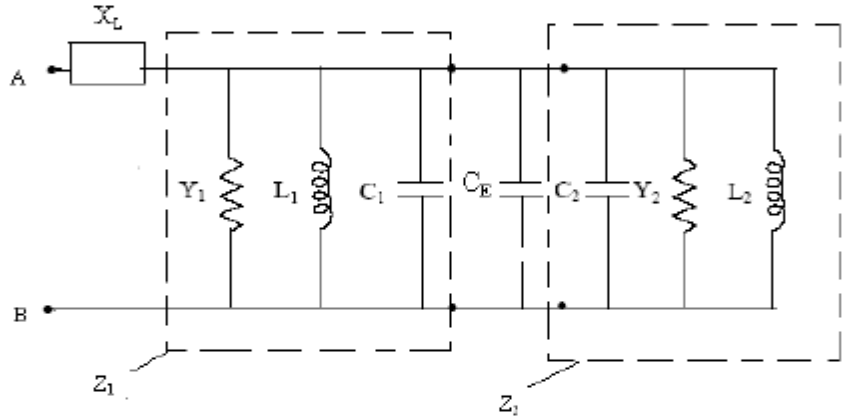

Fig. 4.3 Equivalent circuit model of the two gap-coupled circular microstrip antenna for the even mode.

The equivalent circuit model of the two gap-coupled circular microstrip antenna for the odd mode is given in Fig. 4.4. From Fig. 4.4, the input impedance for odd mode is calculated. The total input impedance of the gap-coupled structures is given by [154]:

$$Z_{in} = Z_{in}^{E} + Z_{in}^{O} \tag{4.26}$$

where Z_{in}^{E} and Z_{in}^{O} are the input impedance for even and odd mode, respectively. Using aforementioned equations, we can calculate the input impedance of the two gap-coupled circular microstrip patch antennas. The gap capacitance between two structures through dielectric (C_{gd}) is directly proportional to the fringe capacitance that is increases with

increasing the fringe capacitance and decreases with decreasing the fringe capacitance as from equation (4.6). While the gap capacitance between the two structures through air (C_{ga}) is independent from the fringing capacitance as from equation (4.7). Both the gap capacitances that is gap capacitance between two structures through dielectric (C_{gd}) and through air (C_{ga}) depends upon the gap between adjacent edges of the feed patch and parasitic patch. The variation of these capacitances with gap distance is shown in table 4.2. From table 4.2, it is clear that both gap capacitances decrease with increasing the gap.

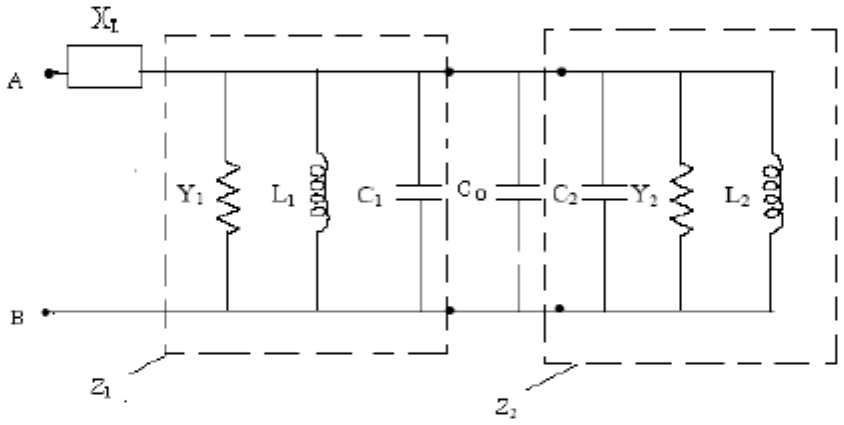

Fig. 4.4 Equivalent circuit model of the two gap-coupled circular microstrip patch antenna for the odd mode.

4.4 Results and Discussion

The input impedance is defined as the ratio of voltage across the patch and ground plane to the feed point current. The microstrip line feeding and probe feeding methods are very similar in operation, and offer essentially one degree of freedom in the design of antenna element through the positioning of the feed point to adjust the input impedance level. The input impedance of the two gap-coupled circular microstrip patch antenna is calculated by using (4.26) and the computed results are compared with simulated results.

Table 4.2 Variation of the gap capacitances of the two gap-coupled circular microstrip antenna with gap distance between adjacent edges of feed patch and parasitic patch ($r_1 = r_2 = 15$ mm, $\varepsilon_r = 2.2$, $h = 1.59$ mm).

Gap distance s (mm)	C_{ga}(pF)	C_{gd}(pF)
0.1	46.4	28.64
0.5	37.37	15.8
1	33.5	11.48
2	29.65	8.178
4	25.86	6.593

The simulation of the proposed antenna is performed by a commercially available MoM based simulator IE3D. The frequency characteristics of the input impedance (real and imaginary part) of two gap-coupled circular microstrip patch antennas are shown in Fig. 4.5. With the increase of frequency, the real part of input impedance increases and attain an optimum value at a particular frequency (3.77GHz) and then start to decrease, whereas the imaginary part of the input impedance almost always decreases as shown in Fig. 4.5. The comparison of simulated and computed results shows good agreement except initial frequencies (3.7 to 3.74 GHz). Initially, in a very short range of frequency the simulated and computed results are differing. In chapter 2, it has been shown that the gap-coupling lead to close resonance of the TM_{11} and TM_{21} mode. Here, we have computed the frequency characteristics of the input impedance only for TM_{21} mode, however, the deviation seen in Fig. 4.5 for initial frequencies is due to presence of the TM_{11} mode in simulation results.

The variation of the real and imaginary part of the input impedance of the proposed antenna with gap distance between adjacent edges of the patch is shown in Fig. 4.6. The computed and simulated results in the particular range of the gap distance between the feed patch and parasitic patch of the proposed antenna are well matched.

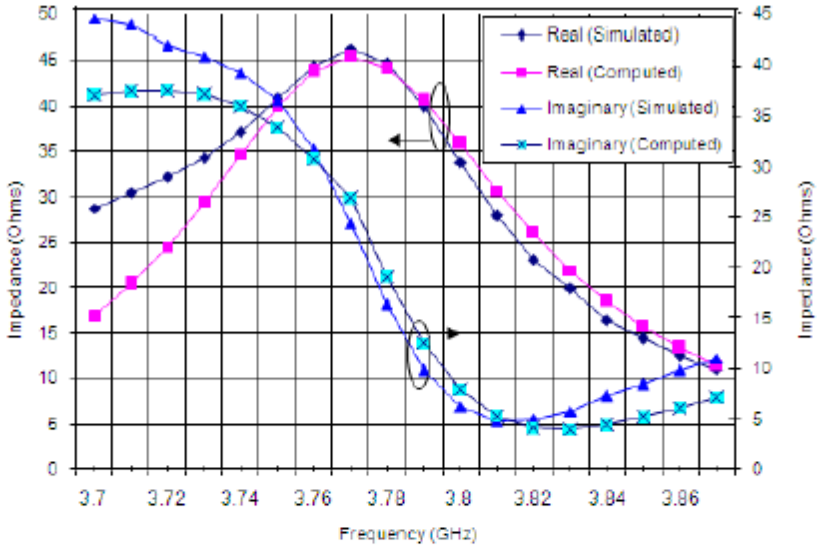

Fig. 4.5 Frequency characteristics of the input impedance of the two gap-coupled circular microstrip patch antenna for gap distance between the feed patch and parasitic patch = 1.5 mm.

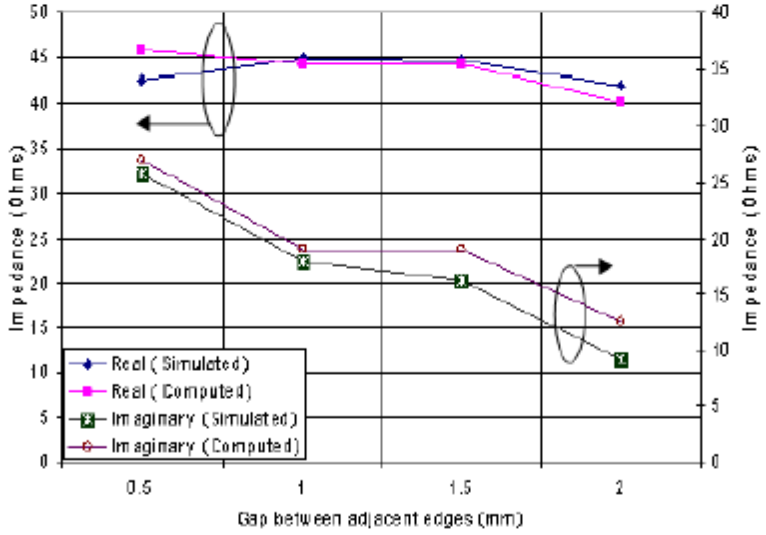

Fig. 4.6 The gap distance characteristics of input impedance of the two gap-coupled circular microstrip patch antenna with gap distance between adjacent edges of the feed patch and parasitic patch at frequency 3.78 GHz.

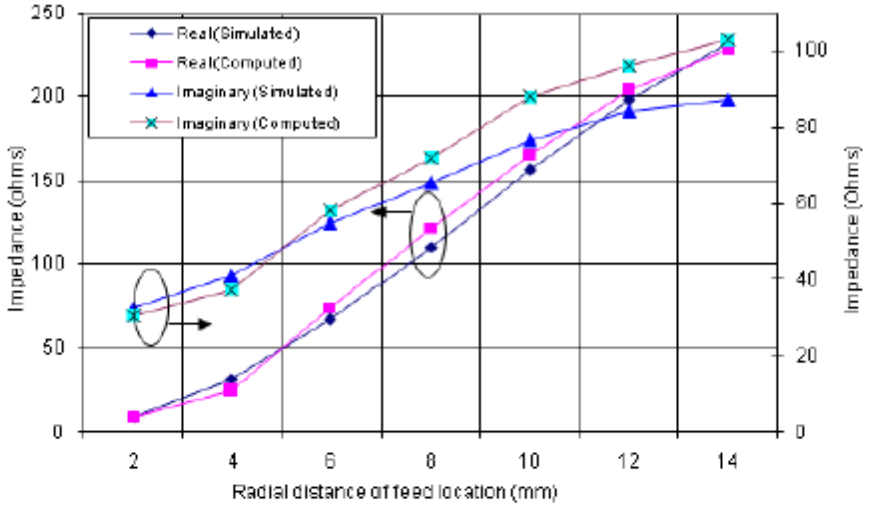

Fig. 4.7 Feed location characteristics of the input impedance of the two gap-coupled circular microstrip patch antenna at 3.72 GHz for gap distance between adjacent edges of the feed patch and parasitic patch is 1.00 mm.

Further, the variation of the real and imaginary part of the input impedance with feed location from the center of the patch is shown in Fig. 4.7. From Fig. 4.7, it is clear that both real and imaginary part of the input impedance of the proposed antenna increase when the feeding probe moves from center towards the edge of the patch. In terms of the transmission line model, the antenna is viewed as a length open circuited transmission line with light loading at the end to account for fringing fields and radiations. The voltage and current on this equivalent transmission line give the input impedance variation of the microstrip antenna. For a feed point at a radiating edge, the voltage is maximum and current is minimum so the input impedance is maximum. For a feed point at the center of patch, the voltage is zero and current is maximum, so the input impedance is zero. Thus the input impedance can be controlled by adjusting the position of feed point.

4.5 Conclusion

A simple and numerically efficient model for the input impedance of two gap-coupled circular microstrip patch antennas is developed. Input impedance for different gap distances between adjacent edges of feed patch and parasitic patch is shown as well as the variation of input impedance with feed location is also discussed. The input impedance depends strongly on the feed location and increases when feed point moves from center towards edge of the patch. The comparison between the analytical and simulated results shows good agreement.

CHAPTER -5

THEORETICAL INVESTIGATION OF INPUT IMPEDANCE OF GAP-COUPLED CIRCULAR MICROSTRIP PATCH ANTENNAS LOADED WITH SHORTING POST

5.1 Introduction

In chapter 3, it is shown that the size of two gap-coupled circular microstrip antennas can be reduced by loading with a shorting post. In the present chapter, the input impedance of the two gap-coupled circular microstrip antennas loaded with shorting post is analyzed. The concept of the analysis described in chapter 4, is extended to gap-coupled circular microstrip patch antennas loaded with the shorting post and the input impedance is analyzed. The analyzed results are compared with the simulated results.

5.2 Antenna Configuration

The geometrical configuration of two gap-coupled circular microstrip antennas loaded with shorting post is shown in Fig 3.1. The patch of radius r_1 = 15 mm is the feed patch and the patch of radius r_2 = 15 mm is the parasitic patch. The parasitic patch is excited by the gap-coupling. The feed patch is shorted by a shorting post of diameter p as shown in Fig. 3.1. The height and permittivity of the substrate is h = 1.59 mm and ε_r = 2.2, respectively. The gap distance between the adjacent edges of the feed patch and parasitic patch is s. The thickness of the patches is neglected.

5.3 Analysis

Coupled microstrip structures can be characterized for the two modes as in chapter 4. These modes are known as even and odd modes. The capacitances can be expressed in

terms of even and odd mode values for the two modes of propagation. The concept of coupled microstrip lines has been applied to the two gap-coupled circular microstrip antennas in chapter 4. The total capacitance of the two gap-coupled circular microstrip antennas can be determined for even mode and odd mode as in chapter 4.

The equivalent circuit models of two gap-coupled circular microstrip antennas loaded with shorting post for even mode and odd mode are shown in Fig. 5.1 and Fig. 5.2, respectively. From Fig. 5.1 and Fig. 5.2, the input impedance for the even mode and odd mode is calculated. In Fig. 5.1 and Fig. 5.2, Y_1, L_1, C_1 and Y_2, L_2, C_2 are the conductance, inductance, capacitance of the feed patch and parasitic patch, respectively, C_E and C_O are the capacitances for the even mode and odd mode, respectively. The feed patch is shorted by a shorting post, which is in shunt to the patch as shown in Fig. 5.1 and Fig. 5.2. The impedance per unit length due to shorting post is given by [157]:

$$X_P = \frac{\eta k}{4}[1 - J_0^2(kr_d) + j\{\frac{2}{\pi}\ln(\frac{2}{\gamma k\Delta}) + J_0(kr_d)N_0(kr_d)\}.F_1] \tag{5.1}$$

where r_d is the radial distance of the post from the center of the patch,

$$F_1 = \frac{\sin(\frac{\pi}{4})\{J_0(\frac{1}{8})\}^2}{J_0^{1.3}\left(\frac{r_d}{r_e}\right)J_0^{1.8}\left(\frac{r_d}{r_e}\right)}$$

where J_0, N_0 are the Bessel function of first and second kind, respectively of order zero and r_e is the effective radius of the patch due to fringing fields and is given by [158]

$$r_e = r_1\sqrt{1+\left(\frac{2h}{\pi\varepsilon_r r_1}\right)\Delta}$$

here $\Delta = \ln\left(\frac{\pi r_1}{2h}\right) + 1.7726$ and the thickness of patch metallization is negligible.

The total input impedance of the gap-coupled structure is given by:

$$Z_{in} = Z_{in}^E + Z_{in}^O \tag{5.2}$$

where Z_{in}^E and Z_{in}^O are the input impedances for the even and odd mode, respectively.

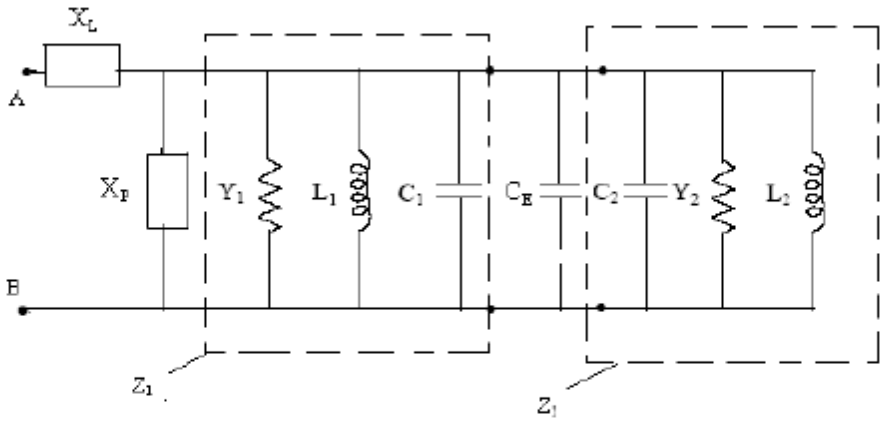

Fig. 5.1 Equivalent circuit of two gap-coupled circular microstrip antennas loaded with shorting post for the even mode.

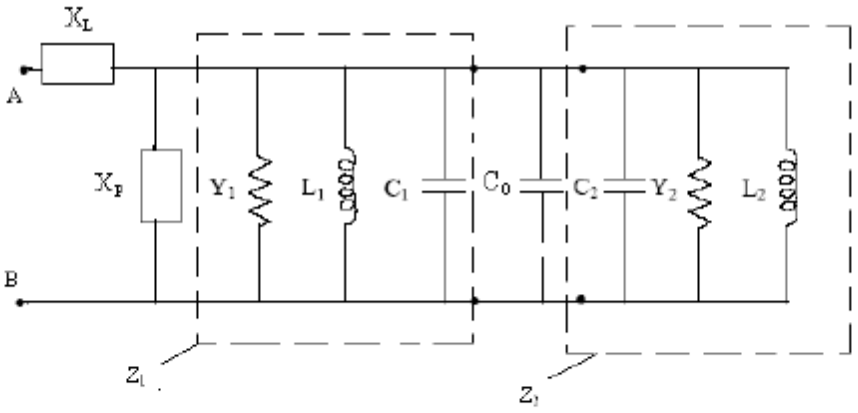

Fig. 5.2 Equivalent circuit of two gap-coupled circular microstrip antennas loaded with shorting post for the odd mode.

5.4 Results and Discussion

The simulation has been performed using the method-of-moment based commercially available simulator IE3D. For the simulation, two circular patches are placed close to each other and the feed patch is shorted by a post as shown in Fig 3.1. The input impedance is calculated using (5.2) and the computed results are compared with

simulated results. The frequency characteristics of the real and imaginary part of the input impedance are shown in Fig 5.3. The variation of real and imaginary part with gap distance between adjacent edges of the patches is shown in Fig 5.4. Further the variation of real and imaginary part of impedance with diameter of shorting post is shown in Fig 5.5. The comparison of simulated and computed results shows good agreement except real part for initial frequencies; it is due to presence of another mode in simulated results.

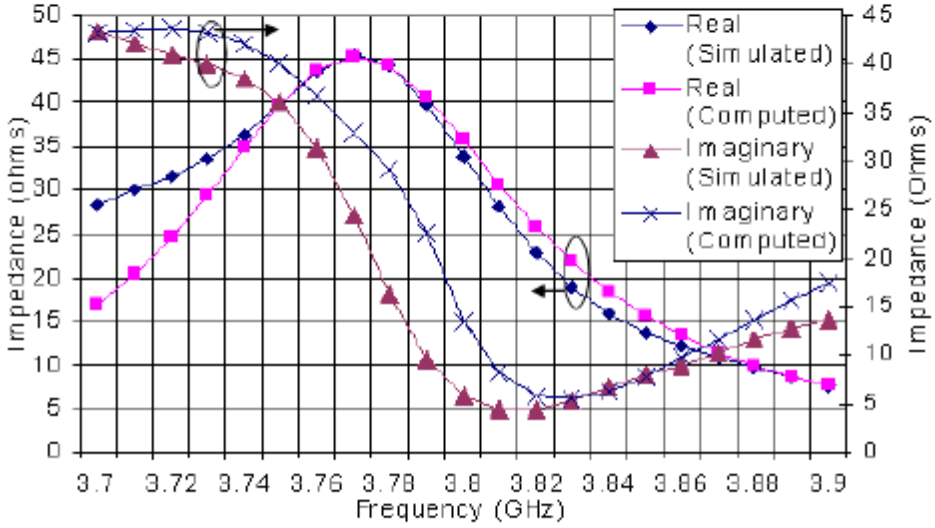

Fig 5.3 Frequency characteristics of the input impedance of the two gap-coupled circular microstrip antenna (diameter of shorting post=0.4 mm and gap distance between adjacent edges=1 mm).

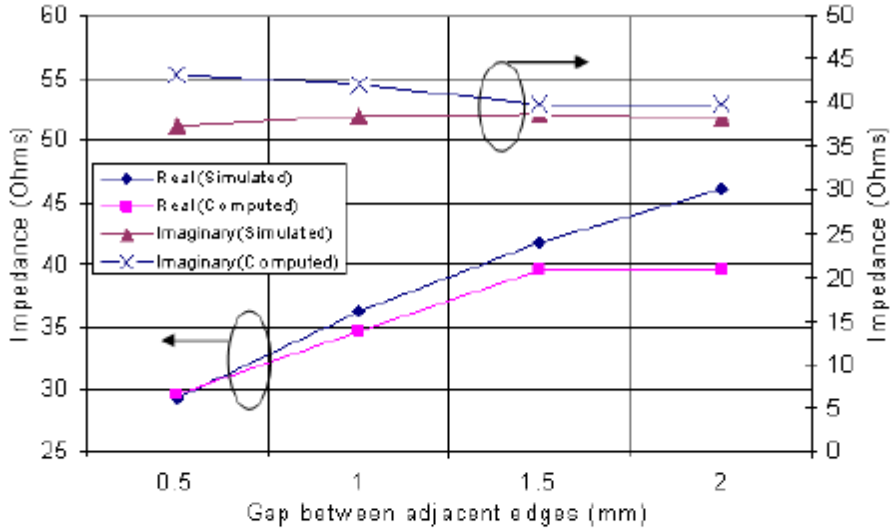

Fig 5.4 Variation of the input impedance of the two gap-coupled circular microstrip antenna with gap distance between adjacent edges at 3.74 GHz (diameter of shorting post = 0.4 mm).

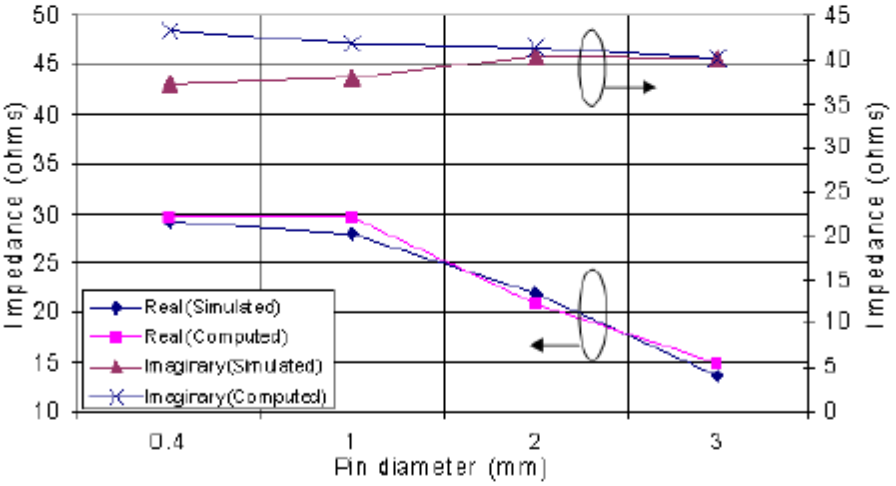

Fig 5.5 Variation of the input impedance of the two gap-coupled circular microstrip antenna with diameter of shorting post at 3.74 GHz (gap distance between adjacent edges = 0.5 mm).

Further, the simulation results of input impedance are shown for the TM_{01} mode. The real and imaginary part of the input impedance of the antenna for different gaps between the adjacent edges of the patches and for different shorting post radius is shown in Fig. 5.6 and in Fig. 5.7, respectively. The variation of the real and imaginary part with gap between adjacent edges at different frequencies is shown in Fig. 5.8 and Fig. 5.9, respectively. Further the variation of the real and imaginary part of the input impedance of the antenna with radius of shorting post is shown in Fig. 5.10 and in Fig. 11, respectively. From Fig. 5.10 and Fig. 5.11, it is clear that the real and imaginary part of the input impedance decreases on increasing the radius of shorting post.

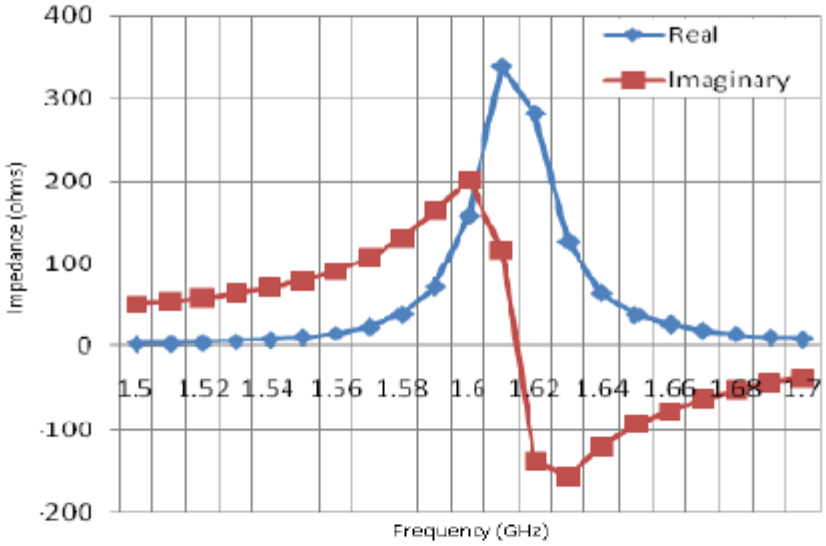

Fig. 5.6 Input impedance of the two gap-coupled circular microstrip antenna loaded with shorting post (gap distance between adjacent edges = 0.5 mm, radius of shorting post = 0.5 mm).

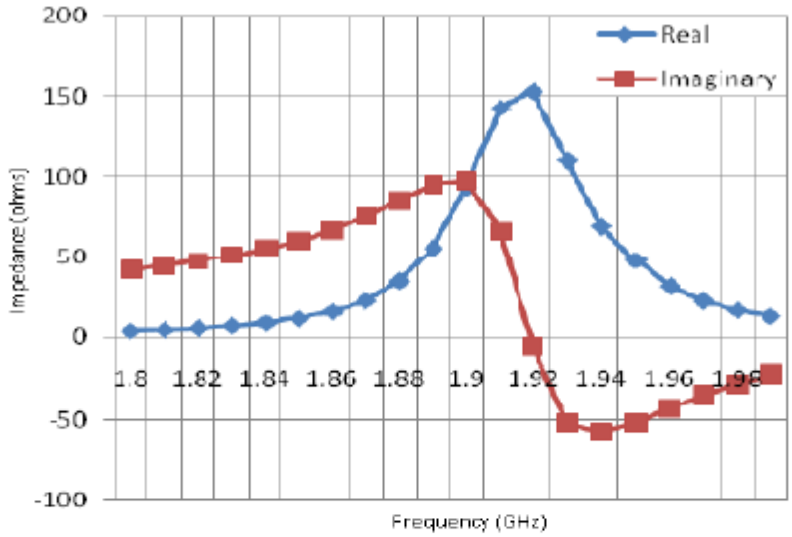

Fig. 5.7 Input impedance of the gap-coupled circular microstrip antenna loaded with shorting post (gap distance between adjacent edges = 1.00 mm, radius of shorting post = 1.00 mm).

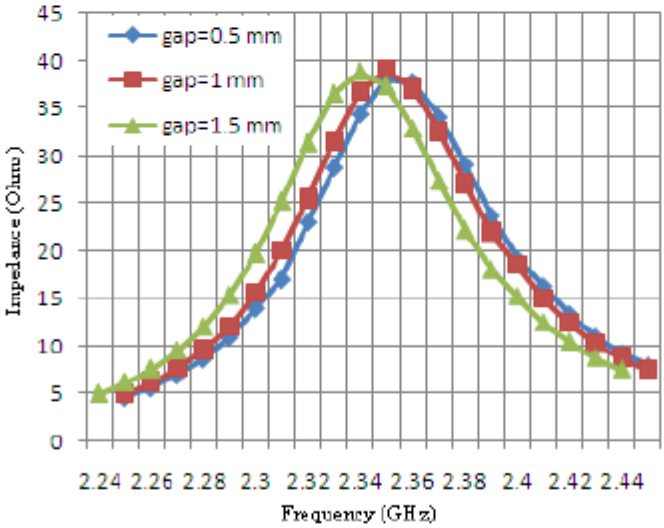

Fig. 5.8 Variation of the real part of the input impedance of the two gap-coupled circular microstrip antenna loaded with shorting post with gap distance between adjacent edges (radius of shorting post = 2.00 mm).

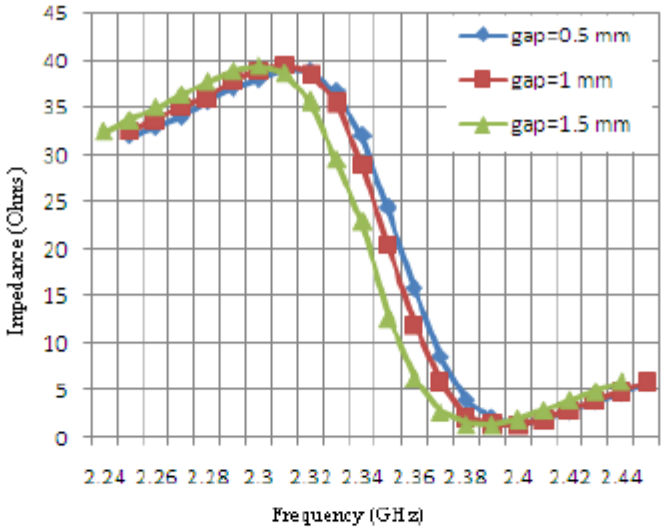

Fig. 5.9 Variation of the imaginary part of the input impedance of the two gap-coupled circular microstrip antenna loaded with shorting post with gap distance between adjacent edges (radius of shorting post = 2.00 mm).

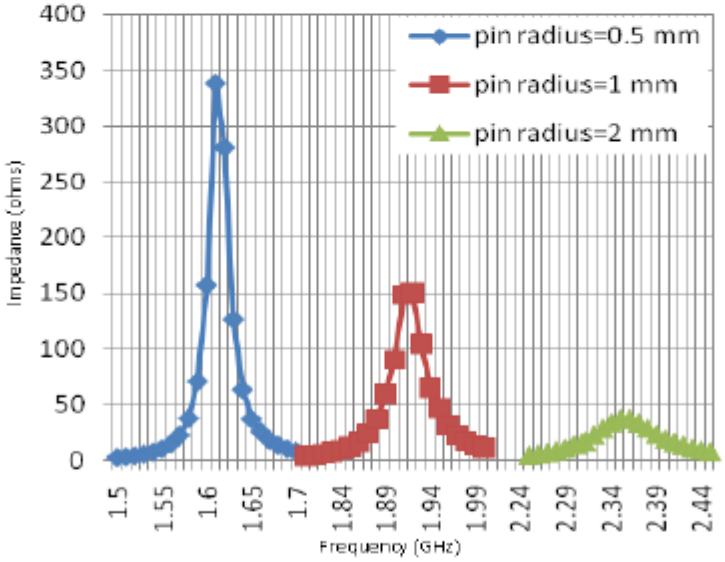

Fig. 5.10 Variation of the real part of the input impedance of the two gap-coupled circular microstrip antenna loaded with shorting post with radius of shorting post (gap distance between adjacent edges = 0.5 mm).

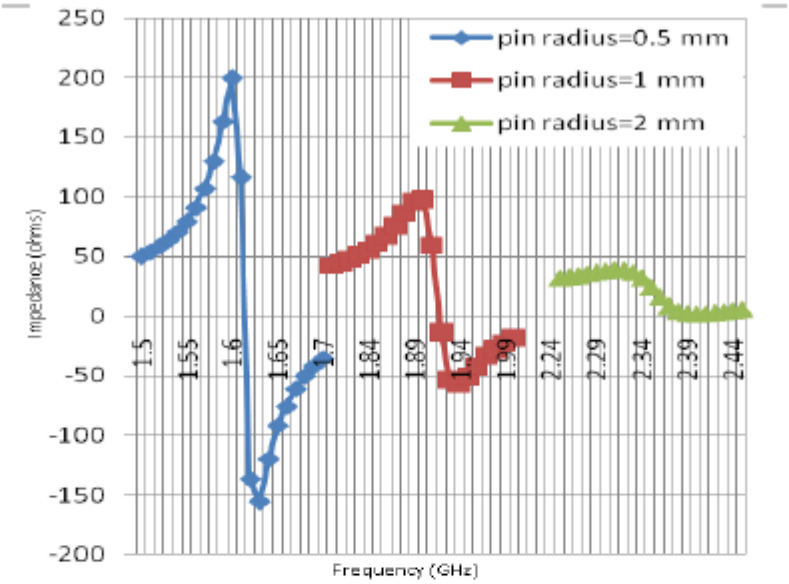

Fig. 5.11 Variation of the imaginary part of the input impedance of the two gap-coupled circular microstrip antenna loaded with shorting post with pin radius (gap distance between adjacent edges = 0.5 mm).

5.5 Conclusion

In this chapter, a numerical model for the two gap-coupled circular microstrip antenna loaded with shorting post has been developed. The input impedance of the two gap-coupled circular microstrip antennas loaded with shorting post for different gap distances between adjacent edges of feed patch and parasitic patch is shown. The effect of the diameter of the shorting post in the proposed configuration is also studied. The analysis presented above can be easily programmed to determine the input impedance of the two gap-coupled circular microstrip patch antenna loaded with shorted post.

CHAPTER -6

COMPUTATION OF MUTUAL COUPLING BETWEEN TWO GAP-COUPLED MICROSTRIP ANTENNAS WITH AND WITHOUT SHORTING POST

6.1 Introduction

The previous analysis of two gap-coupled microstrip patch antennas for the prediction of radiation properties was based on the assumption that the antenna elements are treated as isotropic sensors isolated from one another [159-160]. The electromagnetic influence of one patch on the other that is mutual coupling was ignored hence resulting the disagreement in predicted and measured results [160-161]. The mutual coupling influences the radiation mechanism of the antennas in both ways, namely, constructive and destructive [162]. In the former case, such coupling is helpful and in the latter case, attempt is to be made to reduce the same effect. Thus in all cases the estimation of the mutual coupling is important. Different antenna parameters like antenna element separation, frequency, substrate thickness, patch thickness, dielectric constant, near field scatters and direction of arrival of incoming wave are key parameters affecting the mutual coupling resulting in the change of antenna characteristics like gain, beamwidth and input impedance. The consequences of the mutual coupling can not be overlooked; in fact the affects on the gain influence the pattern directivity which can be exploited for decorrelating antenna elements. Several approaches like cavity model and equivalence theorem [163-164], network model [150], moment method [165], and full-wave methods [166] have been used on different geometries to estimate the mutual coupling between the elements of the antennas. The performance of adaptive array antennas [167, 168] and non linear arrays [169] under the effect of mutual coupling has also been the point of interest for authors [170]. In each analysis the important observation is that the estimation of the

coupling is mandatory and on the basis of this estimation, other analyses like compensation of coupling [171] are being carried out.

In this chapter, an estimation of the mutual coupling between the two gap-coupled circular microstrip antennas with and without shorting post is carried out.

6.2 Mutual Coupling between Two Gap-Coupled Circular Microstrip Patch Antennas

The geometrical configuration of a two gap-coupled circular microstrip antenna is shown in Fig. 2.1. The magnetic current model is used to determine the wall admittances of a patch antenna. In this model, the patch is replaced by the equivalent magnetic current source at its periphery. The wall admittances of the patch are equivalent to the radiation admittances of the corresponding magnetic currents [4]. However, the mutual admittance between two edges at $u = u_1$ and $u = u_2$ can be calculated accurately as:

$$y_{12}^{m} = \frac{< u_1, u_2 >}{V_1 V_2} \tag{6.1}$$

where $\langle u_1, u_2 \rangle$ is the mutual reaction between the sources at $u = u_1$ and $u = u_2$. The mutual reaction $\langle u_1, u_2 \rangle$ is given by [172]:

$$< u_1, u_2 > = \iint (E^{u_1} J^{u_2} - H^{u_1} M^{u_2}) dr \tag{6.2}$$

where J and M are the surface and magnetic current, respectively. We consider that u_1 and u_2 represent the two circular patches hitherto called simply as 'a' and 'b' only. Here J^a is the impressed (source) current and E^b is the electric field generated in 'b' due to J^a. For computation of the mutual admittance of the two circular patches, we consider only the first term of expression (6.2). Fig 6.1 gives the geometry of two gap-coupled circular microstrip patches. A patch of radius r_1 is placed at the center and another patch of radius r_2 is placed around the central patch as shown in Fig 6.1. Here, we have segmented the structure into two regions with origin at the center of region I. The inner radius of region II is 'b' and outer radius is 'c'. The distance between the centers of the patches is 'ρ_0'. In the proposed analysis thickness of the patch is not considered.

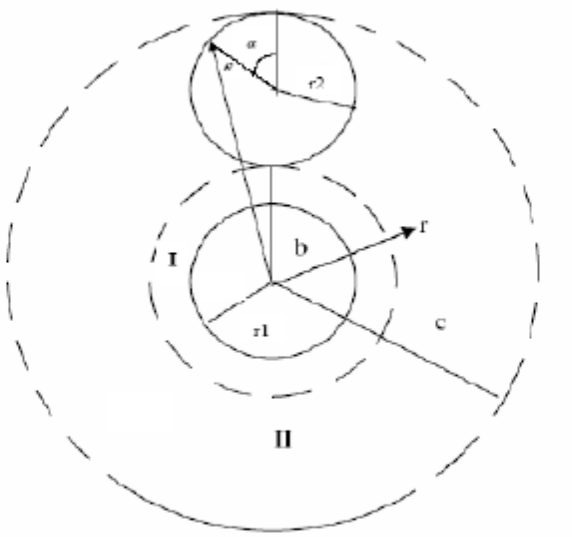

Fig. 6.1 Analytical geometry of a two gap-coupled circular microstrip patch antenna.

The axial electric field and azimuthal magnetic field expressions in region I ($0 \le r \le r_1$) are:

$$E_z^1 = -j\omega\mu C_n^1 F_n^1(kr)\cos n\phi \qquad \text{(rewritten, 2.16)} \qquad (6.3)$$

$$H_\phi^1 = -kC_n^1 F_n^{1\prime}(kr)\cos n\phi \qquad \text{(rewritten, 2.17)} \qquad (6.4)$$

where C_n^1 is a constant, and

$$F_n^1(kr) = J_n(kr) \qquad \text{(rewritten, 2.18)} \qquad (6.5)$$

$F_n^{1\prime}(kr)$ is the first derivative of $F_n^1(kr)$ with respect to argument. The expression for H_r^1 is omitted intentionally. The axial electric field and azimuthal magnetic field expressions in region II ($b \le r \le c$) are:

$$E_z^2 = -j\omega\mu C_n^2 F_n^2(kr)\cos n\alpha \qquad \text{(rewritten, 2.13)} \qquad (6.6)$$

$$H_\phi^2 = -kC_n^2 F_n^{2\prime}(kr)\cos n\alpha \qquad \text{(rewritten, 2.14)} \qquad (6.7)$$

where C_n^2 is a constant dependant on given mode 'n' , and

$$F_n^2(kr) = J_n(kr)I_1 - I_2 N_n(kr) \qquad (6.8)$$

$F_n^{2'}(kr)$ is the first derivative of $F_n^2(kr)$ with respect to arguement. Considering the parasitic patch in isolation the boundary condition of vanishing H_ϕ^2 can be applied as:

$$H_\phi^2 = 0 \text{ , for } r = \rho_0 + r_2.\cos\alpha \text{ and } 0 \le \alpha \le 2\pi$$

Thus

$$\frac{I_2}{I_1} = \frac{\int_0^{2\pi} J_n'(k\rho(\alpha))d\alpha}{\int_0^{2\pi} N_n'(k\rho(\alpha))d\alpha}$$

Using expression (6.2), the reaction is given by:

$$< a,b >= \int_0^{2\pi}\int_{r_2}^{r_2+h} E_z^{(2)}(\rho(\alpha))H_\phi^{(1)}(r_e)rdrd\alpha \qquad (6.9)$$

where r_e is the effective radius introduced to account for the fringe field. The effective radius is slightly greater than the physical radius of the circular patch. The relationship between physical radius and effective radius is given by [158]:

$$r_e = r_1\sqrt{1+\left(\frac{2h}{\pi\varepsilon_r r_1}\right)\Delta} \qquad \text{(neglecting the patch thickness)}$$

here $\Delta = \ln\left(\frac{\pi r_1}{2h}\right) + 1.7726$. The voltages are evaluated at the edges of respective patches and are given by:

$$V_1 = -hE_z^1(r_1) \qquad (6.10)$$

$$V_2 = -hE_z^2(r_2) \qquad (6.11)$$

Therefore using (6.2) the mutual admittance is given by:

$$y_{12}^m = \frac{\int_0^{2\pi}\int_{r_2}^{r_2+h} E_z^{(2)}(\rho(\alpha))H_\phi^{(1)}(r_e)rdrd\alpha}{h^2E_z^{(1)}(r_1)E_z^{(2)}(r_2)} \qquad (6.12)$$

Now mutual admittances for individual excited modes can be computed using equation

(6.12). The theoretical results are compared with published results [173]. In [173], the results are presented in terms of $|S_{12}|^2$ (dB). Therefore, for exact interpretation we have to convert y_{12}^m to $|S_{12}|^2$. This can be done by considering that the two edges of gap-coupled circular patches form a π - type network as shown in Fig 2.2. For such π - type network [174]:

$$S_{12} = -y_{12}^m \tag{6.13}$$

6.3 Mutual Coupling Between Gap-Coupled Circular Microstrip Antennas Loaded With Shorting Post

Fig 6.2 gives the geometry of two gap coupled circular patches. A patch of radius 'r_1' is placed at the center and another patch of radius 'r_2' is placed around the central patch as shown in Fig 6.2. Here we have segmented the structure into two regions with origin at the centre of region I. The inner radius of region II is 'b' and outer radius is 'c'. The distance between the centers of the patches is 'ρ_0'. The central patch is shorted by a pin of diameter 'p'. The thickness t of the patches is neglected.

The field expressions in region I ($0 \le r \le r_1$) are in (3.1) and (3.2), and for region II ($b \le r \le c$), the field expressions are given in (3.3) and (3.4).

Considering the parasitic patch in isolation, the boundary condition of vanishing H_ϕ^2 gives:

$$\frac{C_4}{C_3} = -\frac{\int_0^{2\pi} J_n'(k\rho(\alpha))d\alpha}{\int_0^{2\pi} N_n'(k\rho(\alpha))d\alpha} = \frac{I_2}{I_1} \tag{6.14}$$

where $\rho(\alpha) = \rho_0 + r_2.\cos\alpha$. Therefore the field expression in region II can be written as:

$$E_z^2 = -j\omega\mu C_n^2 F_n^2(kr)\cos n\phi \tag{6.15}$$

$$H_\phi^2 = -kC_n^2 F_n^{2\prime}(kr)\cos n\phi \tag{6.16}$$

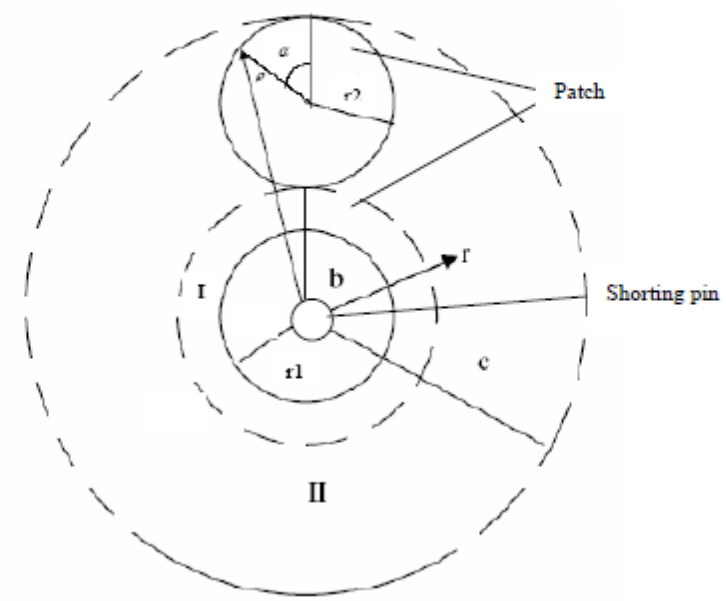

Fig. 6.2 Analytical configuration of the two gap coupled circular patch antennas loaded with shorting post.

where C_n^2 is a constant dependant on given mode 'n' and

$$F_n^2(kr) = J_n(kr)I_1 - I_2N_n(kr) \tag{6.17}$$

Similarly,

$$E_z^1 = 0 \text{ for } r = \frac{p}{2}$$

$$\frac{C_1}{C_2} = -\frac{N_n(\frac{kp}{2})}{J_n(\frac{kp}{2})} = \frac{I_3}{I_4} \tag{6.18}$$

Thus the field expression in region I is:

$$E_z^1 = -j\omega\mu C_n^1 F_n^1(kr)\cos n\phi \tag{6.19}$$

$$H_\phi^1 = -kC_n^1 F_n^{1\prime}(kr)\cos n\phi \tag{6.20}$$

where C_n^1 is a constant and

$$F_n^1(kr) = J_n(kr)I_3 - N_n(kr)I_4 \tag{6.21}$$

Now the mutual admittance is computed using equation (6.12). The computed results are compared with simulated results. The mutual coupling parameter S(1,2) can be calculated using (6.13).

6.4 Results and discussion

We have compared the analyzed results with that obtained through measurements presented in [173]. Using (6.12) the mutual admittance Y(1,2) is calculated and using (6.13) $|S(1,2)|^2$ (dB) is calculated for different gap distances between adjacent edges of feed patch and parasitic patch. From Fig. 6.3, it can be observed that the mutual coupling is stronger for smaller gap distance and it is weaker as the gap distance is increased. The computed results show good agreement with measured data [173] for small gaps between the circular microstrip patches. The dimensions of the antennas for this computation are given in table 6.1.

Table 6.1 Dimensions of the antennas used for Fig. 6.3.

Radius of feed patch (r_1)(mm)	Radius of parasitic patch (r_2) (mm)	Thickness of substrate (h) (mm)	Dielectric constant (ε_r)
38.5	38.5	1.575	2.5

Using (6.12) the mutual admittance Y(1,2) is calculated and using (6.13) $|S(1,2)|^2$ (dB) is calculated. The computed results are compared with the simulated data. One patch is shorted by a shorting post at its center. Both the patches are fed and the driving point impedance is set to approximately 50 Ω by varying the feeding points. For 50 Ω driving point impedance the mutual admittance parameter Y(1,2) is taken. The dimensions of the antennas used here are shown in table 6.2. The comparison of computed and simulated results is shown in Fig. 6.4 to Fig. 6.7. In Fig 6.4 and Fig. 6.5, the variation of mutual coupling parameter S(1,2) with pin radius is shown at various frequencies for the fixed

gap distances between adjacent edges of the feed patch and parasitic patch, is shown. In Fig 6.6 and Fig. 6.7, the variation of mutual coupling parameter S(1,2) with gap between adjacent edges for the fixed shorting post radius is shown.

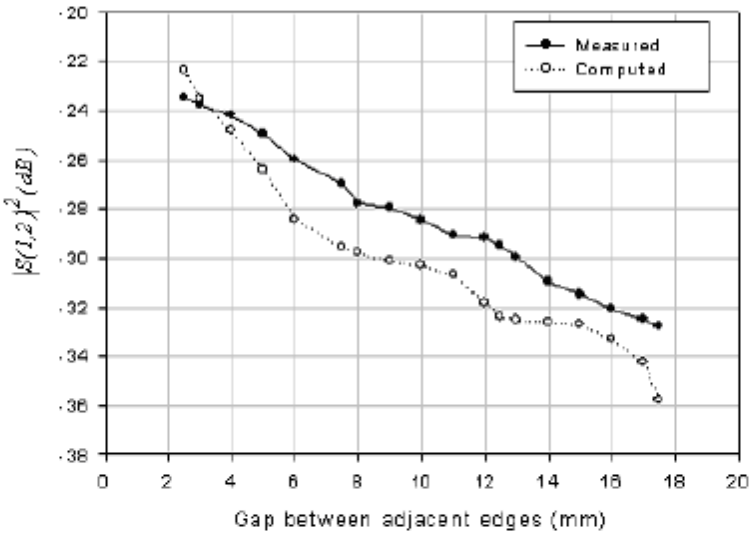

Fig. 6.3 Analyzed and measured [173] values of mutual coupling parameter at 1.44 GHz for two gap-coupled circular microstrip antennas.

Table 6.2 Dimensions of the two gap-coupled circular microstrip antennas loaded with shorting post.

Radius of feed patch (r_1)(mm)	Radius of parasitic patch (r_2) (mm)	Thickness of substrate (h) (mm)	Dielectric constant (ε_r)
15	15	1.59	2.2

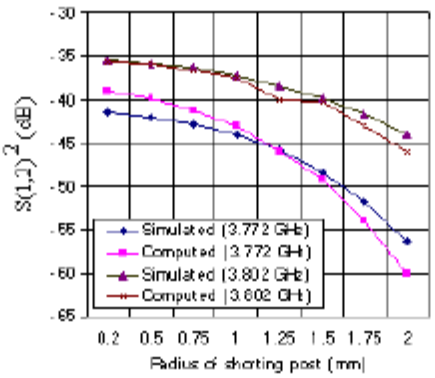

Fig 6.4 Variation of the mutual coupling parameter S(1,2) of two gap-coupled circular microstrip antennas loaded with shorting post with the radius of shorting post for the gap distance between adjacent edges = 0.5 mm.

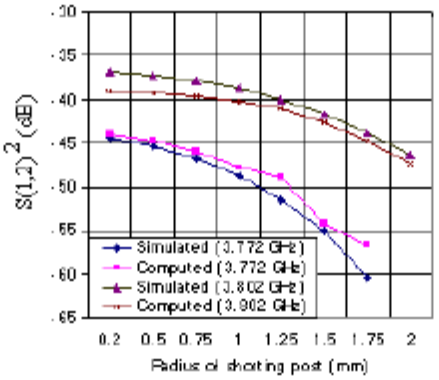

Fig 6.5 Variation of the mutual coupling parameter S(1,2) of two gap-coupled circular microstrip antennas loaded with shorting post with the radius of shorting post for the gap distance between adjacent edges = 1.00 mm.

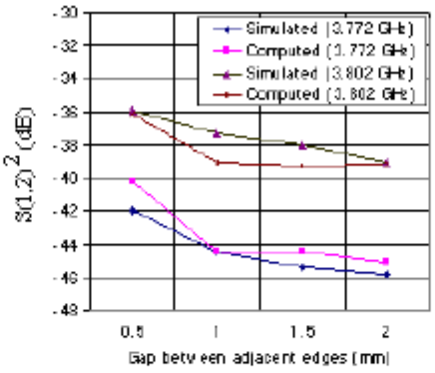

Fig 6.6 Variation of the mutual coupling parameter S(1,2) of two gap-coupled circular microstrip antennas loaded with shorting post with the gap distance between adjacent edges for radius of shorting post = 0.5 mm.

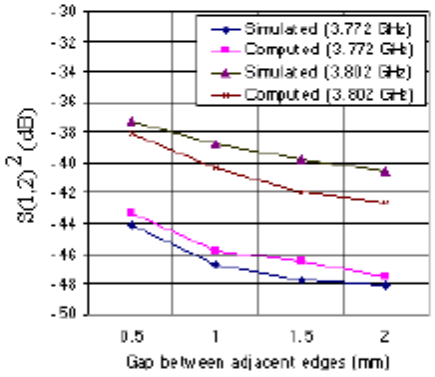

Fig 6.7 Variation of the mutual coupling parameter S(1,2) of two gap-coupled circular microstrip antennas loaded with shorting post with the gap distance between adjacent edges for radius of shorting post = 1.00 mm.

6.5 Conclusion

In this chapter, the numerical models for the mutual coupling between two gap-coupled circular microstrip antennas with and without the shorting post have been investigated. The mutual impedance is calculated using cavity model and reaction theorem. For the

gap-coupled circular microstrip antennas loaded with shorting post, the analyzed results are compared with the simulated results. The comparison between the analyzed and reported literature shows good agreement for small gap distance between circular patches in case of gap-coupled circular microstrip patch antennas. As the gap distance between the adjacent edges increases, the coupling is weaker and vice-versa. The present model can be comfortably extended to the multiple patches.

CHAPTER -7

DESIGN OF A NOVEL PRINTED CROSS ANTENNA FOR WIDEBAND APPLICATIONS

7.1 Introduction

Microstrip antennas are suitable for circuit integration resulting in compact communication systems. The disadvantage of patch antennas, however, lies in the narrow impedance bandwidth of operation. Various techniques for improving bandwidth have been presented [4, 175]. Lee and Lim [176] have designed and fabricated a planar wideband microstrip antenna in which the resonance frequency is controlled. The geometry of the antenna is coplanar waveguide fed double-T microstrip antenna. An antenna impedance bandwidth of 450 MHz is obtained within IMT 2000 frequency bands. Recently a planer printed triangular monopole antenna (PTMA) has been presented for operation in ultra-wideband (UWB) communication system in the frequency range 3.1 GHz to 10.6 GHz [177]. The structure of the antenna consists of a tapered radiating element excited by a microstrip line. The ground plane below the monopole is etched out resulting in omni-directional radiation.

In this chapter, an innovative design of a cross patch antenna, on a substrate with ground plane partially removed, is presented. The antenna is fed by a microstrip line and yields an omnidirectional pattern. Two antennas with different dimensions are presented. Optimization of the design leads to a bandwidth of 28% with sufficient directivity. The proposed antennas can be used for wideband communication applications. Here, a variation to the above structure is presented. The proposed structure utilizes a cross type patch on a substrate with ground plane removed. The antenna is excited by microstrip line. A bandwidth (2:1 VSWR) of 28% has been achieved with reasonable directivity.

7.2 Antenna Configuration

A cross type printed antenna is shown in Fig. 7.1.

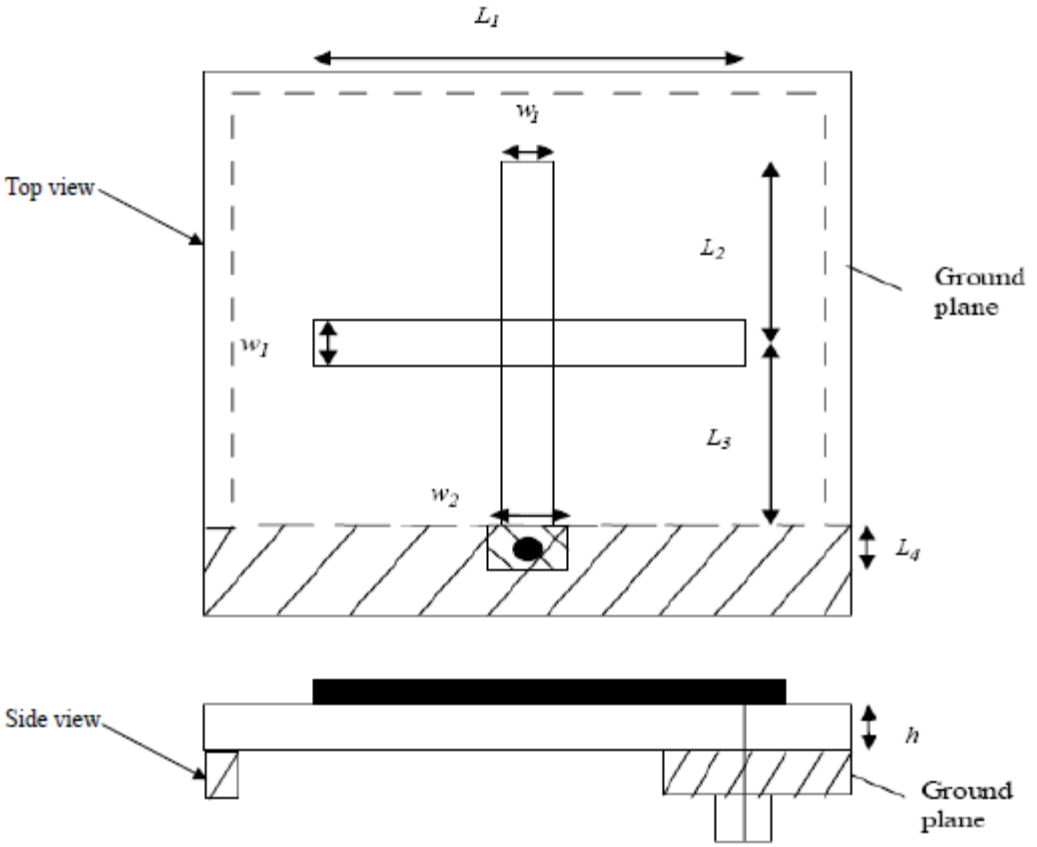

Fig. 7.1 Geometrical configuration of the cross patch antenna.

From the feeding microstrip line of width w_2, a vertical line of 50 Ω and length L is printed, where $L = L_2 + L_3$. It is loaded by a 50 Ω line acting as a dipole of length L_1. The length is chosen be nearly 2λ at the frequency of operation. The loaded impedance is converted to 50 Ω seen by the coaxial probe using a $\lambda/4$ microstrip feed line. However, the feeding line width is optimized using CST Microwave Studio a commercially available software based on finite integral technique to obtain maximum bandwidth around the frequency of operation. The two antennas are designed with parameters given in table 7.1. The simulated results are presented in the following section.

Table 7.1 Dimensions of the proposed antennas (h =1.58 mm, ε_r=4.9).

	L_1 (mm)	L_2 (mm)	L_3 (mm)	L_4 (mm)	w_1 (mm)	w_2 (mm)
Antenna 1	30	15	15	5	2.5	2.5
Antenna 2	40	20	20	5	2.5	0.45

7.3 Results and Discussion

The antennas described in above section are simulated using CST Microwave Studio. The simulated results are presented in this section.

The return losses for both antennas are shown in Fig 7.2. The bandwidth (2:1 VSWR) of antenna 1 is from 8.1 GHz to 10.9 GHz (28%), and of antenna 2 is from 6.1 GHz to 8.7 GHz (36%).

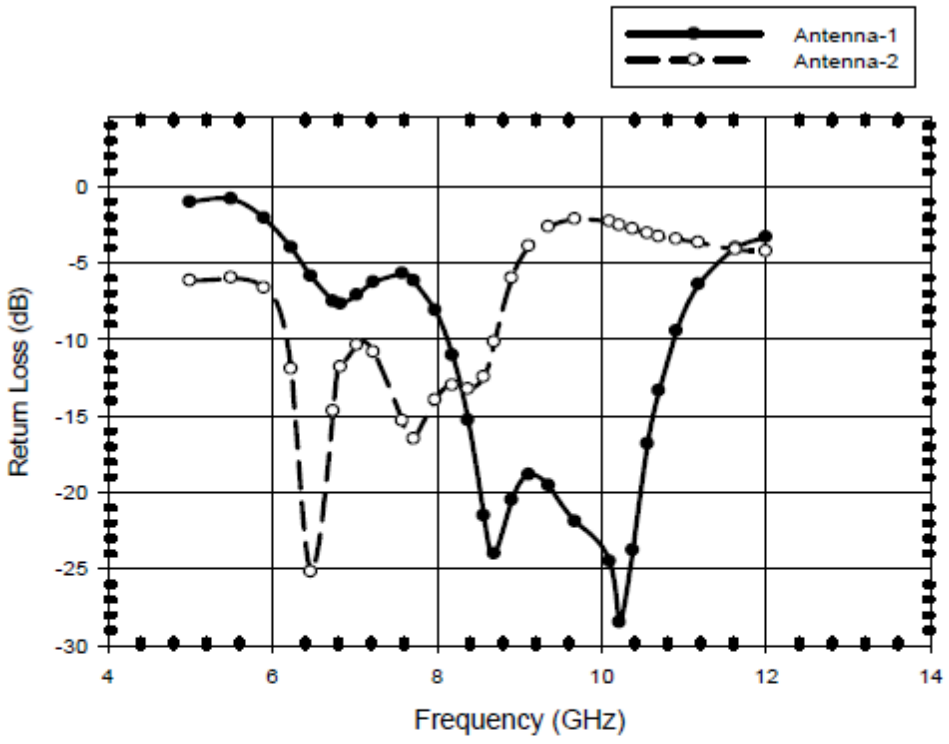

Fig 7.2 Frequency characteristics of the return loss (dB) of the cross patch antenna.

The beam patterns for both antennas at different frequencies are analyzed. All the beam patterns are almost similar; a typical beam pattern at 8.2 GHz is shown in Fig. 7.3. In Fig. 7.3, it is seen that antennas behave like a dipole with a length 2λ with squint angle at 35° from zenith and four lobes as explained in [178].

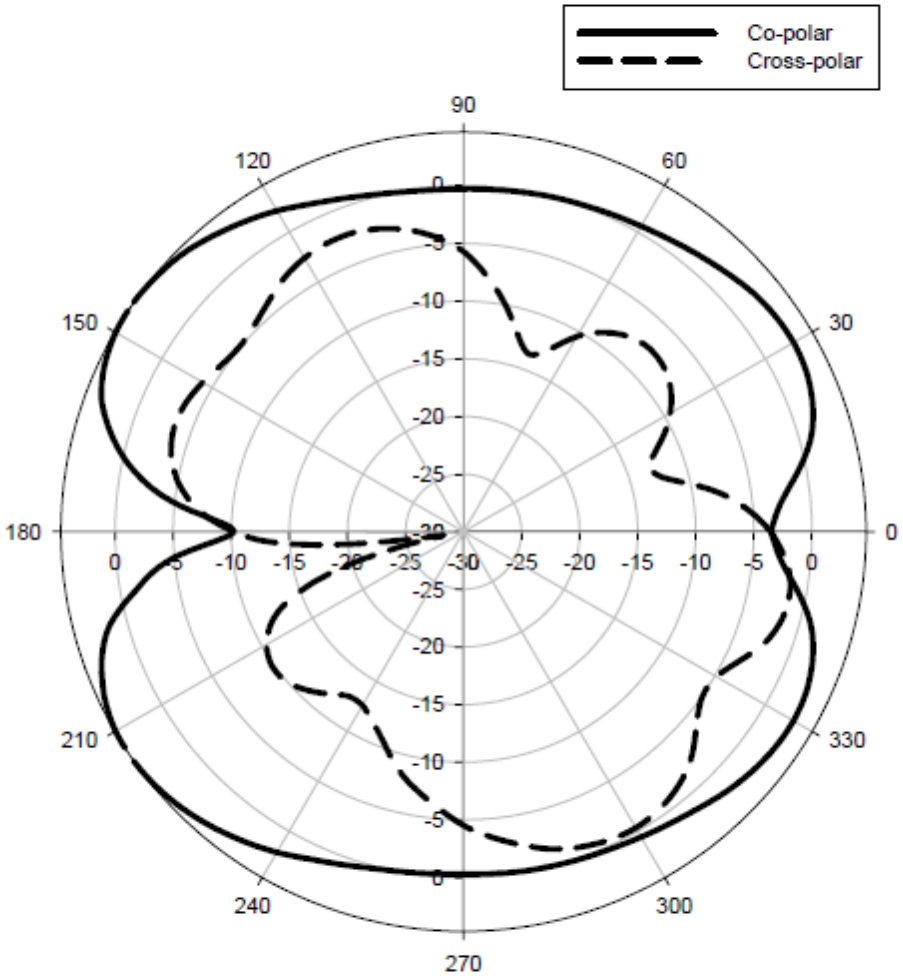

Fig 7.3 Simulated beam pattern of the cross patch antenna at 8.2 GHz.

The beam pattern shows an omnidirectional nature. The cross polarization is relatively high because of the crossed dipole structure. The main radiating element is a

dipole with length L_1. The crossed dipole structure is used for impedance matching. Fig 7.3 shows the plot of directivity. The maximum directivity is 4.7 dBi with a radiation efficiency of 77%.

The theoretical beam pattern at frequency 8.2 GHz is shown in Fig 7.4. The pattern factor (P.F.) for a dipole antenna is given as [172]:

$$\text{P.F.} = \frac{\cos[(\beta L\cos\theta)/2] - \cos(\beta L/2)}{\sin\theta}$$

where β = propagation constant, L = length of antenna. For the present case the length is chosen to be 2λ at 10 GHz. The computed pattern factor is compared with full wave simulation results. Except for the minor lobes, the pattern agree well, thereby suggesting that proposed theory is reasonable accurate.

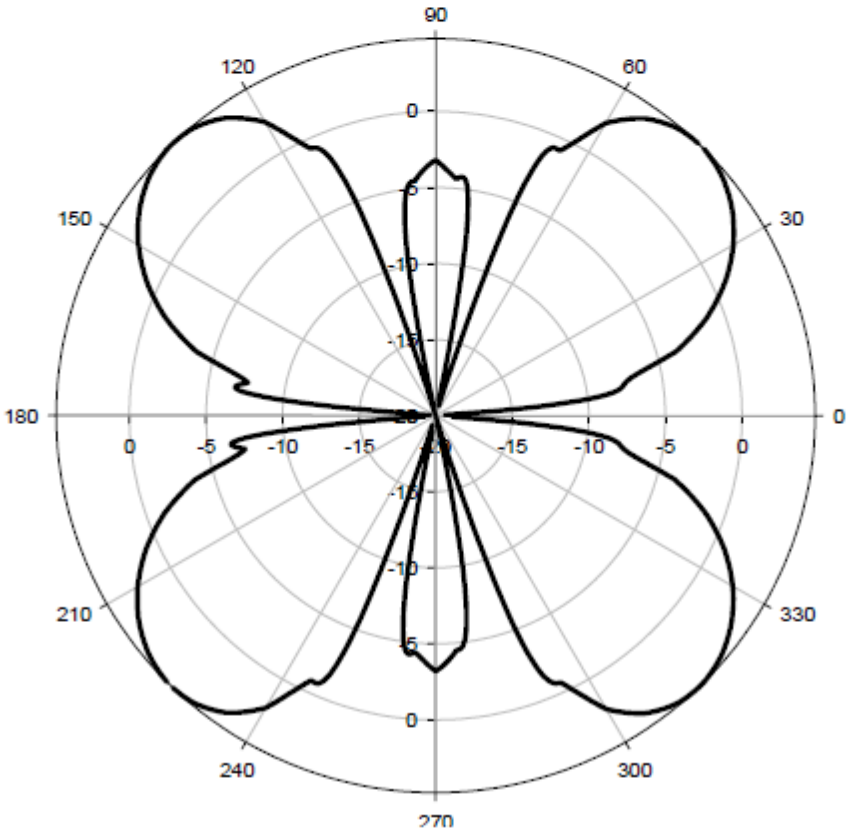

Fig 7.4 Theoretical beam pattern of dipole of the given length at 8.2 GHz.

7.4 Conclusion

In this chapter, a low profile antenna in cross shape for wide band application has been presented. The impedance matching is good over the band of interest and pattern is stable over the frequency range. The cross structure can be modified to operate in different frequency ranges with suitable impedance matching. By loading more than one cross in a single structure it is envisaged that an antenna can be developed for ultra wideband applications ranging from frequency 3.1 GHz to 10.6 GHz.

CHAPTER -8

CONCLUSIONS AND FUTURE SCOPE

8.1 Conclusions

In this thesis, the analytical and simulation studies of the multi-frequency, compact and broadband microstrip antennas have been carried out. A numerical model for the resonant frequency of the two gap-coupled circular microstrip patch antenna has been developed. The gap-coupled circular microstrip structure is divided in to two concentric regions. The field expressions for these two regions are written and different boundary conditions are applied. The gap between the parasitic and fed patch is considered as a π type network circuit and finally the transcendental equation for calculating the resonant frequencies has been derived. The computed results are compared with the simulated for the two gap-coupled circular microstrip antennas. Since cavity model analysis is used in conjunction with circuit theory, the mode number prediction is also done. The same is validated through obtaining the current distribution for full-wave solutions. The presented gap-coupled circular microstrip antenna generates two modes that is TM_{11} and TM_{21}.

A numerical model for computing the resonant frequencies of the gap-coupled circular microstrip patch antennas loaded with shorting post has been developed. The gap-coupled circular microstrip antennas loaded with shorting post generates three modes that is TM_{01}, TM_{11} and TM_{21} mode. The resonant frequency of the TM_{01} mode is lower than the TM_{11} and TM_{21} mode. So the size of the microstrip antennas can be reduced by shorting the patch for same frequency applications. The effect of the gap distance between adjacent edges of patches on resonant frequency for each mode has been presented. The effect of diameter of shorting post on resonant frequency of each mode is also studied. The resonant frequency of the two gap-coupled circular microstrip antennas depends on both parameters that is gap distance between adjacent edges and diameter of shorting post; it increases on increasing the diameter of shorting post and decreases on increasing the gap between adjacent edges of parasitic and fed patch. So the resonant

frequencies as well as the size of the gap-coupled circular microstrip antennas loaded with shorting post can be controlled by varying the gap and diameter post.

The input impedance is one of the major parameters of an antenna. A numerical model for calculating the input impedance of the gap-coupled circular microstrip patch antennas is developed. The concept of coupled microstrip lines is extended to the coupled circular microstrip antennas and the calculated results of the two gap-coupled circular microstrip antennas are compared with the reported literature of the coupled microstrip lines. The even and odd mode impedances are calculated from the even and odd mode equivalent circuits. With the help of the even and odd mode impedances the overall impedance of the structure has been calculated. The calculated results are compared with the simulated results. The comparison of these results shows good agreement except for initial range of frequencies. This slightly deviation may be due to presence of another mode in simulated results. Variation of input impedance of gap-coupled circular microstrip antennas with gap distances between adjacent edges of feed patch and parasitic patch as well as the variation of input impedance with feed location is also discussed. The input impedance depends heavily on the feed location and increases when feed point moves from center towards edge of the patch. By varying the feed position, the input impedance of the two gap-coupled circular microstrip antennas can be controlled.

The size of the gap-coupled circular microstrip antenna can be miniaturized by loading the patch with shorting post. A numerical model for input impedance of gap-coupled circular microstrip antenna loaded with shorting post has been developed. The concept of coupled microstrip line is applied to gap-coupled circular microstrip antennas loaded with shorting post and input impedance is calculated. In the gap-coupled circular microstrip antennas loaded with shorting post, the impedance due to shorting post has been taken in to account and the impedance due to shorting post is shunt to the microstrip patch. The over all impedance of the structure has been calculated with the help of even and odd mode impedance of the structure. The comparison of computed and simulated results shows good agreement except initial range of frequencies. It may be due to presence of another mode in simulated results. Variation of input impedance with gap distance between adjacent edges as well as with diameter of shorting post is studied.

Further, the simulation results for TM_{01} mode have been presented. The variation of input impedance for TM_{01} mode with gap between adjacent edges as well as with diameter of shorting post is shown. The input impedance heavily depends on the diameter of shorting post. So by varying the diameter of shorting post the input impedance can be controlled.

For analysis of the two gap-coupled structures or antenna arrays, mutual coupling is an essential parameter. The numerical models for mutual coupling between two gap-coupled circular microstrip antennas loaded and without loaded have been developed. The mutual impedance is calculated using the cavity model and reaction theorem. The comparison between the analyzed and reported literature shows good agreement for small gap distances between circular patches in case of the two gap-coupled circular microstrip patch antennas. For gap-coupled circular microstrip antennas loaded with shorting post, the calculated results are compared with the simulated results. As the gap between the adjacent edges increases, the coupling is weaker and vice-versa.

As the narrow bandwidth is the major disadvantage of the microstrip antennas. A novel design of wideband microstrip antennas has been presented. A low profile antenna in cross shape for wide band application has been demonstrated. The impedance matching is good over the band of interest and pattern is stable over the frequency range. The cross structure can be modified to operate in different frequency ranges with suitable impedance matching.

8.2 Future Scope

The proposed numerical models of the resonant frequency and input impedance for the two gap-coupled circular microstrip antennas can be extended to multiple resonators as well as analysis with different patch sizes and patch shapes. The proposed models of the resonant frequency and input impedance for the two gap-coupled circular microstrip antennas loaded with shorting post can be extended to multiple resonators as well as with different patch shapes and patch sizes. An asymmetric gap-coupled microstrip antenna configuration has an inherent capability for impedance transformation which can be used for tapered antenna arrays that can be modeled. By using one more cross patch antenna, the design of cross patch antenna for wideband applications can be extended for ultra

wideband applications. The analytical model can be developed for the proposed design of novel cross patch antennas.

REFERENCES

[1] G. A. Deschamps, "Microstrip microwave antennas," *Proceedings* of *3rd USAF Symposium on Antennas*, 1953.

[2] J. Q. Howell, "Microstrip antennas," *Proceedings* of *IEEE Antennas and Propagation Society International Symposium Digest*, pp. 177-180, 1972.

[3] R. E. Munson., "Conformal microstrip antennas and microstrip phased arrays," *IEEE Transactions on Antennas and Propagation,* vol. 22, pp. 74-78, 1974.

[4] R. Garg, P. Bhartia, I. Bahl and A. Ittipiboon, "Microstrip Antenna Design Handbook," *Artrech House Publishers*, Boston, 2001.

[5] Constantine A. Balanis, "Antenna Theory: Analysis and Design," *Wiley*, New Mexico, 2005.

[6] Y. J. Wang and C. K. Lee, "Compact and broadband microstrip patch antenna for the 3G IMT-2000 handsets applying styrofoam and shorting-posts," *Progress In Electromagnetics Research,* vol. 47, pp. 75–85, 2004.

[7] J. P. Thakur, J. S. Park, M. S. Joung, B. J. Jang and H. R. Oh, " Quad band CEIFS antenna for mobile communication," *Proceedings* of *IEEE Microwave Theory and Technique Society International Microwave Symposium Digest*, pp. 198-201, 2006.

[8] A. K. Bhattacharya and R. Garg, "Generalised transmission line model for microstrip patches," *IEE Proceeding on Microwave, Antennas and Propagation,* vol. 132, no. 2, pp. 93-98, 1985.

[9] A. K. Bhattacharya and R. Garg, "Input impedance of annular ring microstrip antennas using circuit theory approach," *IEEE Transactions on Antennas and Propagation*, vol. 33, no. 4, pp. 369-374, 1985.

[10] A. K. Bhattacharya and R. Garg, "Analysis of annular sector and circular sector microstrip antennas," *Electromagnetics*, vol. 6, no. 3, pp. 229-242, 1986.

[11] A. Derneryd, "A theoretical investigation of the rectangular microstrip antenna," *IEEE Transactions on Antennas and Propagation,* vol. 26, no. 4, pp. 532-535, 1978.

[12] A. Derneryd, "Linearly polarized microstrip antennas," *IEEE Transactions on Antennas and Propagation,* vol. 24, no. 6, pp 846-851, 1976.

[13] Y. T. Lo, D. Solomon and W. F. Richards, "Theory and experiment on microstrip antennas," *IEEE Transactions on Antennas and Propagation*, vol. 27, no. 2, pp. 137-145, 1979.

[14] W. F. Richards, Y. T. Lo and D. D. Harrison, "An improved theory for microstrip antennas and applications," *IEEE Transactions on Antennas and Propagation,* vol. 29, no. 2, pp. 38-46, 1981.

[15] Y. T. Lo and W. F. Richards, "Perturbation approach to design of circularly polarized microstrip antennas," *Electronics Letters*, vol. 17, no. 1, pp. 383-385, 1981.

[16] J. R James and P. S. Hall (Eds), "Handbook of Microstrip Antennas," *Peter Prengrinus*, London, 1989.

[17] J. Watkins, "Circular resonant structures in microstrip," *Electronics Letters*, vol. 5, no. 21, pp. 524-525, 1969.

[18] L. C. Shen, S. A. Long, M. R. Allerdin and M. D. Walton., "Resonant frequency of a circular disk printed-circuit antenna," *IEEE Transactions on Antennas and Propagation*, vol. 25, pp. 595-596, 1977.

[19] S. A. Long, L. C. Shen and P. B. Morel, "Theory of the circular disk printed circuit antenna," *IEE Proceeding on Microwave, Antennas and Propagation,* vol. 125, pp. 925-928, 1978.

[20] S. A. Long, L. C. Shen, M. D. Walton and M. R. Allerding, "Impedance of a circular disk printed circuit antenna," *Electronics Letters*, vol. 14, no. 21, pp. 684-686, 1978.

[21] A. G. Derneryd, "Analysis of the microstrip disk antenna element," *IEEE Transactions on Antennas and Propagation*, vol. 27, no. 5, pp. 660-664, 1979.

[22] L. C. Shen, "Analysis of the circular- disk printed-circuit antenna," *IEE Proceeding on Microwave, Antennas and Propagation*, vol. 126, pp. 1220-1222, 1979.

[23] S. Yano and A. Ishimaru, "A theoretical study of the input impedance of a circular microstrip disk antenna," *IEEE Transactions on Antennas and Propagation*, vol. 29, no. 1, pp. 77-83, 1981.

[24] A. K. Bhattacharya, "Characteristics of circular patch on thick substrate and superstrate," *IEEE Transactions on Antennas and Propagation,* vol. 39, no. 7, pp. 1038-1041, 1991.

[25] A. K. Bhattacharya, "Generalised Transmission Line Model of Microstrip Patch Antennas and Some Applications," Ph. D Thesis, *Indian Institute of Technology, Kharagpur, India*, 1985.

[26] W. C. Chew and J. A. Kong, "Analysis of a circular microstrip disk antenna with a thick dielectric substrate," *IEEE Transactions on Antennas and Propagation*, vol-29, no. 1, pp. 68-76, 1981.

[27] K. Araki and T. Itoh, "Hankel transform domain analysis of open circular microstrip radiating structures," *IEEE Transactions on Antennas and Propagation,* vol. 29, no. 1, pp. 84-89, 1981.

[28] K. L. Wu, J. Litva, R. Fralich and C. Wu, "Full wave analysis of arbitrarily shaped line-fed microstrip antenna using triangular finite-element method," *IEE Proceeding on Microwave, Antennas and Propagation,* vol. 138, no. 5, pp. 421-428, 1991.

[29] G. M. Turner and C. G. Christodoulu, "Finite difference time domain analysis of circular microstrip antenna," *Proceedings* of *IEEE Antennas and Propagation Society International Symposium Digest*, pp. 1292-1295, 1996.

[30] C. K. Wu and K. L. Wong, "Broadband microstrip antenna with directly coupled and gap-coupled parasitic patches," *Microwave and Optical Technology Letters,* vol. 22, no. 5, pp. 348–349, 1999.

[31] T. Huynh and K. F. Lee, "Single-layer single-patch wideband microstrip antenna," *Electronics Letters,* vol. 31, no. 16, pp. 1310–1311, 1995.

[32] K. L. Wong and W. H. Hsu, "Broadband triangular microstrip antenna with u-shaped slot," *Electronics Letters,* vol. 33, no. 25, pp. 2085–2087, 1997.

[33] N. Herscovici, "A wide-band single-layer patch antenna," *IEEE Transactions on Antennas and Propagation,* vol. 46, no. 4, pp. 471–473, 1998.

[34] K. L. Wong and W. H. Hsu, "A broadband rectangular patch antenna with a pair of wide slits," *IEEE Transactions on Antennas and Propagation*, vol. 49, no. 9, pp. 1345–1347, 2001.

[35] C. L. Tang, C. W. Chiou and K. L. Wong, "Broadband dual-frequency V-shape patch antenna," *Microwave and Optical Technology Letters,* vol. 25, no. 2, pp. 121–123, 2000.

[36] C. L. Tang, J. Y. Chiou and K. L. Wong, "A broadband probe-fed patch antenna with a bent ground plane," *Proceedings Asia Pacific Microwave Conference*, pp. 1356–1359, 2000.

[37] C. L. Mak, K. M. Luk and K. F. Lee, "Microstrip line-fed L-strip patch antenna," *IEE Proceeding on Microwave, Antennas and Propagation,* vol. 146, no. 4, pp. 282–284, 1999.

[38] K. M. Luk, L. K. Au Yeung, C. L. Mak, and K. F. Lee, "Circular patch antenna with an L-shaped probe," *Microwave and Optical Technology Letters,* vol. 20, no. 4, pp. 256–257, 1999.

[39] P. S. Hall, "Probe compensation in thick microstrip patches," *Electronics Letters,* vol. 23, no. 11, pp. 606–607, 1987.

[40] G. A. E. Vandenbosch and A. R. Vande Capelle, "Study of the capacitively fed microstrip antenna element," *IEEE Transactions on Antennas and Propagation,* vol. 42, no. 12, pp. 1648–1652, 1994.

[41] G. A. E. Vandenbosch, "Network model for capacitively fed microstrip antenna," *Electronics Letters,* vol. 35, no. 19, pp. 1597–1599, 1999.

[42] K. L. Wong and Y. F. Lin, "Small broadband rectangular microstrip antenna with chip resistor loading," *Electronics Letters,* vol. 33, no. 19, pp. 1593–1594, 1997.

[43] K. L.Wong and K. P. Yang, "Modified planar inverted F antenna," *Electronics Letters*, vol. 34, no. 1, pp. 6–7, 1998.

[44] S. Dey, C. K. Aanandan, P. Mohanan and K. G. Nair, "A new broadband circular patch antenna," *Microwave and Optical Technology Letters,* vol. 7, no. 13, pp. 604–605, 1994.

[45] J. Y. Sze and K. L. Wong, "Broadband rectangular microstrip antenna with a pair of toothbrush-shaped slots," *Electronics Letters,* vol. 34, no. 23, pp. 2186–2187, 1998.

[46] J. Y. Sze and K. L. Wong, "Single-layer single-patch broadband rectangular microstrip antenna," *Microwave and Optical Technology Letters,* vol. 22, no. 4, pp. 234–236, 1999.

[47] J. Y. Sze and K. L.Wong, "Slotted rectangular microstrip antenna for bandwidth enhancement," *IEEE Transactions on Antennas and Propagation,* vol. 48, no. 8, pp. 1149–1152, 2000.

[48] J. Y. Jan and K. L. Wong, "A broadband circular microstrip antenna with two open-ring slots," *Microwave and Optical Technology Letters,* vol. 23, no. 4, pp. 205–207, 1999.

[49] S. T. Fang, K. L. Wong and T. W. Chiou, "Bandwidth enhancement of inset-microstrip line-fed equilateral-triangular microstrip antenna," *Electronics Letters,* vol. 34, no. 23, pp. 2184–2186, 1998.

[50] M. C. Pan and K. L. Wong, "A broadband slot-loaded trapezoid microstrip antenna," *Microwave and Optical Technology Letters,* vol. 24, no. 1, pp. 16–19, 2000.

[51] J. H. Lu, C. L. Tang, and K. L. Wong, "Novel dual-frequency and broadband designs of single-feed slot-loaded equilateral-triangular microstrip antennas," *IEEE Transactions on Antennas and Propagation,* vol. 48, no. 7, pp. 1048–1054, 2000.

[52] K. L. Wong and J. Y. Jan, "Broadband circular microstrip antenna with embedded reactive loading," *Electronics Letters,* vol. 34, no. 19, pp. 1804–1805, 1998.

[53] J. Y. Jan and K. L. Wong, "Microstrip-line-fed broadband circular microstrip antenna with embedded reactive loading," *Microwave and Optical Technology Letters,* vol. 22, no. 3, pp. 200–202, 1999.

[54] N. Fayyaz and S. Safavi-Naeini, "Bandwidth enhancement of a rectangular patch antenna by integrated reactive loading," *Proceedings* of *IEEE Antennas and Propagation Society International Symposium Digest*, pp. 1100–1103, 1998.

[55] K. L. Wong and J. S. Kuo, "Bandwidth enhancement of bow-tie microstrip antenna using integrated reactive loading," *Microwave and Optical Technology Letters,* vol. 22, no. 1, pp. 69–71, 1999.

[56] K. L. Wong, J. S. Kuo, S. T. Fang and T.W. Chiou, "Broadband microstrip antennas with integrated reactive loading," *Proceedings of Asia Pacific Microwave Conference*, pp. 352–354, 1999.

[57] D. M. Pozer, "Microstrip antennas," *Proceedings of the IEEE*, vol. 80, pp. 79-91, 1992.

[58] S. A. Long and M. D. Walton, "A dual frequency stacked circular disc antenna," *Proceedings* of *IEEE Antennas and Propagation Society International Symposium Digest*, pp. 260-263, 1978.

[59] F. Crop and D. M. Pozar, "Millimeter wave design of wide band aperture coupled stacked microstrip antennas," *IEEE Transactions on Antennas and Propagation,* vol. 39, no. 12, pp. 1770-1776, 1991.

[60] G. Dubost and A. Zerguerras, "Transmission line model analysis of arbitrary shape symmetrical patch antenna coupled with a director," *Electronics Letters*, vol. 26, no. 13, pp. 952-954, 1990.

[61] J. G. Tagle and C. G. Christodoulou, "Extended cavity model analysis of stacked microstrip ring antennas," *IEEE Transactions on Antennas and Propagation*, vol. 45, no. 11, pp. 1626-1635, 1997.

[62] C. H. Chen, A. Tulintseff and R. Sorbello, "Broadband two layer microstrip antennas," *Proceedings* of *IEEE Antennas and Propagation Society International Symposium Digest*, pp. 252-254, 1984.

[63] R. Q. Lee, K. F. Lee and J. Bobinchak, "Characteristics of a two layer electromagnetically coupled rectangular patch antennas," *Electronics Letters*, vol. 23, no. pp. 1070-1072, 1987.

[64] F. Croq, G. Kossiavas and A. Papiernik, "Stacked resonators for bandwidth enhancement: a comparison of two feeding techniques," *IEE Proceeding on Microwave, Antennas and Propagation,* vol. 140, no. 4, pp. 303-308, 1993.

[65] C. H. Tsao, Y. M. Hwang, F. Kilbarg and F. Dietrich, "Aperture coupled patch antennas with wide bandwidth and dual polarization capabilities," *Proceedings* of *IEEE Antennas and Propagation Society International Symposium Digest*, pp. 936-939, 1988.

[66] A. Ittipiboon, B. Clarke and M. Cuhaci, "Slot coupled stacked microstrip antennas," *Proceedings* of *IEEE Antennas and Propagation Society International Symposium Digest*, pp. 1108-1111, 1990.

[67] S. D. Targonski, R. B. Waterhouse and D. M. Pozar, "Design of wideband aperture stacked patch microstrip antennas," *IEEE Transactions on Antennas and Propagation*, vol. 46, pp. 1245-1251, 1998.

[68] Y. Zehforoosh, C. Ghobadi and J. Nourinia, "Antenna design for ultra wideband application using a new multilayer structure," *Progress In Electromagnetic Research*, vol.2, no.6, pp. 544-549, 2006.

[69] D. H. Schaubert and F. G. Farrar, "Some conformal printed circuit antenna designs," *Proceedings of Workshop Printed Circuit Antenna Technology,* New Mexico State University, Las Cruces, NM, pp. 5.1-5.21, 1979.

[70] G. Kumar and K. C. Gupta, "Broadband microstrip antennas using additional resonators gap coupled to the radiating edges," *IEEE Transactions on Antennas and Propagation*, vol. 32, no. 12, pp. 1375-1379, 1984.

[71] G. Kumar and K. C. Gupta, "Nonradiating edges and four edges gap coupled multiple resonator broadband microstrip antennas," *IEEE Transactions on Antennas and Propagation*, vol. 33, no. 2, pp. 173-178, 1985.

[72] C. Wood, "Improve bandwidth of microstrip antennas using parasitic elements," *IEE Proceedings Microwaves, Optics and Acoustics*, vol. 127, pp. 231-234, 1980.

[73] C. K. Aanandan, P. Mohanan and K. G. Nair, "Broad-band gap coupled microstrip antenna," *IEEE Transactions on Antennas and Propagation*, vol.38, no. 10, pp. 1581-1586, 1990.

[74] M. B. Nile, A. A. Rasheed and G. Kumar, "Broadband gap coupled semicircular and triangular microstrip antennas," *Proceedings* of *IEEE Antennas and Propagation Society International Symposium Digest,* pp. 1202-1205, 1994.

[75] G. Kumar and K. P. Ray, "Stacked gap coupled multi-resonator rectangular microstrip antennas," *Proceedings* of *IEEE Antennas and Propagation Society International Symposium Digest,* vol. 3, pp. 514-517, 2001.

[76] Raj Kumar and V. A. Deshmukh, "On the design of compact broadband gap-coupled microstrip patch antenna with PBG," *Proceedings of IEEE Asia Pacific Microwave Conference*, vol. 2, 2005.

[77] K. P. Ray, S. Ghosh and K. Nirmala, "Compact broadband gap-coupled microstrip antennas," *Proceedings* of *IEEE Antennas and Propagation Society International Symposium Digest,* pp. 3719-3722, 2006.

[78] K. P. Ray and G. Kumar, "Multi-frequency and broadband hybrid-coupled circular microstrip antennas," *Electronics Letters*, vol. 33, no. 6, pp. 437-438, 1997.

[79] P. Bhartia and I. J. Bahl, "A frequency agile microstrip antennas," *Proceedings* of *IEEE Antennas and Propagation Society International Symposium Digest*, vol. 20, pp. 304-307, 1982.

[80] J. T. Aberle, M. Chu and C. R. Birtcher, "Scattering and radiation properties of varactor tuned microstrip antennas," *Proceedings* of *IEEE Antennas and Propagation Society International Symposium Digest*, pp. 2229-2232, 1992.

[81] R. B. Waterhouse and N. V. Shuley, "Dual frequency microstrip rectangular patches," *Electronics Letters*, vol. 28, no. 7, pp. 606-607, 1992.

[82] S. A. Bokhari, J. F. Zurcher, J. R. Mosiq and F. E. Gardiol, "A small microstrip patch antenna with a tuning option," *IEEE Transactions on Antennas and Propagation*, vol. 44, no. 11, pp. 1521-1527, 1996.

[83] V. Palanisamy and R. Garg, "Analysis of circularly polarized square ring and crossed-strip antennas," *IEEE Transactions on Antennas and Propagation*, vol. 34, no. 11, pp. 1340-1346, 1984.

[84] W. S. Chen and H. D. Chen, "Single feed circularly polarized square ring microstrip antenna with a slit," *Proceedings* of *IEEE Antennas and Propagation Society International Symposium Digest*, pp. 1360-1363, 1998.

[85] K. L. Wong and J. Y. Wu, "Single-feed small circularly polarized square microstrip antenna," *Electronics Letters*, vol. 33, no. 22, pp. 1833-1834, 1997.

[86] C. Y. Haung and J. Y. Wu, "Compact microstrip antenna loaded with very high permittivity," *Proceedings* of *IEEE Antennas and Propagation Society International Symposium Digest*, pp. 680-683, 1998.

[87] M. Yawata and H. Arai, "Self-diplexing stacked patch antenna for satellite mobile mode handset system," *Proceedings* of *IEEE Antennas and Propagation Society International Symposium Digest*, pp. 2124-2127, 1998.

[88] H. Imasaki, "A circularly polarized small size microstrip antenna with a cross slot," *IEEE Transactions on Antennas and Propagation*, vol. 44, no. 10, pp. 1399-1401, 1996.

[89] J. H. Lu, C. L. Tang and K. L. Wong, "Single-feed slotted equilateral triangular microstrip antenna for circular polarization," *IEEE Transactions on Antennas and Propagation,* vol. 47, no. 7, pp. 1174-1178, 1999.

[90] B. F. Wang, and Y. T. Lo, "Microstrip antennas for dual-frequency operation," *IEEE Transactions on Antennas and Propagation*, vol. 32, no. 9, pp. 938-943, 1984.

[91] M. Yazidi, M. Himdi and J. P. Daniel, "Aperture coupled microstrip antenna for dual frequency operation," *Electronics Letters*, vol.29, no. 17, pp 1506-1508, 1993.

[92] J. H. Lu, "Single feed dual-frequency rectangular microstrip antenna with pair of step-slots," *Electronics Letters*, vol. 35, no. 5, pp. 354-355, 1999.

[93] Y. M. Antar, A. I. Ittipiboon and A. K. Bhattacharya, "A dual-frequency antenna using a single patch and an inclined slot," *Microwave and Optical Technology Leters.*, vol. 8, no. 6, pp. 309-310, 1995.

[94] Y. Murukami, W. Chujo, I. Chiba and M. Fujise, "Dual slot-coupled microstrip antenna for dual frequency operation," *Electronics Letters*, vol. 29, no. 22, pp 1906-1907, 1993.

[95] D. M. Pozar and S. M. Duffy, "A dual-band circularly polarized aperture-coupled stacked microstrip antenna for global positioning satellite," *IEEE Transactions on Antennas and Propagation*, vol. 45, no. 11, pp. 1618-1624, 1997.

[96] K. P. Yang and K. L. Wong, "Inclined slot-coupled compact dual-frequency microstrip antenna with cross slot," *Electronics Letters*, vol. 34, no. 4, pp 321-322, 1998.

[97] K. L. Wong and K. P. Yang, "Small dual frequency microstrip antenna with a cross slot," *Electronics Letters*, vol. 33, no. 23, pp. 1916-1917, 1997.

[98] W. S. Chen, "Single feed dual frequency rectangular microstrip antenna with square slots," *Electronics Letters*, vol. 34, no. 3, pp 231-232, 1998.

[99] V. Palniswamy and R. Garg, "Rectangular ring and H-shaped microstrip antennas: alternatives to rectangular patch antenna," *Electronics Letters*, vol. 21, no. 19, pp. 874-876, 1985.

[100] W.-L. Chen and G.-M. Wang, "Small size edge-fed sierpinski carpet microstrip patch antennas," *Progress In Electromagnetics Research C, vol. 3, 195–202, 2008.*

[101] A. A. Abdelaziz, "Bandwidth enhancement of microstrip antenna", *Progress In Electromagnetics Research*, vol. 63, pp. 311– 317, 2006.

[102] E. Nishiyama, and M. Aikawa, "FDTD analysis of stacked microstrip antenna with high gain," *Progress In Electromagnetics Research*, vol. 33, pp. 29–43, 2001.

[103] A. Sharma and G. Singh, "Design of single pin shorted three-dielectric-layered substrates rectangular patch microstrip antenna for communication systems," *Progress In Electromagnetics Research Letters*, vol. 2, pp. 157-165, 2008.

[104] D. H. Schaubert, F.G. Farrar, A. Sindoris and S. T. Hayes., "Microstrip antennas with frequency agility and polarization diversity," *IEEE Transactions on Antennas and Propagation*, vol. 29, no. 1, pp.118-123, 1981.

[105] D. L. Sengupta, "Resonant frequency of a tunable rectangular patch antenna," *Electronics Letters*, vol. 20, no. 15, pp. 614-615, 1984.

[106] K. L. Wong and W. S. Chen, "Compact microstrip antennas with dual frequency operation," *Electronics Letters*, vol. 33, no. 8, pp. 646-647, 1997.

[107] W. F. Richards and Y. T. Lo, "Theoretical and experimental investigations of a microstrip radiator with multiple lumped linear loads", *Electromagnetics*, vol. 3, pp. 371-387, 1983.

[108] V. Srinivasan, R. Kapur and G. Kumar, "MNM for compact dual frequency rectangular microstrip antenna," *Proc. APSYM-98*, Cochin, India, pp. 88-91, 1998.

[109] R. B. Waterhouse, "Small microstrip patch antenna," *Electronics Letters*, vol. 31, no. 8, pp. 604-605, 1995.

[110] Z. D. Liu, and P. S. Hall, "Dual-band antenna for hand held portable telephones," *Electronics Letters*, vol. 32, no. 7, pp. 609-610, 1996.

[111] C. R. Rowell and R. D. Murch, "A capacitively loaded PIFA for compact mobile telephone handsets," *IEEE Transactions on Antennas and Propagation*, vol. 45, no. 5, pp. 837-842, 1997.

[112] R. B. Waterhouse, S. D. Targonski and D. M. Kokotoff, "Design and performance of small printed antennas," *IEEE Transactions on Antennas and Propagation*, vol. 46, no. 11, pp. 1629-1633, 1998.

[113] K. L. Wong and W. S. Chen, "Compact microstrip antenna with dual frequency operation," *Electronics Letters*, vol. 33, no. 8, pp. 646-647, 1997.

[114] Porath Rebekka., "Theory of miniaturized shorting-post microstrip antenna," *IEEE Transactions on Antennas and Propagation*, vol. 48, no.1, pp 41-47, 2000.

[115] E. Lee, P. S. Hall and P. Gardner, "Compact dual-band dual-polarization microstrip patch antennas," *Electronics Letters*, vol. 35, no. 13, pp. 1034-1036, 1999.

[116] K. Hirasawa and M. Haneishi, "Analysis, Design and Measurement of Small and Low Profile antennas," *Artech House*, Boston, 1992.

[117] T. C. Edwards, "Fundamentals for Microstrip Circuit Design," *John Wiley and Sons*, New York, 1981.

[118] K. R. Carver and J. W. Mink, "Microstrip antenna technology," *IEEE Transactions on Antennas and Propagation*, vol. 29, no. 1, pp. 2-24, 1981.

[119] K. F. Lee and W. Chen, "Advances in Microstrip and Printed Antennas," *John Wiley and Sons*, New York, 1997.

[120] T. Fujimoto, K. Oyama, K. Tanaka and M. Taguchi, "Stacked square microstrip antenna loading a helical pin," *Proceedings* of *IEEE Antennas and Propagation Society International Symposium Digest*, pp. 833-836, 2007.

[121] N. Ghassemi, J. Rashed-Mohassel, M. H. Neshati and M. Ghassemi, "Slot coupled microstrip antenna for ultra wideband applications in C and X bands," *Progress In Electromagnetics Research M,* vol. 3, pp. 15–25, 2008.

[122] K. P. Ray, M. D. Pandey, A. A. Deshmukh, "Broadband gap-coupled half hexagonal microstrip antennas," *Microwave and Optical Technology Letters*, vol. 50, no. 2, pp. 271 – 275, 2007.

[123] A. A. Deshmukh, G. Kumar, "Compact broadband gap-coupled shorted square microstrip antennas," *Microwave and Optical Technology Letters*, vol. 48, no. 7, pp. 1261 – 1265, 2006.

[124] T. Chakravarty, S. M. Roy, S. K. Sanyal and A. De, "A novel microstrip patch antenna with large impedance bandwidth in VHF/UHF range," *Progress In Electromagnetics Research,* vol. 54, 83–93, 2005.

[125] A. K. Bhattacharya, L. Shafai and R. Garg, "Microstrip antenna-a generalized transmission line," *Progress in Electromagnetics Research*, vol. 4, pp. 45-84, 1991.

[126] M. Mahajan, S. K. Khah, T. Chakarvarty and A. De, "Computation of resonant frequency of annular microstrip antenna loaded with multiple shorting posts," *IET Microwave, Antennas and Propagation*, vol. 2, no. 1, pp. 1-5, 2008.

[127] Aditi Sharma and G. Singh, "Rectangular microstirp patch antenna design at THZ frequency for short distance wireless communication systems," *Journal of Infrared, Millimeter and Terahertz Waves*, vol. 30, no. 1, pp. 1-7, 2009.

[128] Takafumi Fujimotot and Kazumasa Tanakat, "Stacked square microstrip antenna with a shorting post for dual band operation in WLAN applications," *Proceedings of Asia-Pacific Microwave Conference*, no. 3, pp. 1979-1982, 2006.

[129] A. Pandey and A. K. Singh, "Compact H-shaped microstrip antenna with shorting post using IE3D," *Proceedings of International Conference on Recent Advances in Microwave Theory and Applications, Microwave 2008,* pp. 803-805, 2008.

[130] J. S. Roy, N. Chattoraj and N. Swain, "New dual-frequency microstrip antennas for wireless communication," *Romanian Journal of Information Science and Technology*, vol. 10, no. 1, pp. 113-119, 2007.

[131] T. Chakravarty and A. De, "Investigation of modes tunable circular patch radiator with arbitrarily located shorting posts," *IETE Technical Review*, vol. 16, no.1, pp. 109-111, Jan. 1999.

[132] T. Chakravarty and A. De, "Design of tunable modes and dual-band circular patch antenna using shorting posts," *IEE Proceeding on Microwave, Antennas and Propagation*, vol. 146, no. 3, pp 224-228, 1999.

[133] D. M. Pozar and D. H. Schaubert, "Microstrip Antennas," *IEEE Press*, New York 1995.

[134] M. Albooyeh, N. Kamjani and M. Shobeyri, "A novel cross-slot geometry to improve impedance bandwidth of microstrip antennas," *Progress In Electromagnetics Research Letters*, vol. 4, 63-72, 2008.

[135] S. S. Yang, K.-F. Lee, A. A. Kishk and K.-M. Luk, "Design and study of wideband single feed circularly polarized microstrip antennas," *Progress In Electromagnetics Research*, vol. 80, 45-61, 2008.

[136] K. R. Carver and J. W. Mink, "Microstrip antenna technology," *IEEE Transactions on Antennas and Propagation*, vol. 29, pp. 2–24, Jan. 1981.

[137] K. Araki, H. Ueda and M. Takahashi, "Numerical analysis of circular disk microstrip antenna with parasitic elements," *IEEE Transactions on Antennas and Propagation,* vol. 34, no. 12, 1390–1394, Dec. 1986.

[138] I. Park and R. Mittra, "Aperture-coupled small microstrip antenna," *Electronics Letters*, vol. 32, no. 19, pp. 1741–1741, 1996.

[139] S. D. Targonski, R. B. Waterhouse and D. M. Pozar, "Wideband aperture coupled stacked patch antenna using thick substrates," *Electronics Letters*, vol. 32, no. 21, pp. 1941–1942, 1996.

[140] A. Hongming, B. K. J. C. Nauwelaers and A. R. Van de Capelle, "Broadband active microstrip antenna design with the simplified real frequency technique *IEEE Transactions on Antennas and Propagation,* vol. 42, pp. 1612–1619, 1994.

[141] H. F. Pues and A. R. V. D. Capelle, "An impedance-matching technique for increasing the bandwidth of microstrip antennas," *IEEE Transactions on Antennas and Propagation*, vol. 37, pp. 1345–1354, Nov. 1989.

[142] K. P. Ray, V. Sevani and R. K. Kulkarni, "Gap coupled rectangular microstrip antennas for dual and triple frequency operation," *Microwave and Optical Technology Letters*, vol. 49, no. 6, pp. 1480 –1486, 2007.

[143] J. A. Ansari, R. B. Ram, and P. Singh, "Analysis of a gap-coupled stacked annular ring microstrip antenna," *Progress In Electromagnetics Research B*, vol. 4, pp. 147–158, 2008.

[144] L. Zaid, G. Kossiavas, J. Y. Dauvinac, J. Cazajous and A. Papiernik, "Dual frequency and broad-band antennas with stacked quarter wavelength elements," *IEEE Transactions on Antennas and Propagation,*. Vol. 47, no. 4, pp. 654-660, 1999.

[145] J. Ollikainen and P. Vainikainen, "Design of dual-resonant patch antennas," *Proceedings of 4th European Personal Mobile Communications Conference*, Austria, 2001.

[146] K. L. Virga and Y. A. Rashmat-Sammi, "Low profile enhanced bandwidth PIFA antennas for wireless communications packaging," *IEEE Transactions on Microwave Theory and Techniques,* vol. 45, no. 10, pp. 1879-1888, 1997.

[147] H. A. Wheeler, "Fundamental limitations of small antennas," *Proceedings of IRE*, vol. 35. pp. 1479-1484, 1947.

[148] J. S. McLean, "Re-examination of the fundamental limits on the radiation Q of

electrically small antennas," *IEEE Transactions on Antennas and Propagation,* vol. 44, no. 5, pp. 672-676, 1996.

[149] R. Garg, "Design equations for coupled microstrip lines," *International Journal of Electronics*, vol. 47, no. 6, pp. 587-591, 1979.

[150] D. M. Pozar, "Input impedance and mutual coupling of rectangular microstrip antenna," *IEEE Transactions on Antennas and Propagation*, vol. 30, pp.1191-1196, Nov. 1982.

[151] W. C. Chew and J. A. Kong, "Analysis of a circular microstrip disk antenna with a thick dielectric substrate," *IEEE Transactions on Antennas and Propagation*, vol. 29, pp.68-73, Jan. 1981.

[152] M. Davidovitz and Y. T. Lo, "Input impedance of a probe fed circular microstrip antenna with thick substrate," *IEEE Transactions on Antennas and Propagation*, vol. 34, pp. 905-911, July 1986.

[153] A. N. Tulintseff, S. M. Ali and J. A. Kong, "Input impedance of a probe fed stacked circular microstrip antenna," *IEEE Transactions on Antennas and Propagation*, vol. 39, pp. 381-390, March 1991.

[154] Minh-Chau T. Huyngh, "A numerical and experimental investigation of planar inverted-F antennas for wireless communication applications," *MS Thesis*, Virginia Polytechnic Institute and State University, Blacksburg, Virginia, 2000.

[155] F. Abboud, J. P. Damiano and A. Papiernik, "A new model for calculating the input impedance of coax-fed circular microstrip antennas with and without air gaps," *IEEE Transactions on Antennas and Propagation*, vol. 38, no. 11, pp. 1882-1885, 1990.

[156] I. J. Bahal and P. Bhartiya, "Microstrip Antenna," *Artech House*, Bostan, MA, 1988.

[157] T. Chakravarty, S. M. Roy, S. K. Sanyal and A. De, "Loaded microstrip disk resonator exhibits ultra-low frequency resonance," *Progress in Electromagnetics Research*, vol. 50, pp. 1-12, 2005.

[158] Bancroft Randy, "Microstrip and Printed Antenna Design," *Prentice Hall*, India, 2006.

[159] B. D. Van Veen and K. M. Buckley, "Beamforming, a versatile approach to spatial filtering", *IEEE Acoust. Signal Processing Magazine*, vol. 5, no. 2, pp. 4-24, 1998.

[160] I. J. Gupta and A. K. Ksienski, "Effect of mutual coupling on the performance of adaptive arrays," *IEEE Transactions on Antennas and Propagation*, vol.31, pp. 785-791, 1983.

[161] R. S. Adve and T. K. Sarkar, "Compensation for the effects of mutual coupling on direct data domain adaptive algorithm," *IEEE Transactions on Antennas and Propagation,* vol. 48, pp. 86-94, 2000.

[162] G. Y Delisle and J. A. Cummins, "Mutual coupling in the signal to noise ratio optimization of antenna arrays", *IEEE Transactions on Electromagnetic Compatibility*, vol. 15, no. 2, pp. 38-44, 1973.

[163] E. Penard and J. P Daniel, "Mutual coupling between microstrip antennas," *Electronics Letters*, vol. 18, pp. 605-607, 1980.

[164] K. Mahdjoubi, E. Penard, J. P. Daniel and C. Terret, "Mutual coupling between circular disc microstrip antennas," *Electronics Letters*, vol. 23, no. 1, pp. 27-28, 1987.

[165] H. T. Chen, J. S. Row, and Y. T. Cheng., "Mutual coupling between spherical annular-ring and circular microstrip antennas", *Proceedings* of *IEEE Antennas and Propagation Society International Symposium Digest*, vol. 3 pp. 1521-1524, 1997.

[166] E. Van Lil and A. Van De Capelle, "Transmission line model for mutual coupling between microstrip antennas," *IEEE Transactions on Antennas and Propagation*, vol. 32, pp. 816-821, 1984.

[167] Q. Yun, Q. Chen and K. Sawaya, "Performance of adaptive array antenna with geometry in the presence of mutual coupling," *IEEE Transactions on Antennas and Propagation*, vol. 54, no. 7, pp. 1991-1996, 2006.

[168] M. A. Ali and P. Wahid, "Analysis of mutual coupling effect in adaptive array antennas," Antennas and Propagation society Int. Symp., vol. 1, pp. 102-105, 2002.

[169] K. C. Lee and T. H. Chu, "Mutual coupling mechanisms within arrays of nonlinear antennas," *IEEE Transactions on Antennas and Propagation*, vol. 47, no. 4, pp. 963-970, 2005.

[170] M. A. Ali and P. Wahid, "Effect of mutual coupling in adaptive arrays," *Microwave and Optical Technology Letters*, vol. 35, no. 4, pp. 270-274, 2002.

[171] Z. Huang, C. A. Balanis and C. R. Birtcher, "Mutual coupling compensation in UCAs: simulation and experiment", *IEEE Transactions on Antennas and Propagation*, vol. 54, no. 11, pp. 3082-3086, 2006.

[172] R. F. Harrington, "Time-Harmonic Electromagnetic Fields", *John Wiley*, New York, 2000.

[173] R. P. Jedica., M. T. Poe and K. R. Carver, "Measured mutual coupling between microstrip antennas", *IEEE Transactions on Antennas and Propagation*, vol. 29, no. 10, pp. 147-149, 1981.

[174] G. G. Bhise, P. R. Chaddha and D. C. Kulshrestha, "Engineering Network Analysis and Synthesis", *Umesh Publications*, New Delhi, India, 2006.

[175] Wong Kin-Lu, "Compact and broadband microstrip antenna," *John Wiley & Sons*, Inc., New York, 2002.

[176] H. Lee and Y. Lim, "A design of double T type microstrip antennas for broadband and control of resonance," *Microwave Journal*, vol. 49, no.1. January 2006.

[177] H. R. Chaung, C. C. Lin and Y. C. Kan, "A printed UWB Triangular monopole antenna," *Microwave Journal*, vol. 49, no. 1, January 2006.

[178] John D. Kraus and Ronald J. Marhefka, "Antennas for All Applications", *Tata McGra-Hill*, 2002.

Author's Publications

Journals

[1] **Pradeep Kumar**, G. Singh, T. Chakravarty, S. Bhooshan, S. Khah and Asok De, "Numerical computation of Resonant frequency of gap coupled circular microstrip antennas", *J. of Electromagnetic Waves and Applications*, vol. 21, no. 10, pp. 1303-1311, 2007.

[2] **Pradeep Kumar**, G. Singh and T. Chakravarty, "Numerical computation of resonant frequency of shorting post loaded gap coupled circular microstrip antennas", *J. of Electromagnetic Analysis and Applications*, 2009. (accepted)

[3] **Pradeep Kumar** and G. Singh, "Theoretical investigation of input impedance of gap-coupled microstrip antennas", *J. of Infrared, Millimeter and Terahertz Waves,* vol. 30, pp. 1148-1160, 2009.

[4] **Pradeep Kumar** and G. Singh, "Theoretical investigation of input impedance of gap-coupled microstrip antennas loaded with shorting post", *Journal of Computational Electronics,* 2010. (published online)

[5] **Pradeep Kumar** and G. Singh, "Microstrip Antennas Loaded with Shorting Post", *Int. J. of Engineering*, 2009. (accepted)

[6] **Pradeep Kumar** and G. Singh, "Estimation of mutual coupling of shorting post loaded gap coupled circular microstrip antennas", *Int. J. of Electronics Engg.*, vol. 1, no. 1, pp. 99-102, 2009.

[7] **Pradeep Kumar** and G. Singh, "Estimation of mutual coupling of gap coupled circular microstrip antennas", *Int. J. of Intelligent Information Processing*, vol. 2, no. 2, pp. 397-402, Dec. 2008.

Conferences

[8] **Pradeep Kumar**, G. Singh, S. Bhooshan and T. Chakravarty, "Mutual coupling between gap-coupled pin shorted circular patch antennas", *Proc. of IEEE Applied Electromagnetics Conference (AEMC-2007)*, pp. 1-3, Kolkata, India, 19-20 December, 2007.

[9] **Pradeep Kumar**, G. Singh, S. Bhooshan, T. Chakravarty, "On resonant frequency of pin shorted gap-coupled circular patch antennas", *Proc. of IEEE Applied Electromagnetics Conference (AEMC-2007)*, pp. 1-3, Kolkata, India, 19-20 December, 2007.

[10] **Pradeep Kumar,** G. Singh, S. Bhooshan and T. Chakravarty, "Gap-coupled microstrip antennas," *Proc. of Int. Conf. on Computational Intelligence and Multimedia Applications (ICCIMA-07)*, pp. 434-437, Sivakasi, India, 13-15 December, 2007.

[11] **Pradeep Kumar,** G. Singh and S. Bhooshan, "Miniaturization of gap-coupled circular microstrip antennas," *Proceedings of International Conference on Recent Advances in Microwave Theory and Applications (Microwave-08)*, pp. 489-491, Jaipur, India, 21-24 November, 2008.

[12] **Pradeep Kumar,** G. Singh, S. Bhooshan, "Input impedance of shorting post loaded gap-coupled circular microstrip antennas," *Progress in Electromagnetic Research Symposium (PIERS-09)*, pp. 1634-1638, Beijing, China, 23-27 March, 2009.

[13] **Pradeep Kumar,** G. Singh, S. Bhooshan, "Input impedance of gap-coupled circular microstrip antennas," *IEEE International Symposium on Microwave (IEEE-ISM-08)*, Bangalore, India, 3-6 December, 2008.

[14] **Pradeep Kumar,** G. Singh, and S. Bhooshan, "Terahertz Technology-A Technical Review," *Proceedings of International Conference on Microwave and Optoelectronics (ICMO-07)*, pp. 397-402, Aurangabad, India, 17-20 December, 2007.

[15] **Pradeep Kumar**, G. Singh, T. Chakravarty and S. Bhooshan, "Terahertz technology-a new direction," *Proc. of IEEE International Symposium on Microwave (IEEE-ISM-06)*, pp. 195-201, Bangalore, India, 15-17 December, 2006.

[16] **Pradeep Kumar**, G. Singh and S. Bhooshan, "Pin Shorted Rectangular Microstrip Antenna for Mobile Communication", *Proc. of National Conference on Wireless and Optical Communication (WOC-07)*, pp. 77-79, Chandigarh, India, 13-14 December, 2007.

[17] **Pradeep Kumar,** G. Singh, "Loading of Microstrip Antennas", *Proceedings of National Conference of Applied Physics and Radiating Material (APRM-09), 13-14, March 2009.*

[18] **Pradeep Kumar,** A. K. Singh, G. Singh, T. Chakravarty, and S. Bhooshan, "A novel cross patch antenna for wideband application," *Proc. of IEEE Int. Workshop on Antenna Technology: Small and Smart Antennas Metamaterials and Applications (IEEE-IWAT-07)*, pp. 255-258, Cambridge, UK, 21-23 March, 2007. (accepted by antenna center of excellence for excellent research work)